DEVELOPMENT F FAST AND AFFORDABLE METHODS FOR MEASURING QUALITY RELATED PROPERTIES OF CONFECTIONS

by

JUZHONG TAN

(Under the Direction of WILLIAM L. KERR)

ABSTRACT

The global confectionary market was valued at $184 billion in 2015, and is projected to reach $232 billion by 2022. The industry directly employs 55,000 people domestically, and more than 400,000 jobs in agriculture, retail, transportation and other industries rely in part on the sale and manufacture of confections. However, many available analytical methods for measuring the quality of confections are relatively expensive, time consuming, and difficult to operate or maintain, therefore, it is unrealistic for small/medium confection manufacturers to use those methods. The objective of this study was to develop fast-measuring and affordable analytical methods for some important quality related properties. In addition, the developed methods were used to study the properties of confections and compare them with traditional methods, seeking their potential applications in confection quality assurance for small/medium confection manufacturers and other researchers. Two capacitance-based thermal analysis (CTA) methods were developed to study the glass transition and melting properties of different boiled candies and chocolates respectively. Three particle size measurement methods were tested for characterizing cocoa particle size distribution in the refining/conching process. The

microstructure of cocoa particles was also studied by scanning electron microscopy (SEM). Flavor development and volatile compounds profiles of cocoa during roasting and refining/conching processes were studied by electronic nose. The results provide better understandings about quality related properties, such as glass transition, melting, and particle size, of confection by using non-traditional methods. The potential applications of fast-measuring and affordable analytical methods were tested and several of the methods were proved to be useful for small/medium confection manufacturers.

INDEX WORDS: confection, phase transition, volatile compound, capacitor thermal analysis, electronic nose, particle size analysis, refining/conching, roasting

DEVELOPMENT OF FAST AND AFFORDABLE METHODS FOR MEASURING QUALITY RELATED PROPERTIES OF CONFECTIONS

by

JUZHONG TAN

B.E., Northeast Agricultural University, China, 2013

A Dissertation Submitted to the Graduate Faculty of The University of Georgia in Partial Fulfillment of the Requirements for the Degree

DOCTOR OF PHILOSOPHY

ATHENS, GEORGIA

2017

DEVELOPMENT OF FAST AND AFFORDABLE METHODS FOR MEASURING QUALITY RELATED PROPERTIES OF CONFECTIONS

by

JUZHONG TAN

Major Professor: William L. Kerr

Committee: George A. Cavender
Jose I. Reyes De Corcuera
Chanying Li

Electronic Version Approved:

Suzanne Barbour
Interim Dean of the Graduate School
The University of Georgia
August 2017

DEDICATION

This work is dedicated to my parents, Minliang Tan and Xiaolan Yan.

ACKNOWLEDGEMENTS

I would like to first thank my major advisor Dr. Bill Kerr for his advice. His infinite knowledge in food engineering and processing as well as critical thinking has changed me and made me grow as a professional. He also provided me good opportunities of conducting researches that line up with my interests and ambitions. I am also very grateful to Dr. Balu Balasubramanian for the guidance of research, sharing of experience, and advices of career path. I would also like to express my appreciation to Dr. Changying Li for giving me the invaluable information and constructive suggestions on the research electronic nose related. I would like to acknowledge the other members of my committee, Dr. Fanbin Kong, Dr. Jose Reyes De Corcuera, and Dr. George Cavender, for their help, patience, and advices through the journey. I am very grateful to my host family in Athens, Mr. Latimer Heard and Mrs. Linda Heard, who provided me unconditional emotional support and treated me as their own son. I would also like to thank all my friends and colleagues for their technical assistance and patience when I was doing research in Athens. I am also very grateful to all the personnel in the CocoaTown LLC, College of Engineering and Department of Food Science and Technology. They have been so friendly and nice to me and giving me a hand whenever I needed. Finally, I would like to thank Athens. She is the place I started to know this country and it became my second hometown where I will always remember. After the 4-year odyssey, I will start a new Journey, and I will be ready for my next life chapter.

TABLE OF CONTENTS

Page

LIST OF TABLES

Page

LIST OF FIGURES

Page

CHAPTER 1

INTRODUCTION

Candy is a confection that features sugar as a principal ingredient. The production of candy started in Persia between the 6th to 4th centuries BCE. Today, the categories of candy include hard candies, soft candies, caramels, marshmallows, taffy, and other candies, all of which use sugar as the primary ingredient. Commercially, sugar candies are usually classified according to the amount of sugar they contain and their chemical structure (Richardson 2008).

Chocolate is a complex suspension system of solid particles (cocoa, sugar, milk components, additives) in a continuous fat phase that consists of cocoa butter, milk fat and emulsifiers (Afoakwa et al., 2008a, Beckett 2000, Chetana et al., 2013). The history of chocolate started roughly one thousand years ago in Central America. In the early years, it was mainly consumed in beverages and medicines up until the 1800s when solid chocolate became more popular than liquid chocolate (Grivetti and Shapiro 2011). Chocolate can be a snack, special treat, or delicacy to be sampled and evaluated much like wine, in addition, chocolate is an important industry with an estimated global market value of more than $98 billion (World Atlas 2016).

In the confection industry, advanced analytical methods for quality related properties such as phase transition temperature, particle size, and volatile compound profiles, are relatively expensive and time consuming. These methods include differential scanning calorimetry (DSC), rheometry, scanning electron microscopy (SEM), laser scatting particle size analysis, and gas

chromatography-mass spectrometry (GC-MS), which can be difficult to operate and maintain. Therefore, it can be difficult for small/medium confection manufacturers to perform much-needed quality inspection and product development. This research was undertaken to develop fast-measuring, portable, and inexpensive analytical methods that could be used to determine the quality related properties of confections (boiled candy and chocolate). The development of corresponding electronic devices, data acquisition methods, and a data processing algorithm were also included in the studies as a natural extension. Measurements conducted by the proposed methods were compared to the ones obtained by existing methods.

In Chapter 2, the literature review begins with a broad introduction about the candy and chocolate industry. This includes information about chocolate fermentation and tempering. Chocolate roasting and refining/conching are then discussed as they are to the studies in Chapter 5, 6 and 7. Following that, information on the glassy state, glass transition and cocoa butter crystallization are introduced. The working principles of current standard analytical methods and research related to phase transition detection are discussed. These include DSC, thermal rheometry and dielectric analysis (DEA), and are presented in reference to the capacitor based thermal analysis (CTA) that is presented in Chapter 3 and 4. The basis of the proposed CTA consists of two important parts: the device and the algorithm. Therefore, detailed information about the capacitor (device) and genetic algorithm (GA) are provided following the introduction of standard methods.

Evaluating analytical methods that can be used for chocolate particle size measurement is the main topic in Chapter 5. The following parts of the literature review introduce the process of refining/conching, where the particle size reduction of chocolate is achieved, and the microstructure and volatile compounds profiles are developed. Comprehensive reviews about

particle size measurements methods and scanning electron microscopy (SEM) are provided after introduction of cocoa refining/conching.

The subsequent sections of the literature review discuss the roasting process of cocoa and the development of volatile compounds during roasting. The proposed method for studying the volatile compounds developed both in refining/conching and roasting processes uses an electronic nose system. Therefore, in last two sections of the literature review, the electronic nose (device) and the algorithm (artificial neural network (ANN) are discussed.

Chapter 3 and Chapter 4 present two newly developed capacitor thermal analysis (CTA) methods to determine the glass transition of boiled candies and the melting properties of chocolates. Measurements obtained by using DSC and rheometry for the same samples are used as a reference. Chapter 5 examines particle size reduction and the microstructure of cocoa during refining and conching. Three particle size measurement methods were compared to laser scattering methods. The application of an electronic nose in determining the roasting degree of cocoa beans are presented in Chapter 6. In Chapter 7, the application of the e-nose in characterizing the refining/conching process of cocoa is presented.

References

Afoakwa, E.O., Paterson, A., Fowler, M. and Vieira, J., 2008. Characterization of melting properties in dark chocolates from varying particle size distribution and composition using differential scanning calorimetry. Food Res. Int., *41*(7), pp.751-757.

Chetana, R., Reddy, S.R.Y. and Negi, P.S., 2013. Preparation and properties of probiotic chocolates using yoghurt powder. Food Nutr. Sci., *4*(03), p.276.

Grivetti, L.E. and Shapiro, H.Y., 2011. *Chocolate: history, culture, and heritage*. John Wiley & Sons.

Richardson, T., 2008. *Sweets: a history of candy*. Bloomsbury Publishing USA.

Worldatlas. "Top 10 Cocoa Producing Countries.". 22 July 2016. Web. 25 Nov. 2016.

CHAPTER 2

LITERATURE REVIEW

Candy and chocolate processing

Candy processing is typically divided into two steps. The first step is dissolving sugar in water or milk to form a syrup and the second is the boiling of the ingredients until they reach the desirable concentration or caramelization occurs. The type of candy produced depends on the ingredients and the cooking temperature of the candies before they are allowed to cool. Candy comes in a wide variety of textures, from soft and chewy to hard and brittle. In general, higher temperatures and greater sugar concentrations result in hard, brittle candies, while lower temperatures result in softer candies (Cakebread 1975). The cooking temperatures of boiled candies and their corresponding expected textures are shown in Table 2.1 (Hartel and Hartel 2014).

The manufacture of chocolate includes harvesting, fermentation, roasting, cracking, winnowing, refining, conching, tempering, transporting and storing. Each unit operation greatly influences the final quality of the chocolate. Even today, the harvesting of cocoa pods relies heavily on human labor, which includes cutting them from cocoa trees using a machete or knocking them off the tree with sticks. After harvesting, the pulp is removed from the pods and the beans are placed in piles or bins where microorganisms begin the fermentation process.

Cocoa fermentation is one of the most important stages in post-harvest processing that is related to product quality. Fermentation remains empirical and does not give rise to beans of consistent quality, forcing processors continuously to make changes of their formulations. It also helps to trigger biochemical changes inside the beans that reduce bitterness and astringency, and to the development of flavor precursors. The schematic of a microbial succession during cocoa bean fermentations is shown in Figure 2.1 (Schwan and Wheals 2004). The open boxes indicate the periods during the fermentation when a particular microbial group is most abundant and/or important.

After fermentation, cocoa beans must be roasted to improve quality and develop flavor. Cocoa roasting is a dry heating method that uses different heat sources (hot air, flame, and hot plate) to cook cocoa beans. Roasting also makes the cracking and winnowing much easier by decreasing the moisture content in the beans and helping separate the husk from nibs. Refining/conching includes crushing, mixing, and agitating the cocoa with other ingredients such as sugar, milk protein, and cocoa butter, by extreme friction and high heat. This process reduces the particles size of the ingredients and delivers a smooth texture by developing the microstructure of the particles.

The final process of making chocolate is called tempering. This process controls the crystallization of cocoa butter by manipulating temperature. Both the type and the size of the crystals are influenced by the tempering process. The typically desired texture of chocolate is uniform sheen and crisp bite, and this is achieved by consistently producing small cocoa butter crystals during tempering process. Table 2.2 summarizes the melting temperature (T_m) and the texture of 6 type of cocoa butter crystals. And type V crystal is usually desirable because it delivers glossy, firm, and best snap texture.

Glassy state

In nature, the commonly known states of materials are solid, liquid, and gas. The main difference among these states is their molecular mobility. The solid state has the lowest molecular mobility and the molecules in solids are fixed in their position. The crystalline state is a well-known solid state having molecules well arranged in a regular lattice. However, solids can exist in another state where the arrangement of the molecules are randomly distributed, or in other words, a disordered arrangement. This is called a glassy state or amorphous state. The name appears to have originated from glass manufacturing (Debenedetti and Stillinger 2001).

Glassy states are usually formed by rapidly decreasing the temperature of molten liquids to a certain temperature range. Because of this drop in temperature, the molecules in the liquid don't have sufficient time to undergo the association and change in orientation to form to well-arranged crystalline state. Therefore, the molecules are 'frozen' in their original position. The glassy state is characterized by its amorphous molecule distribution, which is similar to molecules in liquid state, and extremely high viscosity, just like solids (Kivelson et al., 1996; Weeks, et al 2000; Johari and Goldstein 1970).

If the liquids are cooled down slowly below their melt temperatures, the molecules form crystals and the liquids solidify. The transition from liquid to solid is a thermodynamic process, as when the temperature is below the melt temperature of the material, the crystal state is energetically more favorable than the liquid. In contrast, the formation of a glass is purely kinetic, where the disordered glassy state does not have enough kinetic energy to reach the potential energy threshold for the movement of its molecules to pass one another. Therefore, molecules of the molecules are fixed in their original locations but in disordered arrangement.

Although, as mentioned before, the molecules in glassy state materials are disordered, it can have short-range molecular order like molecules in a crystalline solid (Yu 2001). One single molecule in glassy solid has similar number of neighbor molecules and similar distance to the nearest neighbor molecule as single molecule in a crystalline structure. However, this short-range order may only vary over a few angstroms. Unlike crystalline structures, the glassy solid doesn't have long range translational orientational symmetry that characterizes a crystal (Hancock and Zografi 1997; Simatos et al., 1995; Johari 1982).

Glass transition and glass transition temperature (T_g)

Glass transition, is a name given to the phenomenon that glass is changed into a supercooled liquid, or the reverse transformation (Meste et al., 2002). The transition of glass to supercooled liquid is usually driven by heating (Rahman 1999; Bhandari and Howes 1999). The main difference between glass and supercooled liquid is short-range vibration and rotation in glass, and long-range translation and rotation in supercooled liquid (Schmidt 2004).

For food materials, there are two commonly known phase transitions: first-order and second order transition. The main difference is absorption or release of latent heat during transition. Transitions include melting, crystallization, evaporation, and condensation are first order transitions. A certain amount of latent heat is released or absorbed to make the transition isothermal. In contrast, second order transitions occur without the release or absorption of latent heat. However, glass transition is typically called a state transition rather than a phase transition because of the nonequilibrium nature of the glass (Schmidt 2004). In addition, glass transitions occur over a temperature range rather than a fixed temperature and the transition is dependent on the experimental condition. Therefore, it is commonly called a kinetic and relaxation transition, rather than a second-order transition (Liu et al., 2006).

Currently, the knowledge about the glass transition in food materials is phenomenological, as little is known about its theoretical aspect (Champion et al., 2000). T_g is the temperature range corresponding to the transition of glass-liquid. Unlike melting temperature (T_m), T_g is a kinetic parameter, depending on the temperature scanning rate and the material's thermal history. When the temperature is between T_g and T_m, the material can be a viscous liquid, and this state is called a 'rubbery' state.

Cocoa butter crystalline states

Cocoa butter is the main structural material in chocolates and the fat content in chocolates is about 30%. Milk fat and protein can also serve as structuring materials in some chocolates such as milk chocolate or white chocolate. The basic lipid form for cocoa butter is triglycerides (TAG), which are known to crystallize in a number of different polymorphic forms depending on processing conditions such as temperature, force, and mass (Sato et al., 1999; Sato 2001). Six different polymorphs of cocoa butter have been identified in in chocolate. The name of each polymorphic form is γ α, β_2', β_1' β_2 β_1. Alternately, the six different polymorphs can be represented by roman numerals I-VI for γ α, β_2', β_1' β_2 β_1 respectively. The melting temperature ranges for type γ, α, β', β are -5-5℃, 17-22 ℃, 20-27 ℃, 29-34 ℃ respectively. Real-time powder X-ray diffraction has been used by other researchers to study the structure of cocoa butter polymorphism. The results reported by other researchers suggested that the unstable γ (orthorhombic subcell) and α (hexagonal subcell) phases, as well as the more stable β_2 (orthorhombic subcell) phase, can crystallize directly from the chocolate melt. However, the stable β (triclinic) polymorph can only be obtained via phase transformation from the β_2 form (Van Malssen et al., 1999; Van Malssen et al., 1996; Loisel et al., 1998). In most cases, β_2 form is desirable for chocolate manufacturers because this type of crystal is stable at room temperature

and melts at body temperature, which brings smooth mouth feel to consumers. However, in some cases, less stable form such as form α is required for making chocolate fillings or chocolate fountains.

All long-chain compounds, including fats and lipids, in nature show polymorphism. TAG is a glycerin fatty acid ester that usually possesses three polymorphs. The crystallization behavior of TAG depends on the molecular structure of TAG and on several external factors such as temperature, pressure, solvent, rate of crystallization, and levels of impurities (Sato 2001). The arrangements of TAGs in crystals is amorphous-like for α, bulky shape for β' and needle shape for β. The structure of α, β', β polymorphs are based on subcell structures, which define cross-sectional packing modes of the zigzag aliphatic chain and single-crystal structure of tricaprin β form (Larsson 1966; Jensen and Mabis 1966). Aliphatic chain conformation in form α is disorder, however, form β' has intermediate packing and β has the densest packing. Therefore, the Gibbs free energy (G) values are highest in α, intermediate in β' and lowest in β. In other words, β is the most stable form, whereas, α is the least stable form (Sato 2001).

The melting properties, microstructure, and crystallization of cocoa butter has been intensively studied by many researchers. Marangoni and McGauley (2003) have correlated the microstructure obtained by polarized light microscope to crystallization behavior. Loisel et al. (1998), Fessas et al. (2005), Dhonsi and Stapley (2006), Lambelet (1984) and Foubert et al. (2003) used differential scanning calorimetry (DSC) to study the phase transition temperature, crystallization kinetics, and solid/fat content of chocolates. Pérez-Martínez et al. (2007), Brunello et al. (2003), and Sterling and Wuhrmann (1960) did comprehensive research on the relationship between crystal microstructure and rheological/mechanical properties.

Melting is a physical process that results in phase transition from solid phase to liquid phase. The transition is driven by the increase of internal energy, typically, introduced by heat, friction or pressure (Atkins and Jones 2007). Except using DSC, and dynamic viscoelastic analysis, there are several other available methods can be used to determine the melting properties, namely, the melting temperature of chocolates. Capillary method is one popular methods for melting point determinations. A thin glass capillary tube containing a compact column of the substance to be determined is introduced into a heated stand in close to a high accuracy thermometer. The temperature in the heating stand is ramped at constant fixed rate until the sample in the tube transitions into the liquid state. This method is relative low-cost; however, it needs the visual observation of users which is sometime inconsistent and biased. Melting collapse tests conducted by home-made devices can be useful for the determination of melting temperature of materials. The devices perform the melting collapse test, in which a static force is applied on the chocolate sample while a temperature ramp is performed (Dicolla 2008). Thermometer and thermal couple are also implemented by many chocolate manufacturers for melting point measurements. The measurements are based visual observation of the users which brings uncontrolled deviation and inconsistency.

Phase transitions determined by differential scanning calorimetry (DSC)

DSC is a thermal analysis technique that measures the change of heat capacity of materials at different temperature and differentiate it with reference (e.g., air). Alternatively, DSC measures the heat required to raise the temperature of the materials by unit degree. A sample of known mass is heated or cooled and the changes in its heat capacity are tracked as changes in the heat flow. During phase transition, denaturation transitions, bio-macromolecule unfolding process, the heat capacity of different materials exhibit different responses to

temperature scan. Since most materials exhibit some sort of transition, DSC is used in many industries, including pharmaceuticals, polymers, food, paper, printing, manufacturing, agriculture, semiconductors, and electronics (Spink 2008; Freire 1995; Höhne et al., 1996).

Chalikian et al. (1999), Cooper and Johnson, (1994) Freire, (1994), Makhatadze and Privalov, (1995), and Plum and Breslauer (1995) studied the unfolding of protein and nucleic acids. They not only found thermodynamic data for the denaturation transitions, but also a better understanding of the underlying complexity of the unfolding process. DSC was also used to study the phase transition of lipid membranes and model membrane systems (Ali et al., 1989; Huang and Li, 1999; Mason, 1998).

The application of DSC in studying the thermodynamic of food material is very broad. Privalov (1974), Brandts (1964), Jackson and Brandts (1970) used DSC to determine the denaturation of proteins. Donovan, (1979), Biliaderis et al. (1980), Eberstein et al. (1980), and Eliasson (1980) did comprehensive studies on the phase transitions and gelatinization in starch by DSC. Tan and Kerr 2017, Ohkuma et al. (2008) and Afoakwa et al. (2008a) studied the phase transition of candies, frozen foods and chocolates by DSC.

Phase transitions determined by rheometry

The rheological properties of the materials that undergo phase transitions exhibit anomalous trends to non-transition states due to the changes in physical/chemical properties such as viscosity, structure, strength of intermolecular bonds and volume. Many researchers (Lai et al., 1999; Xue et al., 2008; Aguilera 1995; Krog and Larsson 1968; Laaksonen and Roos 2000; Cocero and Kokini 1991; Roos and Karel 1991) have used rheometry to study the phase transitions in food materials, including chocolate, starch, whey protein, monoglycerides, wheat

dough, glutenin, polysaccharide and sugar. Their results show that rheological properties can serve as good indicators for glass transition, melting, and crystallization in food materials.

Determination of rheological properties are usually conducted by dynamic mechanical thermal analysis (DMTA) and mechanical spectroscopy, which obtain mechanical modulus data of food materials as a function of temperature. Mechanical properties can be obtained from the materials by periodically changing the stress or stain that are applied in samples under shear, blending, tension or torsion (Ross-Murphy1994).

The distinctive property of glass forming materials is the dramatic slowing down of relaxation and flow with decreasing temperature. The dynamical range of this phenomenon is probably one of the most spectacular in physics: viscosity may increase by about 15 orders of magnitude for a mere 30% decrease in temperature (Ediger et al., 1996; Debenedetti and Stillinger 2001; Liu and Nagel 2001). Tarjus et al. (2005) used a simple Arrhenius equation to describe the viscosity of a glass forming material as a function of temperature:

$$\eta \approx \eta_{\infty} e^{E_{\infty}/kBT}$$

where ŋ is the viscosity of the materials, ŋ∞ is the viscosity at infinite high temperature, and T is temperature in Kelvin. At low sufficiently temperature, this exponential function shows a linear trend. However, at glass transition temperature, the dynamical properties of a liquid change from an ‘ordinary,’ Arrheniuslike temperature dependence to an ‘anomalous,’ stronger than Arrhenius (or super-Arrhenius) one. Conventionally, the point at which the viscosity takes a given value of 1013 poise is defined as glass transition temperature.

To better use the Arrhenius equation to describe the dynamic mechanical properties of different materials, Ngai et al. (1985) introduced the notion ‘fragility,’ which characterizes the

degree of super-Arrhenius behavior, the more fragile the glassformer the greater the super-Arrhenius character. The simple Arrhenius equation was then modified to Vogel-Fulcher-Tammann formula:

$$\eta \approx \eta_{\infty} e^{\frac{DT_0}{T-T_0}}$$

where D is the measurement of fragility. An alternative method to represent the data is focused on the effective activation energy:

$$E(T) = kBT \ln (\eta/\eta_{\infty})$$

Phase transitions determined by dielectric analysis (DEA)

Dielectric analysis (DEA) refers to a group of techniques that measure the polarization, permittivity, and conductivity of materials as a function of temperature or frequency. The reorientation of dipoles and the translational diffusion of charged molecules caused by oscillating electric fields. The basis of the analysis based on alternating-current (AC) dielectric methods principally involve measurements of the complex permittivity (dielectric constant ε' and dielectric loss ε'') in the frequency or time domain and at constant or varying temperature (Vassilikou-Dova and Kalogeras 2009). The dielectric constant and polarizability of the molecules in materials undergo great changes during phase transitions including glass transition, melting, and crystallization, and these changes are easier to detect than enthalpy, volume, or heat capacity. Since the mid-1970s, DEA has received wide recognition as a powerful thermal analysis method, and its applications cover linear-polymers, numerous macromolecular systems with complex molecular architectures such as comb like and branched structures, stars, cycles, copolymers, hyperbranched polymers, and dendrimers (Kremer 2002).

The most common sample configuration for dielectric analysis involves placing the sample in a parallel-plate capacitor. An alternating voltage of angular frequency ω is applied to the parallel plates. Then the dielectric properties of the sample can be described as its capacitance and conductance:

$$C(\omega) = \varepsilon_0\varepsilon'(\omega)S/d;\ G(\omega) = \varepsilon_0\varepsilon''(\omega)S/d$$

where S and d are the sample's cross-sectional area and thickness, and ε_0 is the permittivity of vacuum. The frequency depended parameters ε' and ε'' are the real and imaginary part of the complex dielectric permittivity function:

$$\varepsilon^*(\omega) = \varepsilon'(\omega)-i\varepsilon''(\omega)$$

where $i^2 = -1$. The real part of the complex permittivity expresses the ability of the dielectric material to store energy, while the imaginary part of the complex permittivity describes the energy losses due entirely to the material medium (Macdonald 1987; Jonscher 1999).
In frequency domain, the real part of the dielectric permittivity $\varepsilon'(\omega)$, shows a dispersion. On the other hand, dielectric losses $\varepsilon''(\omega)$, in the idealized case, exhibit a bell-shaped curve with a full width at half-height of 1.14 decades and a maximum occurring at $\log(\omega_{max}\tau) = 0$. The loss peaks for most polymeric materials are broad and distorted (asymmetric). The loss tangent $\delta(\omega) = \varepsilon''(\omega)/\varepsilon'(\omega)$ was also frequently used to characterize polymers for many electrical and engineering applications. δ is the phase lag between the alternating electric field $E(t) = E_0e^{i\omega t}$ and the dielectric induction $D(t) = D_0e^{i(\omega t - \delta)}$, and is a measure of system's polarization inertia with respect to the electric stimulus (McCrum et al., 1967).

Dielectric relaxation is the momentary delay (or lag) in the dielectric constant of a material. This is usually caused by the delay in molecular polarization applied with alternating

electric field in a dielectric medium. Dielectric relaxation in changing electric fields could be considered analogous to hysteresis in changing magnetic fields. Relaxation in general is a delay in the response of a linear system, and therefore dielectric relaxation is measured relative to the expected linear steady state (equilibrium) dielectric values. The time lag between electrical field and polarization implies an irreversible degradation of Gibbs free energy (Williams and Watts 1970).

In physics, dielectric relaxation refers to the relaxation response of a dielectric medium to an external, oscillating electric field. This relaxation is often described in terms of permittivity as a function of frequency, which can, for ideal systems, be described by the Debye equation. On the other hand, the distortion related to ionic and electronic polarization shows behavior of the resonance or oscillator type. The character of the distortion process depends on the structure, composition, and surroundings of the sample (von Hippel and Morgan 1995).

The single relaxation time model of Debye (Debye 1921) was used to describe the dependency of complex permittivity on relaxation time:

$$\varepsilon^*(\omega) = \varepsilon_u + \frac{\varepsilon_r - \varepsilon_u}{1+i\omega\tau} = \varepsilon_u + \frac{\varepsilon_r - \varepsilon_u}{1+\omega^2\tau^2} - i\frac{\varepsilon_r - \varepsilon_u}{1+\omega^2\tau^2}$$

where ε_r is the permittivity at the high frequency limit, ε_u is the static, low frequency permittivity, and τ is the characteristic relaxation time.

The application of DEA in studying the properties of food materials is very broad. Lu and Fuji (1998) conducted DEA by coaxial line reflection to study the denature of hen egg white, and they reported that the denatured gels were stored at 5°C for 13 days to be subjected to a dehydration process that led to a corresponding decrease in dielectric constant and conductivity. Laaksonen and Roos (2000) compared the performance of three methods (DSC, DMA, DEA) for

determining phase transition of wheat dough. They found that the DEA method is an effective method to detect phase transition in wheat dough, and in fact, t was able to detect several more transition regions than DMA and DSC. They later used the same methods to study the wheat dough with sugar, salt and acid, and were able to determine that relaxation temperatures (α, β and γ) increased with increasing frequencies if NaCL was added into the wheat dough (Laaksonen and Roos 2001). Moran et al. (2000) studied the structure and dynamics of sugar/water solution in both the viscous liquid and the glassy state, and they verified that the dielectric response was dominated by the large dipole moment of the water molecule. Both the structural relaxation and a secondary β process were observed. Feng et al. (2002) did a study on how moisture content influences the dielectric properties of microwaved dried apple, and they found that decrease in moisture content resulted in a decrease in ε' and ε''.

Capacitors

The most basic device for DEA is a parallel plate capacitor (Stuchly and Stuchly 1980). A capacitor is an electronic device that has the ability to store energy in the form of an electrical charge, producing a potential difference across its conductors. Its working principal is similar to a rechargeable battery. The conductor may be a foil, thin film, sintered bead of metal, or an electrolyte. The most basic form of a capacitor consists of two or more parallel conductive plates which are not connected or touching each other, but the plates are separated either by air or by an insulating material such as wood, plastic, or rubber. The insulating layer between a capacitors plates is commonly called the dielectric materials or medium (Poynting 1908).

The ability of a capacitor to store charge on its conductors in the form of an electrostatic field is called the capacitance of the capacitor. By applying a voltage to a capacitor and measuring the charge on the plates, the ratio of the charge Q to the voltage V will give the

capacitance value of the capacitor. Ideally the capacitance C of a capacitor is sufficiently characterized by:

$$C = \frac{Q}{V}$$

In practical devices, charge build-up sometimes affects the capacitor mechanically, causing its capacitance deviated from its ideal form. In this case, capacitance is defined in terms of incremental changes:

$$C=\frac{dQ}{dV}$$

When a capacitor is not in a circuit, theoretically, its capacitance is calculated by

$$C=\varepsilon_r\varepsilon_0\frac{A}{d}$$

where A is the area of overlap of the two plates, in square meters, ε_r is the relative static permittivity (sometimes called the dielectric constant) of the material between the plates (for a vacuum, $\varepsilon_r = 1$), ε_0 is the electric constant ($\varepsilon_0 \approx 8.854\times10^{-12}$ F·m^{-1}) and d is the separation between the plates, in meters. There are also many other types of capacitors such as coaxial cable, pairs of parallel wires, concentric sphere, circular disc, and sphere. The calculation of capacitance for different types of capacitor vary accordingly (Houldin 1967).

In a DC (source voltage V_0) circuit where one capacitor and one resistor is in series, Kirchhoff's voltage law can be applied and the relation between capacitance and V_0 is

$$RC\frac{dt(i)}{d(t)}+i(t)=0$$

while in a AC circuit where one capacitor and one resistor is in series, A capacitor connected to a sinusoidal voltage source causes a displacement current to flow through it. In the case that the voltage source is $V_0\cos(\omega t)$, the displacement current can be expressed as:

$$I=C\frac{dV}{dt}=-\omega CV_0\sin(\omega t)$$

where, I is current, C is capacitance, and ω is frequency of the AC voltage that being applied to the capacitor.

Genetic algorithm (GA)

The Genetic algorithm is an adaptive heuristic search method based on natural selection of gene, and GA was firstly introduced by John Holland in the early 1970s (Tsoukalas and Uhrig 1997). Usually the selection is started with a set of solutions called the first generation. The solutions in genetic algorithms are called chromosomes or strings. The population size is either preserved or varied throughout each generation depending on the designed strategy. At each generation, fitness of each chromosome is evaluated through a pre-set fitness function, and then the chromosomes with high fitness values are probabilistically favored to be inherited to the next generation. The next generation is generated by selecting chromosomes as 'parent' and they randomly mate and produce offspring. When producing the next generation, crossover and mutation randomly occurs according to the settings of GA. Because chromosomes with high fitness values have high probability of being selected in the long term, chromosomes of the new generation may have higher average fitness value than those of the old generation. The process of evolution is repeated until the termination criteria is satisfied. The termination criteria can be any chromosome reaching certain fitness value, certain number of generation is generated, or the pre-set time for running the GA is up (Lee and Kim 2005).

The traditional procedure of GA includes initiation, selection, reproduction, and termination. The initial generations are randomly generated and the population size depends on the nature of the problem, varying from tens to thousands. The selection is usually conducted by a fitness-based process, where fitter solutions are typically more likely to be selected. Certain

selection methods rank the fitness of all individuals and preferentially select the best solutions. Other methods rate only a random sample of the population, as this process may be very time-consuming. The reproduction is conducted by two GA operators: crossover and mutation. There are many crossover methods such as single point, two points, uniform, half uniform and adaptive crossover. The selection for crossover method varies by case. Although reproduction methods that are based on the use of two parents are more common, some research suggests more than two "parents" are better for the production good quality children (Eiben et al., 1994).

GA and its upgraded algorithms have many applications including management, robotic, image processing, decision making, and game strategies. Gong and Yang (2001) applied genetic algorithms for stereo image processing. Yasuda and Takai (2001) applied genetic algorithms for sensor-based mobile robot path planning under unstructured environment in real-time. Madureia et al. (2002) suggested genetic algorithms for the resolution of real world scheduling problems, and proposed a coordination mechanism. Potter et al. (1994) used GA to solve a "snake in box" problem and found good solutions. Some researchers (Magnier and Haghighat 2010) also applied GA to improve building designs.

Chocolate refining/conching

Chocolate manufacturing usually includes procedures of mixing, refining and conching. Chocolate refining is the process of reducing the particle sizes of both cocoa solids, sugar crystals and other ingredients (proteins, flavors, milk fat, and liquor etc.,) in finished chocolate. The goal is to reduce the particle size somewhere in the range of 15-25 microns because human tongue loses its ability to determine texture and grittiness at around 30 microns. On the other hand, when the particle size is less than about 10 microns the chocolate can get gummy. In

addition, the particle size of the processed ingredients significantly influences the rheological and melting properties of the final products (Beckett 2011; Beckett 2000).

Typically, refining is conducted by a combination of two- and five-roll refiners. Four grinding rolls are aligned vertically, while the feed roll is placed at an angle to the lowest stack roll. The main factor that determines the throughput and the final fineness of chocolate is the feeding rate, and the feeding rate is adjusted by changing the feed roll gap at a constant roll speed or by changing the roll speed at a constant gap (Ziegler and Hogg 2009). Also, the pressure on the rollers is another critical factor that influences the fineness of the particles (Ripani et al., 1986). Many other studies have reported other refining methods/equipment for chocolate processing. Lucisano et al. (2006) and Alamprese et al. (2007) have used ball mill to refine the ingredients of chocolate, studying the influence of formula and processing variables on the rheological properties of dark, milk, and compound chocolate. Hammer mill and disc mill were also reported as the equipment for chocolate refining (Kurt 1995; Hendry 1952; Zoumas et al., 2004). A malenger can also be used for chocolate refining. A traditional melanger has a rotating pan, often with a granite bed, on which two granite rollers rotate. Scrapers ensure mixing by directing the material under the rollers. The modern requirement for continuous higher throughput methods has often led to the mixing, grinding, even conching being carried out separately (Beckett 2011).

The procedure after refining is conching, however, by using certain equipment, such as melanger, the two steps are conducted at almost the same time. Chocolate conching is basically a process of stirring and agitating the chocolate for an extended period of time at temperature >50 ℃ (Jolly et al., 2003; Beckett 2000). Conching is not very well understood. It is believed that conching contributes many things that improve the flavor and texture of chocolates.

Babin (2005) described the conching as a three-step process. At the first stage, the ingredients are crushed but still dry. At the second stage, melted cocoa butter are released from the cells of cocoa and chocolate paste is generated. In the last stage, the ingredients become liquid like, and this stage is called liquid conching. In the early stages of conching, the moisture is reduced, certain undesirable flavor-active volatiles such as acetic acid are removed, and interactions between disperse and continuous phase are promoted. In later stages, conching rounds off the particulates within the chocolate through the use of friction. In addition, the high heat allows volatile oils and other ingredients to evaporate. Desirable flavors are developed during conching, as it allows the flavor components to permeate the cocoa butter more fully (Afoakwa et al., 2007). The time needed for conching varies from several hours to days depending on the processing requirements, what type of equipment is used, and the formula of chocolates (Awua 2002; Chaveron et al., 1987).

As mentioned above, during conching, the physical and chemical properties of chocolate undergo great changes. The texture, rheological properties, and volatile compounds profiles of chocolate are developed during conching. Schnermann and Schieberle (1997) have studied the key odorants in milk chocolate and cocoa mass by aroma extract dilution analysis (AEDA). They found that 13 odorants had great contribution to the overall chocolate flavor. These odorants are 3-methylbutanal (malty); 2-ethyl-3,5-dimethylpyrazine (potato chip-like); 2- and 3-methylbutanoic acid (sweaty); 5-methyl-(E)-2-hepten-4-one (hazelnut-like); 1-octen-3-one (mushroom-like); 2-ethyl-3,6-dimethylpyrazine (nutty, earthy); 2,3-diethyl-5-methylpyrazine (potato chip-like); (Z)-2-nonenal (green, tallowy); (E,E)-2,4-decadienal (fatty, waxy); (E,E)-2,4-nonadienal (fatty); R-δ-decalactone (sweet, peach-like); and 2-methyl-3-(methyldithio)furan. Based on their study, Counet et al. (2002) carried out comparison between the odorants before

and after conching. The results indicated that although no new key odorant is synthesized during the conching process, levels of 2-phenyl-5-methyl-2-hexenal, Furaneol, and branched pyrazines are significantly increased while most Strecker aldehydes are lost by evaporation. Owusu et al. (2012) used dynamic headspace sampling/gas chromatography-mass spectrometry (GC-MS) to isolate and identify aroma volatiles in cocoa before and after conching at low and high temperatures. They reported that at high temperature (80°C), conching didn't significantly change the volatile compound profiles. They also found that no conching or short conching time results in higher concentrations of most aroma compounds. These aroma compounds include acetic acid, 2,5-dimethylpyrazine (popcorn) and 2-ethyl-5-methylpyrazine (roasted, coffee) and 2,3,5-trimethylpyrazine (fried potato), 2- and 3-methylbutanal, 5-methyl-2-phenyl-2-hexenal (sweet/cocoa/roasted), aldehydes, 1,2/3-butanediol and benzyl acetate.

Rheological properties of chocolate are developed by conching mainly because of particle size reduction, releasing of cocoa butter and the development microstructure of the ingredients source. Afoakwa et al. (2008b) did comprehensive studies on how particle size distribution influence the rheology properties (apparent viscosity and yield stress) plus textural parameters (firmness, index of viscosity and hardness) and melting properties (duration or time) of dark chocolate, indicating that those parameters are all highly positively correlated to the particle size of the chocolate. Findings from other researchers including Glicerina et al. (2013), Do et al. (2007), Sokmen. and Gunes (2006) and Ziegler et al. (2001) echoed the conclusions claimed by Afoakwa et al. (2008b).

Methods for particle size analysis

Particle size analysis is very important for the food industry, as particle size controls the taste and feel (chocolate), viscosity (chocolate, emulsions), dissolution rate (milk, coffee),

freeze-drying rate (coffee), creaming/flocculation (e.g. milk/cream), stability (cream liqueurs) of products. In addition, particle size characterizes emulsification (shear rate), indicator of (unwanted) processes (e.g. creaming), phase separation, crystallization (e.g.sugar), QC control parameters (Servais et al., 2002). The application areas for particle size analysis in the food industry include milk products (powders/liquid), chocolate, coffee (dry), sugar (dry, crystallization), emulsions (dairy cream liqueurs, ice cream, margarine, butter, mayonnaise etc.). There are additional methods available for sizing particles in many different fields. These methods include physical methods based on sieving, sedimentation, electrical properties, and impactors, imaging methods based on microscopy, photography and holography images, light scattering methods based on laser light.

The particle size for a spherical particle can be described using a single number, the diameter for every dimension is identical. For non-spherical particles, the particle size can be described by using multiple length and width measurements such as horizontal and vertical length. Although these descriptions provide better accuracy, complexity of the measurement also increase greatly. Thus, many techniques are based on the assumption that all the particles being measured are a perfect sphere for convenience. The reported value is typically an equivalent spherical diameter. This is essentially taking the physical measured value such as scattered light and determining the size of the sphere that could produce the data. Although this approach is not perfectly accurate, the shapes of particles generated by most industrial processes are unproblematic. There will be problems if the measured particles have a very large aspect ratio, such as fibers or needles. In addition, shape factor causes disagreements when particles are measured by different type of particle size analyzers. Different particle size analysis techniques are based on different physical principles. For example, sieving will tend to emphasize the

second smallest dimension because in order to pass through the mesh opening, the particles must orient themselves (Konert and Vandenberghe 1997). A sedimentometer measures the rate of fall of the particle through a viscous medium, and the surrounding particles plus the container walls tend to slow the dropping speed of the particles. Flaky or plate-like particles tend to orient to maximize drag while sedimenting, resulting the measurements of particle size in the smaller size than their real size (Allen 2013). A light scattering device will average the various dimensions as the particles flow randomly through the light beam, producing a distribution of sizes from the smallest to the largest dimensions (Eshel et al 2004). The only techniques that implement multiple values to describe the particle size are image analysis including microscopy. The parameters such as the longest and shortest diameters, perimeter, projected area, and equivalent spherical diameter are used by image analysis to describe the particle size of non-spherical. When reporting a particle size distribution, the most common format used for image analysis systems is equivalent spherical diameter on the x axis and percent on the y axis. It is only for elongated or fibrous particles that the x axis is typically displayed as length rather than equivalent spherical diameter.

Laser scattering based particle size analyses are currently most widely used in food industry because they provide comprehensive information about the particle size distribution of food materials. Because of the nature of the laser, it is particularly useful for determining particle size information based on properties of scattered light. Properties that make the laser a useful tool include nearly planar wave front, its monochromatic nature, coherence and spectral power (Black et al., 1996). Laser diffraction measures particle size distributions by measuring the angular variation in intensity of light scattered as a laser beam passes through a dispersed particulate sample. The principle of Laser diffraction is based on the Fraunhofer

diffraction theory, stating that the intensity of light scattered by a particle is directly proportional to the particle size (Mudroch et al., 1996). Large particles scatter light at small angles relative to the laser beam and small particles scatter light at large angles (McCave et al., 1986). The Fraunhofer approximation is accurate for large particles (~50 um), however, for measuring smaller particles, Mie theory needs to be applied. Mie theory calculates the particle size distribution, assuming a volume equivalent sphere model. And Mie theory requires knowledge of the optical properties (refractive index and imaginary component) of both the sample being measured, along with the refractive index of the dispersant. Usually the optical properties of the dispersant are relatively easy to find from published data, and many modern instruments will have in-built databases that include common dispersants.

There are many types of particle diameter used to specify the size of particles. This is because of the variety of situations encountered by those using particle-size measurement systems. For different processes, different parameters of the size distribution are important. In addition, the methods being used to conduct the particle size measurements decide which diameters being reported (Azzopardi 1979). Laser-based particle analyzers generally determine the distribution of the equivalent spherical particle sizes. Commonly used diameters for this method include arithmetic mean d_{l0}, Normal average particle diameter of the size distribution; surface mean d_{20}, Diameter of a sphere with the average surface area of the particles in the size distribution; volume mean d_{30}, Diameter of a sphere with the average volume of the particles in the size distribution; Sauter mean d_{32}, diameter of a sphere with the equivalent surface to volume ratio as all the particles in the size distribution; weight mean d_{34}, Diameter of a sphere having the average weight of all the particles in the size distribution. In addition, dxx is also used to describe the xx% of the particles are smaller than dxx, such as, d_{10}, d_{50} and d_{90}. Some of the

diameters obtained by other measurement methods are sieve diameter ds, the width of the minimum square aperture through which the particle will pass; Martin's diameter d_M, the mean chord length of the projected outline of the particle; Feret's diameter d_F, the mean value of the distance between pairs of parallel tangents to the projected outline of the particle; project area da, diameter of a circle having the same area as the projection of the particle; Stoke's diameter d_{st}, diameter of a sphere of similar density having the same freefall velocity as the particle (Irani and Callis 1963).

Particle size measurement is involved in many previous research projects and it is critical for characterizing the properties of food materials. The selection of particle size measurement method depends on the properties of the samples. Qian and McClements (2011), Huang et al. (2001), Kim and Morr (1996), Mirhosseini et al. (2008) used laser scattering particle size analyzer to measure the particle size distribution of nanoemulsions. Tan and Kerr (2015), Ahmed et al. (2000), Sato and Cunha (2009), Corredig et al. (2001) conducted studies that involve particle size measurements for vegetable/fruit puree and pulp. Sieves were also used by many researchers (Peyron et al., 2004; Olthoff et al., 1984) as the principal particle size measurement method for peanut, almond, pistachio cauliflower, radish, chili pepper, and carrot powders. Van der Bilt et al. (1993) introduced an optical scanning method for particle size measurement for food materials and compared the methods to sieving methods. In industry, other methods such as micrometer, Hegman gauge are used by small food manufacturers producing chocolate, candy, peanut butter and almond milk. Those methods are currently not standardized and the applications rely on individual experience.

Microstructure obtained by scanning electron microscopy (SEM)

The microstructure of chocolate has been well studied by previous researchers. A stereoscopic binocular microscope was used by Afoakwa et al. (2008c) to study the microstructure of dark chocolate. Confocal scanning laser microscopy (CSLM) methods have also been developed to identify fat and protein in milk chocolate and milk powders by Auty et al. (2001) and Svanberg et al. (2011). Hodge and Rousseau (2002) applied atomic force microscopy (AFM) and powder X-ray diffraction (XRD) to study the surface microstructure and polymorphic behavior of milk chocolate. James and Smith (2009) have compared the performance of X-ray photoelectron spectroscopy, cyro-scanning electron microscopy and environmental scanning electron microscopy in studying the surface of blooming chocolate. However, no study has investigated the microstructure of cocoa solid because of the difficulty in separating the cocoa solids alone from fat phase.

Unlike traditional light microscope, SEMs use an electron beam instead of a beam of light, which is directed towards the specimen under examination. SEM is a type of electron microscope that produces images of a sample by scanning the surface with a focused beam of electrons. The electrons interact with atoms from the surface of the sample, producing various signals that contain information about the sample's surface topography and composition (Stokes 2008). Prior to the examination, the specimens need to be dried or frozen below -80°C and then coated by a thin layer (5-20 nm) of gold that provides electric conductivity unless using back scatter. During examination, an electron gun located at the top of the device shoots out a beam of highly concentrated electrons. There are two main types of electron guns used by SEMs. The first is called a thermionic gun, which heats a filament until electrons stream away. The second electron gun is field emission gun, which rips electrons away from their atoms by generating a

strong electrical field (Kaláb et al., 1995). The microscope is composed of a series of lenses within a vacuum chamber and the vacuum environment prevents collision between electron and other molecules. Lenses direct the electrons towards the specimen in order to maximize efficiency. Greater magnification is achieved by more using more electrons. When a specimen is hit with a beam of the electrons known as the incident beam, it emits X-rays and three kinds of electrons: primary backscattered electrons, secondary electrons and Auger electrons. The SEM uses primary backscatter electrons and secondary electrons to construct images that include information about the surface topography and composition. An electron recorder picks up the rebounding electrons and records their imprint. This information is translated onto a screen which allows three-dimensional images to be represented clearly. For traditional SEMs, the images generated are not color images (Bozzola and Russell 1999; Reimer 2013).

The application of SEM is very common in studying the microstructure of food materials. Kalab and Harwalkar (1973) and Verheul and Roefs (1998) have studied the structure of a variety of food gels by SEM. They reported that heat-induced milk gels consisted of casein micelles linked together by short, thin fibers. Such fibers were not in acid-heat gels, which were composed of expanded protein particles closely attached to each other forming thick chains and networks. Renneted milk gels contained a high proportion of long fibers, and casein micelles were fused together. SEM has also been applied by Rosenberg et al. (1985) and Dalgleish et al. (2004) for the morphological study of various microcapsule systems. They reported that SEM is a useful tool for the selection of wall materials. The core materials distribution in microcapsules can be observed in SEM images, and the images elucidate the mechanisms of capsule formation and the effects of water-vapor uptake on microcapsule properties. Tatsumi et al. (1991), Roman-Gutierrez et al. (2002), Caldwell et al. (1992), and Zounis et al. (2002) have done comprehensive

research on the surface structure of carrot, wheat power, ice cream and wheat dough by SEM. They reported that the surface structure can be used as a tool to monitor the quality related properties such as rheology, and texture of food materials.

Cocoa roasting and flavor development

The cocoa roasting procedure usually happens after cocoa fermentation and before cracking and winnowing. Roasting is a heating method that uses different heat source (hot air, flame, and hot plate) to cook the food. The food is cooked evenly on all sides with temperatures of at least 150 °C (~300 °F) by radiation, conduction and convection (Martins et al., 2000). Roasting is a very critical step in chocolate processing. It is believed that roasting accomplishes many things. Firstly, roasting helps separate the outer husk from the inner bean and makes lateral steps such as cracking and winnowing much easier. Secondly, it also kills microorganisms in the cocoa beans. This is important as the conditions in which cocoa beans are fermented are naturally full of bacteria, fungi and molds. There is a "quantifiable" risk of infection from unroasted cocoa beans. By roasting, the fermentation is terminated and deterioration is prevented. Various chemical reactions also occur when cocoa beans are roasted and proper roasting is integral to the production of chocolate with good flavor. The vinegar smell (acetic acid) from fermentation is driven off by the high heat introduced by roasting (Jinap et al., 1998; Ramli et al., 2006).

Maillard reactions play a major role in the formation of the flavors of cocoa beans during roasting (Ziegleder 1991). The Maillard reactions involve the reaction between free amino acids and reducing sugars, which develop during fermentation ((Ziegleder and Biehl 1988). Keeney (1972) reported that the roasting process not only generates new volatile compounds for specific flavor through pyrolysis of sugars, but also loss of minor compounds such as acids and

polyphenol that influence the final flavor of chocolate products. It was reported that roasting produces approximately 400–500 chemical compounds (Dimick 1983) including pyrazines, aldehydes, ethers, thiazoles, phenols, ketones, alcohols, furans and esters (Paul and Jeanne 1981). Aldehydes and pyrazines are the major compound groups formed during roasting, and the chemical reactions involved in their formation are Maillard reaction and Strecker degradation of amino acids and sugars during roasting (Heinzler and Eichner 1992). Strecker degradation is a chemical reaction, which converts an α-amino acid into an aldehyde containing the side chain by way of an imine intermediate (Schonberg and Moubacher 1952).

A study conducted by Jinap et al. (1998) indicated that over different compounds can be identified in roasted cocoa beans by using simultaneous distillation extraction based GC-MS. In total, 14 pyrazines, 20 esters, 3 carbonyls, 3 phenols, 3 alcohols, 2 hydrocarbons, 2 ketones, 2 acids, 2 monoterpenes hydrocarbons, 1 benzenoid hydrocarbons, and 1 furan were identified, it was reported that the number of pyrazines present in nib increase with longer roasting time. In contrast, the amount of esters present in the nibs seems to be more affected by roasting temperature rather than roasting time, while alcohols and phenols were decreased by both increasing roasting temperature and time. Ramli et al. (2006), however, identified 28 major compounds by gas chromatography using a mass selective detector. The identified compounds include nine pyrazines (2,5-dimethyl-, 2,3-dimethyl-, 2-ethyl-6-methyl-, trimethyl-, 3-ethyl-2, 5-dimethyl-, tetramethyl-, 2-ethenyl-6-methyl- and 3,5-dimethyl-2- methylpyrazine); five aldehydes (5-methyl-2-phenyl-2-hexenal, benzaldehyde, benzalacetaldehyde and a-ethyliden-benzenacetaldehyde); one methyl ketone (2-nonanone); two alcohols (linalool and 2-heptanol); and two esters (4-ethylphenyl acetate and 2-phenylethyl acetate). Serveral of the compounds, specifically, benzaldehyde, 2-nonanone, linalool and 2-phenylethyl acetate, aldehydes, ketones,

alcohols, esters trimethyl- and tetramethylpyrazine can be used as indicators of the roasting process. Hashim and Chaveron (1994) also reported that methylpyrazine can be used as good indicator of the roasting process. They concluded that the amount of monomethyl-; 2,3-dimethyl-; 2,5-dimethyl-; 2,6-dimethyl-; trimethyl- and the tetramethylpyrazine in unroasted beans were significantly different from the ones in roasted beans.

In addition to mapping volatile compounds by GC-MS systems and classifying the roasting degree based on that, other methods have been implemented in classifying the roasting degree of cocoa beans. Stark et al. (2005), Stark and Hofmann (2005) and Jinap et al. (2004) conducted sensory evaluation tests on cocoa beans with different roasting degree. They correlated compounds such as quercetin, naringenin, luteolin, apigenin, catechin theobromine and caffeine, to certain sensory perception such as astringent mouthfeel. Although training sensory panels has been widely accepted for detecting the roasting degree of cocoa, they are inconsistant, as human smell assessment is affected by many factors. Bias within panels is inevitable and the panelists may be affected by poor physical and mental health as well as fatigue. In addition, sensory tests may take hours for testing and it may take months to train the panel (Pearce et al., 2006). Krysiak (2006) correlated the color of cocoa nibs to the roasting condition of cocoa beans. He concluded that roasting of cocoa beans at 110 °C resulted in the least advanced brown pigments and more pronounced changes in pigment content was achieved during roasting at 135 and 150 °C.

Electronic nose (E-nose)

An e-nose system is a combination of gas sensors that give a fingerprint response to a given odor and pattern recognition software that performs odor identification, classification and discrimination. The e-nose is a cost-effective, unbiased, and fast-measuring solution to the

problems associated with sensory panels and with chromatographic and mass-spectrometric techniques. The portable form of e-nose can accommodate real time performance in the field and it may be operated remotely (Arshak et al., 2004).

The e-nose attempts to simulate mammalian olfactory responses to aromas by using gas sensors. The e-nose usually has a sealed chamber where gas sensors are distributed in the space created by the chamber. The odor molecules are drawn into the e-nose chamber by pumping, headspace sampling, diffusion methods, bubblers or pre-concentrators, where they interact with the gas sensors (Pearce et a., 2006). The reaction between gas sensors and the odor molecules induces a reversible physical and/or chemical change in the sensing material, which causes an associated change in electrical properties, such as conductivity. And the measurement of conductivity of the sensors are typically obtained by measuring the output voltages of the gas sensors since they are linearly correlated. (Harsányi 2000). Each gas sensor behaves just like a receptor by responding differently in sensitivity to different odors. The responses of the gas sensor are transduced into electrical signals (voltage, current, capacitance, etc.) and collected by data acquisition system. Finally, the overall response patterns of the gas sensors are processed by designed recognition models for discrimination, classification, and identification (Shurmer, and Gardner 1992; Gardner et al., 1992; Röck et al., 2008).

The response of a gas sensor when exposed to target gases is considered to be a first order time response. In this first stage of measurement conducted by gas sensors, reference gas, usually fresh air, is introduced and reacts with gas sensors to obtain baselines. Then sensors are exposed to the target gases, which causes changes in its output signal until the sensor reaches steady-state. The odorant is finally flushed out of the sensor by using the reference gas and the responses of gas sensors return back to baseline. Several important parameters are used to

describe the sensor response as a function of time. The parameters include response time, the time during which the sensor is exposed to the odorant; relaxation time or recovery time, the time it takes the sensor to return to its baseline; peak value, the maximum response that the sensor exhibited during exposure to the target gases.

Pearce et al. (2006) suggested three data processing methods to remove any noise or drift by sensor response manipulation with respect to the baseline. The first one is Differential: the baseline $x_s(0)$ is subtracted from the sensor response $x_s(t)$ to remove any noise or drift δ_A present. The baseline manipulated response $y_s(t)$ is determined by:

$$y_s(t)=(x(t)+\delta_A)-(x_s(0)+\delta_A)$$

$$y_s(t)=x(t)-x_s(0)$$

Relative: the sensor response is divided by the baseline. By doing this, multiplicative drift δ_M is eliminated and a dimensionless response $y_s(t)$ is obtained.

$$y_s(t)=\frac{x(t)(1+\delta_A)}{x(0)(1+\delta_A)}=\frac{x(t)}{x(0)}$$

Fractional: combine differential and relative methods, the baseline is subtracted from the response $x_s(t)$ and then divided by the baseline $x_s(0)$ from the sensor response which provides a dimensionless, normalized response $y_s(t)$ that can compensate for inherently large or small signals.

$$y_s(t)=\frac{x(t)-x(0)}{x(0)}$$

The selection of baseline depends on the type of gas sensor and also the preference of researchers. However, the selection of certain manipulation techniques mainly depends on sensor type (Arshak et al., 2004). As mentioned before, different gas sensors have different sensitivities to different target gas. The sensitivity is defined as the change in output of a sensor (e.g. voltage)

for a change in the input (target gas concentration) (Fraden and Rubin 1994; Johnson 1993; Boll and Overshott 2008). In the case of e-nose sensors, the sensitivity of the sensor (S) to the odorant is the change in the sensor output parameter (y) results from change of the concentration of the odorant (x):

$$S=\frac{\Delta y}{\Delta x}$$

Some other researchers use different values to measure the sensitivity, usually calculated from baseline-manipulated data.

The commonly used gas sensors are conductivity sensor, piezoelectric sensor, optical sensor, and MOSFET sensors. In the food industry, conductivity sensor is widely used and it have been proved to be a good tool for food quality examination. Conducting polymer composites, intrinsically conducting polymers (ICP) and metal oxides semiconductor (MOS) are three of the most commonly utilized classes of sensing materials in conductivity sensors. The basic working principle for these three type of conductivity sensors is the same: a change in some property of the material resulting from interaction with a gas/odor leads to a change in resistance in the sensor. However, the mechanisms that lead to these resistance changes are different for the three conductivity sensors.

Conducting polymer composites consist of conducting particles such as polypyrrole and carbon black interspersed in an insulating polymer matrix (Albert et al., 2000). When the conducting polymer composites are exposed to target gas, the change of resistance is led by percolation effects or more complex mechanisms in the case of polypyrrole filled composites. The vapor permeates into the polymer and causes the polymer film to expand. The vapor-induced expansion of the polymer composite causes an increase in the electrical resistance of the

polymer composite because the polymer expansion reduces the number of conducting pathways for charge carriers (Munoz et al., 1999). ICP have linear backbones composed of unsaturated monomers, such as, alternating double and single bonds along the backbone, that can be doped as semiconductors or conductors (Heeger 2001). The principle of operation for ICP e-nose sensors is that the odorant is absorbed into the polymer and alters the conductivity of the polymer. Intrachain conductivity, intermolecular conductivity, and ionic conductivity are affected in intrinsically conducting polymers. Intrachain conductivity is changed because the conductivity along the backbone is altered. The changes of intermolecular conductivity is due to electrons hopping to different chains. Ionic conductivity is affected by proton tunneling induced by hydrogen bond interaction at the backbone and also by ion migration through the polymer (Albert et al., 2000; Charlesworth et al., 1993; Dickinson et al., 1998).

MOS type gas sensors are widely used because they have high precision, low cost, and good repeatability. Many metal oxides are suitable for detecting combustible, reducing, or oxidizing gases by conductive measurements. The following oxides show a gas response in their conductivity: Cr2O3, Mn2O3, Co3O4, NiO, CuO, SrO, In2O3, WO3, TiO2, V2O3, Fe2O3, GeO2, Nb2O5, MoO3, Ta2O5, La2O3, CeO2, Nd2O3 (Kanazawa et al., 2001). There are two types of metal oxide sensors. The first one is n-type which is made from zinc oxide, tin dioxide, titanium dioxide or iron (III) oxide. The n-type sensor responds to reducing gases such as H2, CH4, CO, C2H5 or H2S. However, the p-type which is made from nickel oxide, cobalt oxide, which respond to oxidizing gases like O2, NO2, and Cl2 (Pearce et al., 2006). The sensing mechanism of a MOS type gas sensor is mainly due to the trapping of electrons at adsorbed molecules and band bending induced by these charged molecules. This phenomenon is responsible for the change in conductivity. The negative charge trapped in these oxygen species

causes an upward band bending and thus a reduced conductivity compared to the flat band situation. The reactions occurring at the surface of the MOS sensor is described as:

$$\frac{1}{2}O_2+e^- \rightarrow O^-(s)$$

$$R(g)+O^-(s) \rightarrow RO(g)+e$$

where R(g) is the reducing gas and g and s are the surface and gas, respectively, e represent electron from the oxide (Pearce et al., 2006; Albert et al., 2000).

The application of e-nose in food industry is very broad. Foods are characterized by the presence of a large number of different chemical species, many of them are responsible of the qualitative differences existing in terms of taste and aroma and in terms of edibility as well. In the past, electronic noses have been developed for the classification and recognition of a large variety of foods. Gardner et al. (1992) used twelve tin oxide sensors to sense the headspace of coffee packs and achieved success rate of 95.5% in discriminating and classifying 90 samples. Pardo et al. (2000) classified 12 types of coffees by principal component analysis (PCA) based e-nose and achieved 87.5% classification performance. Di Natale et al. (1996) and García et al. (2006) reported that e-nose can discriminate between for different types of wine and the same wine from different locations. They use (PCA) and probabilistic neuronal network (PNN) as discrimination tools. The quality of meat and meat products can be also determined by e-nose technology. Many researchers (Winquist et al., 1993; Rajamäki et al., 2006; El Barbri et al., 2008) reported accurate rates of identification, discrimination and classification achieved by an e-nose based system. Quality related properties of cheese (Drake et al., 2003; Benedetti et al., 2005), vegetable oil (Hai and Wang 2006), vinegar (Zhang et al., 2006), and fruit (Brezmes et al., 2000) have all been studied using e-nose technologies and the accuracy of these e-nose systems tends to be excel 90%.

Artificial neural network (ANN)

A neural network is a computing system made up of a number of simple, highly interconnected processing elements, which process information by their dynamic state response to external inputs (Caudill 1987). ANN is computational model used in machine learning, computer science and other research disciplines, mimicking the neuronal structure of the mammalian cerebral cortex but on much smaller scale. The learning and training process of ANN is similar to human cognitive process. Like the human cerebral cortex, a ANN consist of layers of artificial neurons, or simply “neurons” or “nodes”. The number of neurons and layers, theoretically, can be infinite. However, the time needed for running ANNs with huge number of neurons and layers is too long and large systems are not typically necessary to solve most problems. In a most basic mathematical model of the ANN, the effects of the synapses are represented by connection weights that modulate the effect of the associated input signals, and the nonlinear characteristic exhibited by neurons is represented by a transfer function. The neuron impulse is then computed as the weighted sum of the input signals, transformed by the transfer function. The learning capability of an artificial neuron is achieved by adjusting the weights in accordance to the chosen learning algorithm (Abraham 2005).

In a most simplified process of ANN, from the first layer (input layers) of neuron (inputs) x1, ..., xn is considered to be unidirectional, which are indicated by forward or backward detection. The output Oi of the first layer is the sum of each input that connected to the output node multiplied by the weight of the connection.

$$O_i = f\left(\sum_{j=1}^{n} \omega_j x_j\right)$$

where ω_j j is the weight vector, and the function f is referred to as an activation (transfer) function such as tansig, logsig, and purelin.

$$\text{tansig}(x)=\frac{2}{1+e^{-2x}}-1$$

$$\text{logsig}(x)=\frac{1}{1+e^{-x}}$$

$$\text{purelin}(x)=x$$

O_i must be greater than a threshold before it can be transferred to the next layer. Once threshold value is reached, O_i become the input for the next layer and this process keeps going until the values of the nodes in the last layer (output layer) are calculated. This process is called feed-forward networks, and it consists of three types of neuron layers: input, hidden, and output layers. The signal flow is from input to output units, strictly in a feed-forward direction. Contrary to feed-forward networks, there is feedback ANN where is signals can flow backward before being transferred to the last layers. In addition to that, there are several other neural network architectures such as adaptive resonance theory maps, and competitive networks (Bishop 1995).

Learning or training of a ANN is based on the modification of the weights on synaptic connections between neurons. The basic idea is that if two neurons are active simultaneously, their interconnection must be strengthened. The perceptron is a single layer neural network whose weights and biases could be trained to produce a correct target vector when presented with the corresponding input vector. The principles underlying this statement have become known as Hebbian Learning. Backpropagation (BP) is one basic training method and one BP process stated as follows: first, start with random weights for the connections. Second, select an input vector x from the set of training samples. If output is not equal to desirable output, which is $y_k \neq d(k)$, modify all connections weight wi according to: $\delta w_i = \eta(d_k - y_k)x_i$; ($\eta$ = learning rate). Go back to second step until termination criteria is reached. There are many other training

methods such as Levenberg-Marquardt, scaled conjugate gradient, Fletcher-Powell conjugate gradient, and resilient backpropagation. The selection of training algorithm depends on the problem need to be solved and preference of the researchers. In addition, the performance of the ANN is heavily depending on factors such as the number of node, layer, transition function, and parameter setting for each training method (Yegnanarayana 2009; Dayhoff and DeLeo 2001; Fyfe 2005). The application of ANN is very broad. ANN has been used to solve classification, optimization, feature detection, data compression, approximation, prediction, control, association and pattern completion.

ANN was introduced to study food materials many years ago. Doganis et al. (2006) applied ANN to forecast the sale of milk products. García-Gimeno et al. (2002), Argyri et a., (2010) and Geeraerd et al. (1998) used ANN as the tool to predict bacteria growth in chilled food products and beef fillet. Research conducted by Goni et al. (2008) reported that ANN can predict freezing and thawing times of foods. The neural network had an average absolute relative error of less than 10%. Some researchers have combined ANN and electronic nose to study the quality of food materials such as olive oil (Cosio et al., 2006), beef (Panigrahi et al., 2006) and honey (Benedetti et al., 2004). Overall, electronic nose based ANN have achieved high accuracy (>90%) in these studies.

References

Abraham, A., 2005. Artificial neural networks. Handbook of measuring system design.

Afoakwa, E. O., Paterson, A. and Fowler, M., 2007. Factors influencing rheological and textural qualities in chocolate-a review. Trends Food Sci. Technol., *18*(6), pp.290-298.

Afoakwa, E. O., Paterson, A., Fowler, M. and Vieira, J., 2008a. Characterization of melting properties in dark chocolates from varying particle size distribution and composition using differential scanning calorimetry. Food Res. Int., *41*(7), pp.751-757.

Afoakwa, E. O., Paterson, A., Fowler, M. and Vieira, J., 2008b. Relationship between rheological,textural and melting properties of dark chocolate as influenced by particle size distribution and composition. Eur. Food Res. Technol., *227*(4), pp.1215-1223.

Afoakwa, E. O., Paterson, A., Fowler, M. and Vieira, J., 2008c. Effects of tempering and fat crystallisation behaviour on microstructure, mechanical properties and appearance in dark chocolate systems. J. Food Eng., *89*(2), pp.128-136.

Aguilera, J. M., 1995. Gelation of whey proteins: Chemical and rheological changes during phase transition in food. Food Technol., *49*(10), pp.83-89.

Ahmed, J., Shivhare, U. S. and Raghavan, G. S. V., 2000. Rheological characteristics and kinetics of colour degradation of green chilli puree. J. Food Eng., *44*(4), pp.239-244.

Alamprese, C., Datei, L. and Semeraro, Q., 2007. Optimization of processing parameters of a ball mill refiner for chocolate. J. Food Eng., *83*(4), pp.629-636.

Albert, K. J., Lewis, N. S., Schauer, C. L., Sotzing, G. A., Stitzel, S. E., Vaid, T. P. and Walt, D. R., 2000. Cross-reactive chemical sensor arrays. Chem. Rev., *100*(7), pp.2595-2626.

Allen, T., 2013. Particle size measurement. Springer.

Ali, S., Lin, H.N., Bittman, R. and Huang, C. H., 1989. Binary mixtures of saturated and unsaturated mixed-chain phosphatidylcholines. A differential scanning calorimetry study. Biochemistry, *28*(2), pp.522-528.

Argyri, A. A., Panagou, E. Z., Tarantilis, P. A., Polysiou, M. and Nychas, G. J., 2010. Rapid qualitative and quantitative detection of beef fillets spoilage based on Fourier transform infrared spectroscopy data and artificial neural networks. Sens. Actuators, B, *145*(1), pp.146-154.

Arshak, K., Moore, E., Lyons, G. M., Harris, J. and Clifford, S., 2004. A review of gas sensors employed in electronic nose applications. Sens. Rev., *24*(2), pp.181-198.

Atkins, P. and Jones, L., 2007. Chemical principles: The quest for insight. Macmillan.

Auty, M. A., Twomey, M., Guinee, T. P. and Mulvihill, D. M., 2001. Development and application of confocal scanning laser microscopy methods for studying the distribution of fat and protein in selected dairy products. J. Dairy Res., *68*(03), pp.417-427.

Awua, P. K., 2002. Cocoa Processing and Chocolate Manufacture in Ghana: The success story that demolished a myth. Saffron Walden, UK: David Jamieson and Associates.

Azzopardi, B. J., 1979. Measurement of drop sizes. Int. J. Heat Mass Transfer, *22*(9), pp.1245-1279.

Babin, H., 2005. Colloidal properties of sugar particle dispersions in food oils with relevance to chocolate processing (Doctoral dissertation, University of Leeds).

Beckett, S., 2000. The science of chocolate (Vol. 22). R. Soc. Chem..

Beckett, S. T. ed., 2011. Industrial chocolate manufacture and use. John Wiley & Sons.

Benedetti, S., Sinelli, N., Buratti, S. and Riva, M., 2005. Shelf life of Crescenza cheese as measured by electronic nose. J. Dairy Sci., *88*(9), pp.3044-3051.

Benedetti, S., Mannino, S., Sabatini, A. and Marcazzan, G., 2004. Electronic nose and neural network use for the classification of honey. Apidologie, *35*(4), pp.397-402.

Bhandari, B. R. and Howes, T., 1999. Implication of glass transition for the drying and stability of dried foods. J. Food Eng., *40*(1), pp.71-79.

Biliaderis, C. G., Maurice, T. J. and Vose, J. R., 1980. Starch gelatinization phenomena studied by differential scanning calorimetry. J. Food Sci., *45*(6), pp.1669-1674.

Bishop, C.M., 1995. Neural networks for pattern recognition. Oxford University Press.

Black, D. L., McQuay, M. Q. and Bonin, M. P., 1996. Laser-based techniques for particle-size measurement: a review of sizing methods and their industrial applications. Prog. Energy Combust. Sci., *22*(3), pp.267-306.

Brandts, J. F., 1964. The thermodynamics of protein denaturation. I. The denaturation of chymotrypsinogen. J. Am. Chem. Soc., *86*(20), pp.4291-4301.

Brezmes, J., Llobet, E., Vilanova, X., Saiz, G. and Correig, X., 2000. Fruit ripeness monitoring using an electronic nose. Sens. Actuators, BSens. Actuators, B, *69*(3), pp.223-229.

Brunello, N., McGauley, S. E. and Marangoni, A., 2003. Mechanical properties of cocoa butter in relation to its crystallization behavior and microstructure. LWT--Food Sci. Technol., *36*(5), pp.525-532.

Boll, R. and Overshott, K. J., 2008. Sensors, Magnetic Sensors (Vol. 5). John Wiley & Sons.

Bozzola, J. J. and Russell, L. D., 1999. Electron microscopy: principles and techniques for biologists. Jones & Bartlett Learning.

Cakebread, S., 1975. Sugar and chocolate confectionery. Oxford University Press.

Caldwell, K. B., Goff, H. D. and Stanley, D. W., 1992. A low-temperature scanning electron microscopy study of ice cream. I Techniques and General Microstructure. Food Structure, *11*(1), p.1.

Caudill, M., 1987. Neural networks primer, part I. AI expert, *2*(12), pp.46-52.

Champion, D., Le Meste, M. and Simatos, D., 2000. Towards an improved understanding of glass transition and relaxations in foods: molecular mobility in the glass transition range. Trends Food Sci. Technol., *11*(2), pp.41-55.

Chalikian, T. V., Völker, J., Plum, G. E. and Breslauer, K. J., 1999. A more unified picture for the thermodynamics of nucleic acid duplex melting: a characterization by calorimetric and volumetric techniques. Proceedings of the National Academy of Sciences, *96*(14), pp.7853-7858.

Charlesworth, J. M., Partridge, A. C. and Garrard, N., 1993. Mechanistic studies on the interactions between poly (pyrrole) and organic vapors. J. Phys. Chem., *97*(20), pp.5418-5423.

Chaveron, H., Pontillon, J., Billon, M., Adenier, H. and Kamoun, A., Clextral, 1987. Process for preparing a chocolate paste. U.S. Patent 4,713,256.

Cocero, A. M. and Kokini, J. L., 1991. The study of the glass transition of glutenin using small amplitude oscillatory rheological measurements and differential scanning calorimetry. J. Rheol., *35*(2), pp.257-270.

Corredig, M., Kerr, W. and Wicker, L., 2001. Particle size distribution of orange juice cloud after addition of sensitized pectin. Food Chem.J. Agric. Food Chem., *49*(5), pp.2523-2526.

Cooper, A. and Johnson, C. M., 1994. Differential scanning calorimetry. Microscopy, optical spectroscopy, and macroscopic techniques, pp.125-136.

Cosio, M. S., Ballabio, D., Benedetti, S. and Gigliotti, C., 2006. Geographical origin and authentication of extra virgin olive oils by an electronic nose in combination with artificial neural networks. Analytica Chimica Acta, *567*(2), pp.202-210.

Counet, C., Callemien, D., Ouwerx, C. and Collin, S., 2002. Use of gas chromatography-olfactometry to identify key odorant compounds in dark chocolate. Comparison of samples before and after conching. J. Agric. Food Chem.., *50*(8), pp.2385-2391.

Dalgleish, D. G., Spagnuolo, P. A. and Goff, H. D., 2004. A possible structure of the casein micelle based on high-resolution field-emission scanning electron microscopy. Int. Dairy J., *14*(12), pp.1025-1031.

Dayhoff, J. E. and DeLeo, J. M., 2001. Artificial neural networks. Cancer, *91*(S8), pp.1615-1635.

Debye, P., 1921. Molecular forces and their electrical interpretation. Phys. Z., *22*, pp.302-308.

Debenedetti, P. G. and Stillinger, F. H., 2001. Supercooled liquids and the glasstransition. Nature, *410*(6825), pp.259-267.

Di Natale, C., Davide, F. A., D'Amico, A., Nelli, P., Groppelli, S. and Sberveglieri, G., 1996. An electronic nose for the recognition of the vineyard of a red wine. Sens. Actuators, B, *33*(1-3), pp.83-88.

Dickinson, T. A., White, J., Kauer, J. S. and Walt, D. R., 1998. Current trends inartificial-nose'technology. Trends Biotechnol., *16*(6), pp.250-258.

Dicolla, C. B., 2008. Characterization of Heat Resistant Milk Chocolates.

Dimick, P. S., 1983. Development of flavour in chocolate. Proceedings Towards Better Acceptance of Malaysian Cocoa, pp.15-21.

Do, T. A., Hargreaves, J. M., Wolf, B., Hort, J. and Mitchell, J. R., 2007. Impact of particle size distribution on rheological and textural properties of chocolate models with reduced fat content. J. Food Sci., *72*(9), pp.E541-E552.

Dhonsi, D. and Stapley, A. G. F., 2006. The effect of shear rate, temperature, sugar and emulsifier on the tempering of cocoa butter. J. Food Eng., *77*(4), pp.936-942.

Doganis, P., Alexandridis, A., Patrinos, P. and Sarimveis, H., 2006. Time series sales forecasting for short shelf-life food products based on artificial neural networks and evolutionary computing. J. Food Eng., *75*(2), pp.196-204.

Donovan, J. W., 1979. Phase transitions of the starch-water system. Biopolymers, *18*(2), pp.263-275.

Drake, M. A., Gerard, P. D., Kleinhenz, J. P. and Harper, W. J., 2003. Application of an electronic nose to correlate with descriptive sensory analysis of aged Cheddar cheese. LWT--Food Sci. Technol., *36*(1), pp.13-20.

Eberstein, K., Höpcke, R., Konieczny-Janda, G. and Stute, R., 1980. DSC-Untersuchungen an Stärke Teil I. Möglichkeiten thermoanalytischer Methoden zur Stärkecharakterisierung. Starch-Stärke, *32*(12), pp.397-404.

Ediger, M. D., Angell, C. A. and Nagel, S. R., 1996. Supercooled liquids and glasses. J. Phys. Chem., *100*(31), pp.13200-13212.

Eiben, A. E., Raue, P. E. and Ruttkay, Z., 1994, October. Genetic algorithms with multi-parent recombination. In International Conference on Parallel Problem Solving from Nature (pp. 78-87). Springer Berlin Heidelberg.

El Barbri, N., Llobet, E., El Bari, N., Correig, X. and Bouchikhi, B., 2008. Electronic nose based on metal oxide semiconductor sensors as an alternative technique for the spoilage classification of red meat. Sensors, *8*(1), pp.142-156.

Eliasson, A. C., 1980. Effect of water content on the gelatinization of wheat starch. Starch Stärke, *32*(8), pp.270-272.

Eshel, G., Levy, G. J., Mingelgrin, U. and Singer, M. J., 2004. Critical evaluation of the use of laser diffraction for particle-size distribution analysis. Soil Sci. Soc. Am. J., *68*(3), pp.736-743.

Fyfe, C., 2005. Artificial neural networks. In Do Smart Adaptive Systems Exist? (pp. 57-79). Springer Berlin Heidelberg.

Feng, H., Tang, J. and Cavalieri, R. P., 2002. Dielectric properties of dehydrated apples as affected by moisture and temperature. Trans. ASAE, *45*(1), pp.129-136.

Fessas, D., Signorelli, M. and Schiraldi, A., 2005. Polymorphous transitions in cocoa butter: a quantitative DSC study. J. Therm. Anal. Calorim., *82*(3), pp.691-702.

Foubert, I., Vanrolleghem, P. A. and Dewettinck, K., 2003. A differential scanning calorimetry method to determine the isothermal crystallization kinetics of cocoa butter. Thermochim. Acta, *400*(1), pp.131-142.

Fraden, J. and Rubin, L. G., 1994. AIP Handbook of Modern Sensors. Physics Today, *47*, p.74.

Freire, E., 1994. Statistical thermodynamic analysis of differential scanning calorimetry data: Structural deconvolution of heat capacity function of proteins. Methods Enzymol., *240*, pp.502-530.

Freire, E., 1995. Differential scanning calorimetry. Protein Stability and Folding: Theory and Practice, pp.191-218.

García, M., Aleixandre, M., Gutiérrez, J. and Horrillo, M. C., 2006. Electronic nose for wine discrimination. Sens. Actuators, B, *113*(2), pp.911-916.

García-Gimeno, R. M., Hervás-Martınez, C. and de Silóniz, M. I., 2002. Improving artificial neural networks with a pruning methodology and genetic algorithms for their application in microbial growth prediction in food. Int. J. Food Microbiol., *72*(1), pp.19-30.

Gardner, J. W. and Bartlett, P. N. eds., 1992. Sensors and sensory systems for an electronic nose (Vol. 212, p. 303). Kluwer Academic.

Gardner, J. W., Shurmer, H. V. and Tan, T. T., 1992. Application of an electronic nose to the discrimination of coffees. Sens. Actuators, B, *6*(1-3), pp.71-75.

Geeraerd, A. H., Herremans, C. H., Cenens, C. and Van Impe, J. F., 1998. Application of artificial neural networks as a non-linear modular modeling technique to describe bacterial growth in chilled food products. Int. J. Food Microbiol., *44*(1), pp.49-68.

Glicerina, V., Balestra, F., Dalla Rosa, M. and Romani, S., 2013. Rheological, textural and calorimetric modifications of dark chocolate during process. J. Food Eng., *119*(1), pp.173-179.

Gong, M. and Yang, Y. H., 2001. Multi-resolution stereo matching using genetic algorithm. In Stereo and Multi-Baseline Vision, 2001. (SMBV 2001). Proceedings. IEEE Workshop on (pp. 21-29). IEEE.

Goni, S. M., Oddone, S., Segura, J. A., Mascheroni, R. H. and Salvadori, V. O., 2008. Prediction of foods freezing and thawing times: Artificial neural networks and genetic algorithm approach. J. Food Eng., *84*(1), pp.164-178.

Grivetti, L. E. and Shapiro, H. Y., 2011. Chocolate: history, culture, and heritage. John Wiley & Sons.

Hai, Z. and Wang, J., 2006. Electronic nose and data analysis for detection of maize oil adulteration in sesame oil. Sens. Actuators, B, *119*(2), pp.449-455.

Hancock, B. C. and Zografi, G., 1997. Characteristics and significance of the amorphous state in pharmaceutical systems. J. Pharm. Sci., *86*(1), pp.1-12.

Harsányi, G., 2000. Polymer films in sensor applications: a review of present uses and future possibilities. Sens. Rev., *20*(2), pp.98-105.

Hashim, L. and Chaveron, H., 1994. Extraction and determination of methylpyrazines in cocoa beans using coupled steam distillation-microdistillator. Food Res. Int., *27*(6), pp.537-544.

Hartel, R. W. and Hartel, A., 2014. Candy Bites: The Science of Sweets. Springer Science & Business Media.

Heeger, A. J., 2001. Semiconducting and metallic polymers: the fourth generation of polymeric materials (Nobel lecture). Angew. Chem., Int. Ed., *40*(14), pp.2591-2611.

Heinzler, M. and Eichner, K., 1992. The role of amodori compounds during cocoa processing–formation of aroma compounds under roasting conditions. Z. Lebensm.-Unters.-Forsch, 21, pp.445-450.

Hendry Jr John, L., Pederson Richard R, 1952. Process of Comminuting Food Products. U.S. Patent 2,583,697.

Hodge, S. M. and Rousseau, D., 2002. Fat bloom formation and characterization in milk chocolate observed by atomic force microscopy. J. Am. Oil Chem. Soc., *79*(11), pp.1115-1121.

Houldin, J. E., 1967. Fundamentals of Electronics. Phys. Bull., *18*(10), p.354.

Höhne, G. W. H., Hemminger, W. and Flammersheim, H. J., 1996. Theoretical Fundamentals of Differential Scanning Calorimeters. In Differential Scanning Calorimetry (pp. 21-40). Springer Berlin Heidelberg.

Huang, X., Kakuda, Y. and Cui, W., 2001. Hydrocolloids in emulsions: particle size distribution and interfacial activity. Food Hydrocolloids, *15*(4), pp.533-542.

Huang, C. H. and Li, S., 1999. Calorimetric and molecular mechanics studies of the thermotropic phase behavior of membrane phospholipids. Biochimica et Biophysica Acta (BBA)-Reviews on Biomembranes, *1422*(3), pp.273-307.

Irani, R. R. and Callis, C. F., 1963. Particle size: measurement, interpretation, and application (Vol. 3). New York: Wiley.

James, B. J. and Smith, B. G., 2009. Surface structure and composition of fresh and bloomed chocolate analysed using X-ray photoelectron spectroscopy, cryo-scanning electron microscopy and environmental scanning electron microscopy. LWT--Food Sci. Technol., *42*(5), pp.929-937.

Jensen, L. H. and Mabis, A. J., 1966. Refinement of the structure of β-tricaprin. Acta Crystallogr., *21*(5), pp.770-781.

Jinap, S., Rosli, W. W., Russly, A. R. and Nordin, L. M., 1998. Effect of roasting time and temperature on volatile component profiles during nib roasting of cocoa beans (Theobroma cacao). J. Sci. Food Agric., *77*(4), pp.441-448.

Jinap, S., Jamilah, B. and Nazamid, S., 2004. Sensory properties of cocoa liquor as affected by polyphenol concentration and duration of roasting. Food Quality and Preference, *15*(5), pp.403-409.

Jolly, M. S., Blackburn, S. and Beckett, S. T., 2003. Energy reduction during chocolate conching using a reciprocating multihole extruder. J. Food Eng., *59*(2), pp.137-142.

Johnson, C. D., 1993. Process Control Instrumentation Technology. Prentice Hall PTR.

Kalab, M. and Harwalkar, V.R., 1973. Milk gel structure. I. Application of scanning electron microscopy to milk and other food gels. J. Dairy Sci., *56*(7), pp.835-842.

Kaláb, M., Allan-Wojtas, P. and Miller, S. S., 1995. Microscopy and other imaging techniques in food structure analysis. Trends Food Sci. Technol., *6*(6), pp.177-186.

Kanazawa, E., Sakai, G., Shimanoe, K., Kanmura, Y., Teraoka, Y., Miura, N. and Yamazoe, N., 2001. Metal oxide semiconductor N_2O sensor for medical use. Sens. Actuators, B, *77*(1), pp.72-77.

Keeney, P. G., 1972. Various interactions in chocolate flavor. Journal of the American Oil Chemists Society, *49*(10), pp.567-572.

Konert, M. and Vandenberghe, J. E. F., 1997. Comparison of laser grain size analysis with pipette and sieve analysis: a solution for the underestimation of the clay fraction. Sedimentology, *44*(3), pp.523-535.

Kremer, F., 2002. Dielectric spectroscopy–yesterday, today and tomorrow. J. Non-Cryst. Solids, *305*(1), pp.1-9.

Krog, N. and Larsson, K., 1968. Phase behaviour and rheological properties of aqueous systems of industrial distilled monoglycerides. Chem. Phys. Lipids, *2*(1), pp.129-143.

Krysiak, W., 2006. Influence of roasting conditions on coloration of roasted cocoa beans. J. Food Eng., *77*(3), pp.449-453.

Kim, Y. D. and Morr, C. V., 1996. Microencapsulation properties of gum arabic and several food proteins: spray-dried orange oil emulsion particles. J. Agric. Food Chem., *44*(5), pp.1314-1320.

Kivelson, D., Tarjus, G., Zhao, X. and Kivelson, S. A., 1996. Fitting of viscosity: Distinguishing the temperature dependences predicted by various models of supercooled liquids. Phys. Rev. E, *53*(1), p.751.

Kurt, W. H., 1955. Apparatus for the Production of Chocolate Paste. U.S. Patent 2,711,964.

Jackson, W. M. and Brandts, J. F., 1970. Thermodynamics of protein denaturation. Calorimetric study of the reversible denaturation of chymotrypsinogen and conclusions regarding the accuracy of the two-state approximation. Biochemistry, *9*(11), pp.2294-2301.

Johari, G. P. and Goldstein, M., 1970. Viscous liquids and the glass transition. II. Secondary relaxations in glasses of rigid molecules. J. Chem. Phys., *53*(6), pp.2372-2388.

Johari, G. P., 1982. Effect of annealing on the secondary relaxations in glasses. J. Chem. Phys., *77*(9), pp.4619-4626.

Jonscher, A. K., 1999. Dielectric relaxation in solids. J. Phys. D: Appl. Phys., *32*(14), p.R57.

Laaksonen, T. J. and Roos, Y. H., 2000. Thermal, dynamic-mechanical, and dielectric analysis of phase and state transitions offrozen wheat doughs. J. Cereal Sci., *32*(3), pp.281-292.

Laaksonen, T. J. and Roos, Y. H., 2001. Dielectric relaxations of frozen wheat doughs containing sucrose, NaCl, ascorbic acid and their mixtures. J. Cereal Sci., *33*(3), pp.331-339.

Lai, V. F., Huang, A. L. and Lii, C. Y., 1999. Rheological properties and phase transition of red algal polysaccharide–starch composites. Food Hydrocolloids, *13*(5), pp.409-418.

Lambelet, P., 1984. Comparison of NMR and DSC methods for determining solid content of fats. Application to cocoa butter and its admixtures with milk fat. Nestle Research News.

Larsson, K., 1966. Classification of glyceride crystal forms. Acta Chem. Scand, *20*(8), pp.2255-2260.

Lee, W. and Kim, H. Y., 2005. Genetic algorithm implementation in Python. In Computer and Information Science, 2005. Fourth Annual ACIS International Conference on (pp. 8-11). IEEE.

Liu, A. J. and Nagel, S. R. eds., 2001. Jamming and rheology: constrained dynamics on microscopic and macroscopic scales. CRC Press.

Liu, Y., Bhandari, B. and Zhou, W., 2006. Glass transition and enthalpy relaxation of amorphous food saccharides: a review. J. Agric. Food Chem., *54*(16), pp.5701-5717.

Loisel, C., Keller, G., Lecq, G., Bourgaux, C. and Ollivon, M., 1998. Phase transitions and polymorphism of cocoa butter. J. Am. Oil Chem. Soc., *75*(4), pp.425-439.

Lu, Y. and Fujii, M., 1998. Dielectric analysis of hen egg white with denaturation and in cool storage. Int. J. Food Sci. Technol., *33*(4), pp.393-399.

Lucisano, M., Casiraghi, E. and Mariotti, M., 2006. Influence of formulation and processing variables on ball mill refining of milk chocolate. Eur. Food Res. Technol., *223*(6), pp.797-802.

Magnier, L. and Haghighat, F., 2010. Multiobjective optimization of building design using TRNSYS simulations, genetic algorithm, and Artificial Neural Network. Build. Sci., *45*(3), pp.739-746.

Marangoni, A. G. and McGauley, S. E., 2003. Relationship between crystallization behavior and structure in cocoa butter. Cryst. Growth Des., *3*(1), pp.95-108.

Martins, S. I., Jongen, W. M. and Van Boekel, M. A., 2000. A review of Maillard reaction in food and implications to kinetic modelling. Trends Food Sci. Technol., *11*(9), pp.364-373.

McCave, I. N., Bryant, R. J., Cook, H. F. and Coughanowr, C. A., 1986. Evaluation of a laser-diffraction-size analyzer for use with natural sediments: research method paper. J. Sediment. Res., *56*(4).

McCrum, N. G., Read, B. E. and Williams, G., 1967. Anelastic and dielectric effects in polymeric solids.

Makhatadze, G. I. and Privalov, P. L., 1995. Energetics of protein structure. Adv. Protein Chem., *47*, pp.307-425.

Mirhosseini, H., Tan, C. P., Hamid, N. S. and Yusof, S., 2008. Optimization of the contents of Arabic gum, xanthan gum and orange oil affecting turbidity, average particle size, polydispersity index and density in orange beverage emulsion. Food Hydrocolloids, *22*(7), pp.1212-1223.

Moran, G. R., Jeffrey, K. R., Thomas, J. M. and Stevens, J. R., 2000. A dielectric analysis of liquid and glassy solid glucose/water solutions. Carbohydr. Res., *328*(4), pp.573-584.

Mason, J. T., 1998. Investigation of phase transitions in bilayer membranes. Methods Enzymol., *295*, pp.468-494.

Meste, M. L., Champion, D., Roudaut, G., Blond, G. and Simatos, D., 2002. Glass transition and food technology: a critical appraisal. J. Food Sci., *67*(7), pp.2444-2458.

Macdonald, J. R., 1987. Impedance Spectroscopy (Vol. 11). New York etc: Wiley.

Mudroch, A., Azcue, J. M. and Mudroch, P., 1996. Manual of Physico-Chemical Analysis of Aquatic Sediments. CRC Press.

Munoz, B. C., Steinthal, G. and Sunshine, S., 1999. Conductive polymer-carbon black composites-based sensor arrays for use in an electronic nose. Sens. Rev., *19*(4), pp.300-305.

Ngai, C. A. K. and Wright, G. B., 1985. Relaxation in Complex Systems, US Govt. Printing O ce, Washington DC.

Ohkuma, C., Kawai, K., Viriyarattanasak, C., Mahawanich, T., Tantratian, S., Takai, R. and Suzuki, T., 2008. Glass transition properties of frozen and freeze-dried surimi products: effects of sugar and moisture on the glass transition temperature. Food Hydrocolloids, *22*(2), pp.255-262.

Olthoff, L. W., Van Der Bilt, A., Bosman, F. and Kleizen, H. H., 1984. Distribution of particle sizes in food comminuted by human mastication. Arch. Oral Biol., *29*(11), pp.899-903.

Owusu, M., Petersen, M. A. and Heimdal, H., 2012. Effect of fermentation method, roasting and conching conditions on the aroma volatiles of dark chocolate. J. Food Process. Preserv., *36*(5), pp.446-456.

Panigrahi, S., Balasubramanian, S., Gu, H., Logue, C. and Marchello, M., 2006. Neural-network-integrated electronic nose system for identification of spoiled beef. LWT--Food Sci. Technol., *39*(2), pp.135-145.

Paul, S. D. and Jeanne, M. H., 1981. Chemico-physical aspects of chocolate processing–a review. Can. Inst. Food Sci. Technol. J., *14*(4), pp.269-282.

Pardo, M., Niederjaufner, G., Benussi, G., Comini, E., Faglia, G., Sberveglieri, G., Holmberg, M. and Lundstrom, I., 2000. Data preprocessing enhances the classification of different brands of Espresso coffee with an electronic nose. Sens. Actuators, B, *69*(3), pp.397-403.

Pearce, T. C., Schiffman, S. S., Nagle, H. T. and Gardner, J. W. eds., 2006. Handbook of Machine Olfaction: Electronic Nose Technology. John Wiley & Sons.

Pérez-Martínez, D., Alvarez-Salas, C., Charó-Alonso, M., Dibildox-Alvarado, E. and Toro-Vazquez, J. F., 2007. The cooling rate effect on the microstructure and rheological properties of blends of cocoa butter with vegetable oils. Food Res. Int., *40*(1), pp.47-62.

Peyron, M. A., Mishellany, A. and Woda, A., 2004. Particle size distribution of food boluses after mastication of six natural foods. J. Dent. Res., *83*(7), pp.578-582.

Plum, G. E. and Breslauer, K. J., 1995. Calorimetry of proteins and nucleic acids. Curr. Opin. Struct. Biol., *5*(5), pp.682-690.

Poynting, J. H. and Thomson, J. J., 1908. A Text-book of Physics. C. Griffin, limited.

Potter, W. D., Robinson, R. W., Miller, J. A., Kochut, K. and Redys, D. Z., 1994, May. Using the Genetic Algorithm to Find Snake-in-the-Box Codes. In IEA/AIE (pp. 421-426).

Privalov, P. L., 1974. Thermal investigations of biopolymer solutions and scanning microcalorimetry. FEBS letters, *40*, pp.S133-S139.

Qian, C. and McClements, D. J., 2011. Formation of nanoemulsions stabilized by model food-grade emulsifiers using high-pressure homogenization: factors affecting particle size. Food Hydrocolloids, *25*(5), pp.1000-1008.

Rahman, M. S., 1999. Glass transition and other structural changes in foods. Food Science and Technology-New York-Marcel Dekker-, pp.75-94.

Rajamäki, T., Alakomi, H.L., Ritvanen, T., Skyttä, E., Smolander, M. and Ahvenainen, R., 2006. Application of an electronic nose for quality assessment of modified atmosphere packaged poultry meat. Food control, *17*(1), pp.5-13.

Ramli, N., Hassan, O., Said, M., Samsudin, W. and Idris, N. A., 2006. Influence of roasting conditions on volatile flavor of roasted Malaysian cocoa beans. J. Food Process. Preserv., *30*(3), pp.280-298.

Reimer, L., 2013. Transmission Electron Microscopy: Physics of Image Formation and Microanalysis (Vol. 36). Springer.

Richardson, T., 2008. Sweets: a history of candy. Bloomsbury Publishing USA.

Ripani, S. and Serafini, G., Carle & Montanari SPA, 1986. Control System for Controlling the Pressure on Chocolate Refining Machine Roll Bearings. U.S. Patent 4,620,477.

Roman-Gutierrez, A. D., Guilbert, S. and Cuq, B., 2002. Description of microstructural changes in wheat flour and flour components during hydration by using environmental scanning electron microscopy. LWT--Food Sci. Technol., *35*(8), pp.730-740.

Ross-Murphy, S. B., 1994. Rheological methods. In Physical Techniques for The Study of Food Biopolymers (pp. 343-392). Springer US.

Roos, Y. and Karel, M., 1991. Phase transitions of mixtures of amorphous polysaccharides and sugars. Biotechnol. Prog., *7*(1), pp.49-53.

Rosenberg, M., Kopelman, I. J. and TALMON, Y., 1985. A scanning electron microscopy study of microencapsulation. J. Food Sci., *50*(1), pp.139-144.

Röck, F., Barsan, N. and Weimar, U., 2008. Electronic nose: current status and future trends. Chem. Rev., *108*(2), pp.705-725.

Sato, K., Ueno, S. and Yano, J., 1999. Molecular interactions and kinetic properties of fats. Prog. Lipid Res., *38*(1), pp.91-116.

Sato, K., 2001. Crystallization behaviour of fats and lipids-a review. Chem. Eng. Sci., *56*(7), pp.2255-2265.

Sato, A. C. K. and Cunha, R.L., 2009. Effect of particle size on rheological properties of jaboticaba pulp. J. Food Eng., *91*(4), pp.566-570.

Schmidt, S. J., 2004. Water and solids mobility in foods. Adv. Food Nutr. Res., *48*, pp.1-103.

Schnermann, P. and Schieberle, P., 1997. Evaluation of key odorants in milk chocolate and cocoa mass by aroma extract dilution analyses. J. Agric. Food Chem., *45*(3), pp.867-872.

Schonberg, A. and Moubacher, R., 1952. The Strecker Degradation of α-Amino Acids. Chem. Rev., *50*(2), pp.261-277.

Schwan, R. F. and Wheals, A. E., 2004. The microbiology of cocoa fermentation and its role in chocolate quality. Crit. Rev. Food Sci. Nutr., *44*(4), pp.205-221.

Shurmer, H. V. and Gardner, J. W., 1992. Odour discrimination with an electronic nose. Sens. Actuators, B, *8*(1), pp.1-11.

Servais, C., Jones, R. and Roberts, I., 2002. The influence of particle size distribution on the processing of food. J. Food Eng., *51*(3), pp.201-208.

Stark, T., Bareuther, S. and Hofmann, T., 2005. Sensory-guided decomposition of roasted cocoa nibs (Theobroma cacao) and structure determination of taste-active polyphenols. J. Agric. Food Chem., *53*(13), pp.5407-5418.

Stark, T. and Hofmann, T., 2005. Structures, sensory activity, and dose/response functions of 2, 5-diketopiperazines in roasted cocoa nibs (Theobroma cacao). J. Agric. Food Chem., *53*(18), pp.7222-7231.

Sterling, C. and Wuhrmann, J. J., 1960. Rheology of cocoa butter. I. Effect of contained fat crystals on flow properties. J. Food Sci., *25*(4), pp.460-463.

Stokes, D., 2008. Principles and Practice of Variable Pressure: Environmental Scanning Electron Microscopy (VP-ESEM). John Wiley & Sons.

Stuchly, M. A. and Stuchly, S. S., 1980. Coaxial line reflection methods for measuring dielectric properties of biological substances at radio and microwave frequencies-A review. IEEE Trans. Instrum. Meas., *29*(3), pp.176-183.

Simatos, D., Blond, G. and Perez, J., 1995. Basic physical aspects of glass transition. Food Preserv. Moisture Control, pp.3-31.

Sokmen, A. and Gunes, G., 2006. Influence of some bulk sweeteners on rheological properties of chocolate. LWT--Food Sci. Technol., *39*(10), pp.1053-1058.

Spink, C. H., 2008. Differential scanning calorimetry. Methods Cell Biol., *84*, pp.115-141.

Svanberg, L., Ahrné, L., Lorén, N. and Windhab, E., 2011. Effect of sugar, cocoa particles and lecithin on cocoa butter crystallisation in seeded and non-seeded chocolate model systems. J. Food Eng., *104*(1), pp.70-80.

Tan, J. and Kerr, W. L., 2017. Determination of glass transitions in boiled candies by capacitance based thermal analysis (CTA) and genetic algorithm (GA). J. Food Eng., *193*, pp.68-75.

Tatsumi, Y., Watada, A. E. and Wergin, W. P., 1991. Scanning electron microscopy of carrot stick surface to determine cause of white translucent appearance. J. Food Sci., *56*(5), pp.1357-1359.

Tarjus, G., Kivelson, S. A., Nussinov, Z. and Viot, P., 2005. The frustration-based approach of supercooled liquids and the glass transition: a review and critical assessment. J. Phys.: Condens. Matter, *17*(50), p.R1143.

Tsoukalas, L. H. and Uhrig, R. E., 1997. Fuzzy and Neural Approaches in Engineering (Adaptive and Learning Systems for Signal Processing, Communications and Control Series. NYUSA: John Wiley and Sons, Inc.

Van der Bilt, A., Van Der Glas, H. W., Mowlana, F. and Heath, M. R., 1993. A comparison between sieving and optical scanning for the determination of particle size distributions obtained by mastication in man. Arch. Oral Biol., *38*(2), pp.159-162.

Van Malssen, K., Peschar, R. and Schenk, H., 1996. Real-time X-ray powder diffraction investigations on cocoa butter. I. Temperature-dependent crystallization behavior. J. Am. Oil Chem. Soc., *73*(10), pp.1209-1215.

Van Malssen, K., van Langevelde, A., Peschar, R. and Schenk, H., 1999. Phase behavior and extended phase scheme of static cocoa butter investigated with real-time X-ray powder diffraction. J. Am. Oil Chem. Soc., *76*(6), pp.669-676.

Vassilikou-Dova, A. G. L. A. I. A. and Kalogeras, I. M., 2009. Dielectric analysis (DEA). In Thermal analysis of polymers: Fundamentals and applications (pp. 497-613). John Wiley, Hoboken, New Jersey.

Verheul, M. and Roefs, S. P. F. M., 1998. Structure of whey protein gels, studied by permeability, scanning electron microscopy and rheology. Food hydrocolloids, *12*(1), pp.17-24.

von Hippel, A. R. and Morgan, S. O., 1955. Dielectric materials and applications. J. Electrochem. Soc., *102*(3), pp.68C-68C.

Winquist, F., Hornsten, E. G., Sundgren, H. and Lundstrom, I., 1993. Performance of an electronic nose for quality estimation of ground meat. Meas. Sci. Technol., *4*(12), p.1493.

Williams, G. and Watts, D. C., 1970. Non-symmetrical dielectric relaxation behaviour arising from a simple empirical decay function. Trans. Faraday Soc., *66*, pp.80-85.

Weeks, E. R., Crocker, J. C., Levitt, A. C., Schofield, A. and Weitz, D. A., 2000. Three-dimensional direct imaging of structural relaxation near the colloidal glass transition. Science, *287*(5453), pp.627-631.

Xue, T., Yu, L., Xie, F., Chen, L. and Li, L., 2008. Rheological properties and phase transition of starch under shear stress. Food Hydrocolloids, *22*(6), pp.973-978.

Yasuda, G. I. and Takai, H., 2001. Sensor-based path planning and intelligent steering control of nonholonomic mobile robots. In Industrial Electronics Society, 2001. IECON'01. The 27th Annual Conference of the IEEE (Vol. 1, pp. 317-322). IEEE.

Yegnanarayana, B., 2009. Artificial neural networks. PHI Learning Pvt. Ltd..

Yu, L., 2001. Amorphous pharmaceutical solids: preparation, characterization and stabilization. Adv. Drug Delivery Rev., *48*(1), pp.27-42.

Zhang, Q., Zhang, S., Xie, C., Zeng, D., Fan, C., Li, D. and Bai, Z., 2006. Characterization of Chinese vinegars by electronic nose. Sens. Actuators, B, *119*(2), pp.538-546.

Ziegleder, G. and Biehl, B., 1988. Analysis of cocoa flavour components and flavour precursors. In Analysis of Nonalcoholic Beverages (pp. 321-393). Springer Berlin Heidelberg.

Ziegleder, G., 1991. Composition of flavor extracts of raw and roasted cocoas. Z. Lebensm.-Unters. -Forsch. A, *192*(6), pp.521-525.

Ziegler, G. R., Mongia, G. and Hollender, R., 2001. The role of particle size distribution of suspended solids in defining the sensory properties of milk chocolate. Int. J. Food Prop., *4*(2), pp.353-370.

Ziegler, G. R. and Hogg, R., 2009. Particle size reduction. Industrial Chocolate Manufacture and Use, Fourth Edition, pp.142-168.

Zoumas, B. L., Azzara, C. D. and Bouzas, J., 2004. Chocolate and cocoa. Kirk-Othmer Encyclopedia of Chemical Technology.

Zounis, S., Quail, K. J., Wootton, M. and Dickson, M. R., 2002. Studying frozen dough structure using low-temperature scanning electron microscopy. J. Cereal Sci., *35*(2), pp.135-147.

Figures

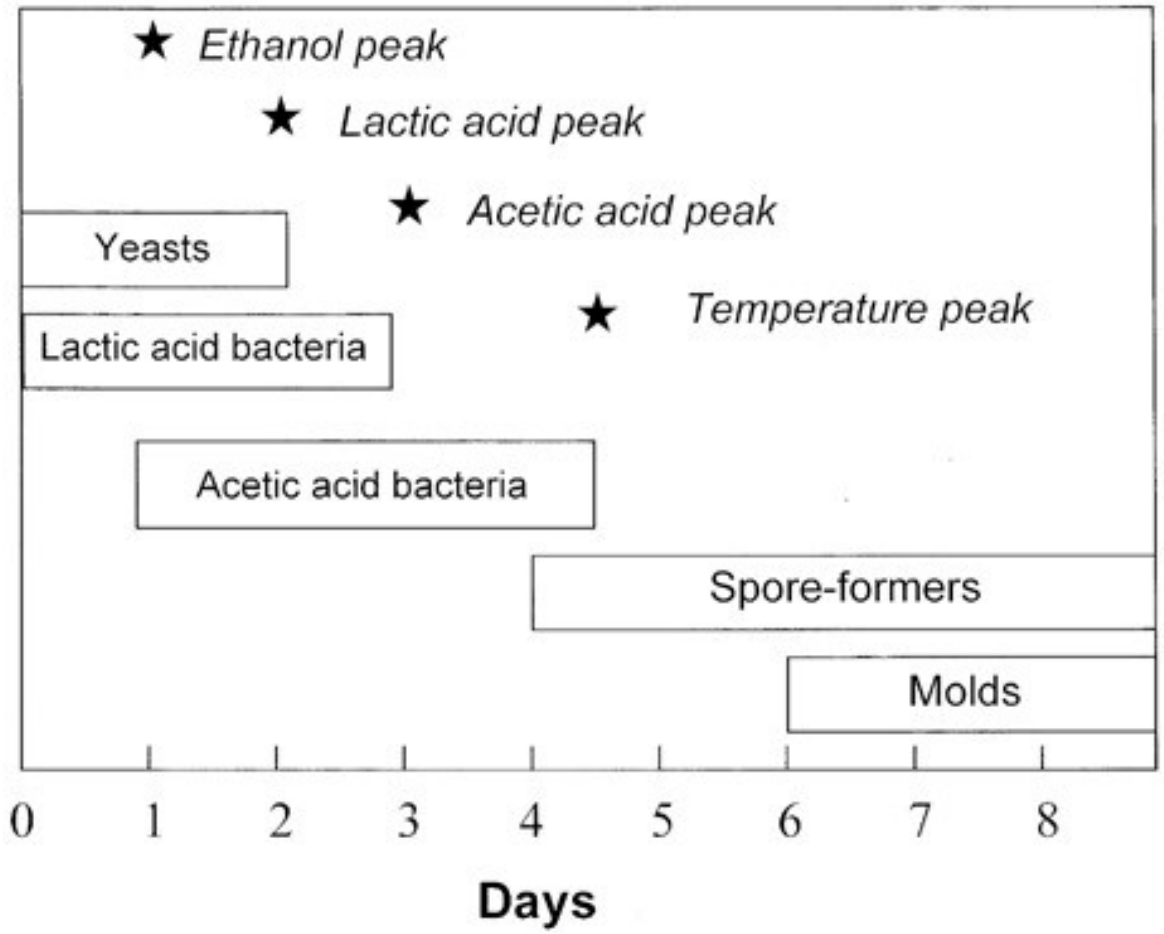

Figure 2.1. Schematic of a microbial succession during cocoa bean fermentations.

Tables

Table 2.1. Cooking tempering of candies of different stages

Stage	Cooking temperature (°C)	Sugar contents
Thread (e.g., syrup)	110-112	80%
Soft ball (e.g., fudge)	112-116	85%
Firm ball (e.g., soft caramel)	118-120	87%
Hard ball (e.g., nougat)	121-130	90%
Soft crack (e.g., salt water taffy)	132-143	95%
Hard crack (e.g., toffee)	146-154	99%
Clear liquid	160	100%
Brown liquid	170	100%
Burnt sugar	177	100%

Table 2.2. Melting temperature and texture of different type cocoa butter crystalline

Type	T_m (°C)	Texture
I (γ)	17	Soft, crumbly, melts too easily
II (α)	21	Soft, crumbly, melts too easily
III (β_1')	26	Firm, poor snap, melts too easily
IV (β_2')	28	Firm, good snap, melts too
V (β_2)	34	Glossy, firm, best snap, melts
VI (β_1)	36	Hard, takes weeks to form

CHAPTER 3

DETERMINATION OF GLASS TRANSITIONS IN BOILED CANDIES BY CAPACITANCE BASED THERMAL ANALYSIS (CTA) AND GENETIC ALGORITHM (GA)[1]

[1] Tan, J. and Kerr, W.L., 2017. *Journal of Food Engineering*, *193*, pp.68-75.
Reprinted here with permission of the publisher.

ABSTRACT

The glass transition temperature (Tg) is an important property that influences the processing and textural characteristics of candy. Measurement of Tg is done by comparably expensive and complex instruments. In this study, we tested a new system which uses capacitance thermal analysis (CTA) of candy trapped between stainless plates, as the system is caused to heat at an uncontrolled rate. The data of capacitance as a function of temperature were processed by a genetic algorithm (GA), and fitted to a three-section model to determine Tg. Tg of the candies were independently measured by DSC as a reference. The results showed that when the Tg of the candy was below ~15 ℃, the measurement from the GA-CTA was higher (2-3 ℃) than that from DSC. However, if Tg of the candy was higher than 15 ℃, the two methods gave similar values. GA based CTA provides a feasible new way to measure phase transitions in candies with relatively inexpensive equipment, and with less need for user interpretation of data.

Keywords: Glass transition, capacitance, genetic algorithm, three-section model

1. Introduction

Candies, or sugar confections, are popular food products characterized by relatively high sugar content. This definition may encompass several distinctly different items such as chocolate, boiled sweets, and chewing gum. Confectionery foods are popular throughout the world and have been consumed for thousands of years. Some studies date the first production of candy to ca. 2000 BC in ancient Egypt (Richardson, 2003). In the past, candies have served a medicinal role, as in the relief of sore throats, and were often only accessible to wealthy individuals. In the United States, sugar confections became more available to the general public in the 1830s. This coincided with the increase in sugar production in Louisiana and the West Indies, and the greater availability of cocoa beans. In addition, the industrial age had provided technological advances that allowed for mass production of sugary sweets. While the production and types of candies has increased since those times, much of the basic composition has remained much the same.

The texture, appearance, and storage stability are very importance factors which can influence consumer perception of candy. A unique feature of candies is that they can appear in many physical and structural forms, which in turn have a profound impact on their perceived texture. Candies containing only sugar (or glucose syrup) can manifest as chewy caramels or solid hard candies. The former are often present as rubbery states with no crystalline material, although graining or whipping may be used to create small sugar crystals that shorten the texture. Hard candies are usually produces as clear amorphous glassy states, although some confections such as rock candy may have sucrose crystals. Other confections incorporate gelling agents such as pectin to create very chewy products such as gummy bears and jelly beans. Of course, a very

prominent category of candy are chocolates. These contain fine dispersions of sugar and cocoa mass particles trapped in a solid fat phase.

The glass transition temperature (T_g) is one of the important factors that determines the physical properties of candies. A glassy state can be defined as an amorphous solid, or the amorphous portion of a semi-crystalline solid. Upon heating, the temperature at which a glassy solid transform into a rubbery state is defined as the glass transition temperature (T_g). At temperatures below T_g, molecules exist in an amorphous solid with limited motion. At a macroscopic level, such materials are often clear and have a relatively hard, brittle structure. At temperatures above T_g, molecules can undergo rotational and translational movement in a 'rubbery' or liquid amorphous state. These materials can be fairly viscous or malleable, properties that influence the chewability of candies.

Controlling the physical states of candy is critical in the confection industry as desirable characteristics, texture, and storage stability are influenced by these states (Hartel et al., 2011). In general, food materials maintain better physical and chemical stability in the glassy state than in the rubbery state (Humagai and Kumagai 2002). Ergun and Hartel (2009) summarized some of the desirable states for confections, and indicated that hard candies should have a T_g which is much higher than room temperature, so that it can maintain its desired brittleness and hard texture over a range of ambient temperatures. Some other candies including ungrained caramels, chewy nougats, and marshmallows have a T_g lower than room temperature, thus exhibit a chewy texture.

To make glassy candies, both glass-formers and modifiers are needed. In addition, the candies need to be rapidly cooled down from a molten state so that crystals do not have time to form. The most common glass-formers are sugar (sucrose) and glucose syrup (Smidova et al.,

2003). Other components such as maltodextrin, gum, color, and flavor serve either as glass-formers working to adjust the T_g of the candy glass, or as additives, changing the appearance and flavor. For most candy production, water is used as a plasticizer that can break down the network connectivity of glass-formers. Plasticizers lower the T_g by increasing the free volume in which molecules are free to move. The agents soften the material but may decrease chemical stability. Therefore, it is important to control the ratio of plasticizers to glass-formers, so that the candies can be made into desirable forms. Previous studies (Ergun et al., 2010; Tananuwong and Reid, 2004; Labuza and Labuza, 2004; Lourdin el al., 1997; Forssell et al., 1997) indicated that water content has great influence on the T_g, and lowering the water content of foods such as starchy materials, dried foods, confections, and frozen foods leads to a greater than linear increase in T_g. In addition, several studies (Bhandari and Howes, 1999; Roos and Karel, 1991; Roos, 1993) have shown that the molecular weight of the primary glass-former has a major impact on T_g, with higher molecular weight compounds producing greater T_g values. The influence of the weight ratio of different components (glass-former and plasticizer) on T_g of food materials has been summarized by the Gordon-Taylor equation (Roos, 1995):

$$T_g = \frac{\omega_1 T_{g1} + k\omega_2 T_{g2}}{\omega_1 + k\omega_2} \qquad (1)$$

where, ω_1 and ω_2 are the weight fractions of components 1 and 2 while T_{g1} and T_{g2} are the glass transition temperature of each component. The constant k is related to the difference in specific heat values for the two components between glass and fluid state ($k = \Delta C_{P1}/\Delta C_{P2}$).

Differential scanning calorimetry (DSC) is one of the most commonly used methods to determine glass transition temperatures. Thermodynamic transitions are classified as first- or second-order. In a first-order transition, there is a transfer of latent heat between system and surroundings, and the system undergoes an abrupt volume change. In a second-order transition,

often called a continuous phase transition, there is no change in latent heat but the heat capacity does change. First-order transitions occur, for example, between the solid and melted states of crystalline sucrose. Glass transitions are second-order, as the greater motional freedom in the rubbery state give it a greater heat capacity than in the glassy state. In some systems, a material may undergo more than one glass transition, such as α and β relaxations. The DSC compares the relative heat flow of a sample and reference (such as an empty pan) during a linear temperature scan (Roos, 1995). The glass transition presents as a step in the heat-flow baseline. The change is not usually abrupt, but occurs over a temperature range. Thus, glass transitions are often characterized by onset, endset and midpoint temperatures (Hartel et al., 2010).

Another common approach to measure glass transitions is through rheological tests. Typically, this involves measurement of an elastic or viscous property as the sample temperature is gradually increased. This often involves small amplitude oscillations of the sample, with measurements of the phase lag between the stress and strain, from which the storage (E' or G') or loss (E" or G") moduli are derived. Generally, the oscillation frequency can be varied to mimic process conditions, or to adjust the relative stiffness of the material. Cocero and Kokini (1991), Kasapis et al (2003) and Madeka and Kokini (1996) measured rheological properties of different food materials over various temperature ranges, and found that at T_g there was a drastic drop of storage modulus G' and viscosity. In addition, a peak of loss modulus G'' appears when the samples reach T_g. Other existing methods to determine T_g include dilatometry (Biliaderis et al., 1986), which measures the volume change during a temperature scan, and nuclear magnetic resonance (NMR) or electronic paramagnetic resonance (EPR), which measure the mobility of nuclei (mainly ^{1}H and ^{13}C) or spin probes (Ruan and Chen, 1997).

Yet another method for determining T_g is dielectric thermal analysis (DETA), which measures the variations of the dielectric constant as a function of temperature or frequency. This technique was demonstrated as particularly effective for the study of secondary relaxations in products with low water content (Champian et al., 2000). The typical DETA consists of parallel metal plates with a small gap between the plates to accommodate the sample being tested. As with DSC and thermal rheological methods, the sample temperature can be increased systematically as it moves from the glassy to rubbery states. The frequency dependence can also be investigated, typically over the range of 1mHz to 1 MHz, allowing researchers to determine different electrical properties that manifest at different frequencies (Räsänen et al., 1998). The instrument measures the stored electrical energy component (the dielectric constant ε') as well as that lost as heat (the dielectric loss ε"). As with dynamic rheological methods, the ratio tan δ (ε"/ε') may help identify and characterize changes in material properties. The peak of tan δ that appears in some isochronal tan δ vs temperature plots is defined as T_g (Laaksonen and Roos, 2000). Some researchers have suggested that DETA is a more sensitive measurement than dynamic rheology, as often only one transition can be seen by rheological tests (Rotter and Ishida, 1992). As T_g measured by DETA varies substantially with frequency, it is important to specify and understand the measurement frequency before comparing results.

DSC, DETA and dynamic rheological thermal analyzers are relatively expensive instruments and require substantial user training to ensure reliable results. In addition, each require careful consideration of the data curves to determine T_g parameters, an exercise that may allow individual interpretations to bias the results. Thus, such approaches are often available only to large candy manufacturers.

The objective of this research was to construct and test a simple and relatively inexpensive device that could be used to measure glass transitions in candies. The device consisted of a parallel metal plate assembly to hold the sample, which was then frozen in a commercial freezer. The temperature of the sample was increased by bringing it to a constant temperature environment. While this does not allow linear increase in temperature, it greatly simplifies the instrument construction. As a measure of the increased mobility of molecules as temperature increased, the capacitance was monitored using an inexpensive capacitance meter. Capacitance is the ability of a subject to store electrical charge, and the capacitance of a parallel-plate capacitor can be determined as:

$$C=\varepsilon'\varepsilon_0\frac{A}{d} \qquad (2)$$

where ε' is the dielectric constant or permittivity of the sample between the parallel-plates, ε_0 is the dielectric constant when the medium is air, A is the overlap area of the two parallel plates, and d is the distant between the plates. While related to the complex moduli measured by DETA, the capacitance is only a measure of the storage moduli and at a fixed frequency. Again, this approach greatly simplified and reduced the cost of the instrument.

A general description of capacitance may help describe the operation of the cell. A capacitor consists of two conductors (here the metal plates), separated by a dielectric material (the candy samples), causing the conductors to develop opposite charges and a potential difference between them. Thus, the plates can store charge because of the influence of the dielectric material. The potential difference between plates filled with a dielectric increases by a factor κ, compared to the same plates *in vacuo*. That is, more charge can be stored at a given potential difference because of increased capacitance. In general, this best occurs for dielectric media that are polarizable or contain permanent dipoles. When an electric field (E_o) is applied,

dipoles align with the field, causing an opposing electric field (E_i). The net field is $E = E_0 - E_i$, thus the charges on the plate are somewhat shielded by the effects of the dielectric.

To test the system, candy samples were prepared to different moisture levels, and thus had differing T_g values, as well as different physical states at ambient temperature. Data was collected of the capacitance versus temperature as the sample temperature increased. To deal with the data interpretation, and to reduce the need for user input, a genetic algorithm (GA) was developed to determine the glass transition regions. A genetic algorithm is an adaptive heuristic search algorithm based on the evolutionary ideas of natural selection and genetics (Sivaraj et al., 2011). The initial "generation" starts with a selection of random solutions (say 100). These are tested as to their fitness, for example through standard regression statistics such as the coefficient of determination. The best-fitting solutions are retained as bit-strings of 0s or 1s. In addition, new solutions are generated by using these "individuals" and allowing them to pass on their "genes", typically though crossover or mutation methods, or mixtures of both. In the former, sections of the bit string array are transferred between "parent" solutions. In the latter method, parts of the array are randomly changed. As the generations pass, the members of the population should get fitter and fitter (Goldberg, 1990). After a set number of generations, a best-fitting solution is determined. The advantage of the GA approach is that a good-fitting function can be obtained relatively quickly, as all possible solutions to the problem do not have to be considered.

In this study, a three-section model was defined based on capacitance versus temperature data, which contained two linear sections for the pre- and post- glass transition temperature range, and one exponential section for the transition temperature range. Two demarcation points for the three sections were determined by a genetic algorithm, which determined the best demarcation points to provide the best overall fitting for the three-section model.

2. Materials and Methods

2.1 Materials

Granulated sugar (Domino Foods Inc.), high-fructose light corn syrup (ACH Food Companies Inc.) and commercial hard candies (Kroger Starlight mints and Kroger Butterscotch Disks) were purchased from Kroger at Athens Georgia.

2.2 Candy preparation

Boiled sugar candies were made with 450g sucrose, 134g light corn syrup and 100g deionized water. The ingredients were mixed in a stainless pan (18 cm in diameter and 14 cm in depth) before being heated on a stove (Model BP90W, Profile, General Electric Company, Inc.). The cooking temperature was 220℃ and the moisture contents of the samples were controlled by their boiling temperature, which was measured by a thermometer (Model TCF400, CDN, Component Design Northwest, Inc.). In this study, six candies with different water contents were made by controlling their boiling temperatures range from the firm ball stage (125℃) to the hard crack stage (150℃). Details of the candies are summarized in Table 1.

When the specific end temperature was reached for each candy, the pan was removed from the burner, and approximately 2 ml of the sample transferred to the parallel-plate capacitor cell, and the gap adjusted to 1 mm. The assembly was then placed in a walk-in freezer at -5°C and left for ~2 h. The remaining candy sample was placed into metal pouches, sealed and kept frozen for subsequent moisture and DSC analyses. Samples of commercial hard candies were also tested. These were first broken into small pieces with a rubber hammer, then melted directly on the lower metal plate by heating it on the stove. All treatment groups were prepared in triplicate, with sample measurements repeated three times.

2.3 Capacitor Based Thermal Analysis (CTA)

The parallel-plate capacitance cell was built at the University of Georgia Instrument Shop in Athens, Georgia. The cell consisted of two separate 50 mm diameter stainless steel plates (Fig. 1). Each plate had a 4 mm hole drilled into the side in which a screw was provided. Single stranded silver-plated copper wire (18 gauge) was wrapped around the screw. The two wires were used to connect the sensor with a capacitance meter (RadioShack 46-range Digital Multimeter with PC interface). An 8 mm diameter hole cut into the center of the upper plate allowed a nylon screw to pass through and be screwed into the lower plate. A 1 mm hole was drilled part way into the the upper plate, allowing a thermocouple to measure the temperature near the surface of the sample. A ring spacer for the parallel-plate capacitor was made from cast nylon rod (Model 1UPX9, Grainger, Lake Forest, IL). The spacer had an outer diameter of 5 cm, an inner diameter of 4.2 cm, and a height of 6 mm. The inner faces of the parallel plates that touched the samples were trimmed by 4 mm in diameter and 2 mm in depth, so the spacer could be fixed between the two the parallel plates.

To operate the CTA, sample was placed between the plates and the plates to give a 4 mm gap. The samples were cooled to ~ 0 ℃ before the tests were commenced. A hot plate was set to 105℃ and used to heat the CTA cell. The capacitance meter and a thermocouple were connected to the cell and the signals directed to a data logger (Model XL100, Omega) set to collect data at 1 point/s. Typically, samples had finished the transition between glassy and rubbery states between 50 and 70°C, depending on the sample. The capacitance data were recorded at 1 point/s and transferred to a laptop computer using LabView software (National Instruments, Austin, TX).

2.4 T_g determined by differential scanning calorimetry (DSC)

The glass transition temperature of each sample was determined using a differential scanning calorimeter (Model DSC 3, Mettler-Toledo International Inc., Columbus, OH). Approximately 12 mg of each sample was sealed into a 40 ul aluminum pan. An empty pan was used as a reference sample. Dry nitrogen gas was used to minimize water condensation in the measuring cell environment. The temperature scan for each sample was from -5℃ to 70 ℃ at a heating rate of 5℃ per minute. Before each scan the sample was heated to 85℃ and held for 1 min, then cooled to 25℃ and held an additional 1 min. This helped eliminate any differences in morphology of each sample, and so that the material would have good contact with the bottom surface of the pan. Also, some previous studies (Angell, 2002) reported that sugar glasses are not completely static, and many of them may exhibit a phenomenon known as enthalpic relaxation (Schmidt and Lammert, 1996). Therefore, melting the sample before undergoing a temperature scan could help eliminate enthalpic relaxation peaks and makes transitions more evident. The data acquired by the DSC were analyzed by STAR^e Thermal Analysis software (version 3.1., Mettler-Toledo, Columbus, OH) to determine the onset and endset glass transition temperatures.

2.5 Genetic algorithm development

Data of capacitance versus temperature of each sample from the CTA test was processed by a GA program using Matlab (2013b, MathWorks, Natick, MA). In the GA, there were 100 individuals in each generation, that is, sets of solutions to be tested as to how well they fit the data. Each individual solution carried one 'gene' represented by a 14-bit string. The first 7 bits and the last 7 bits represented the position of the two demarcation points (in binary numbers), for three regions of the data curve (see Figure 3). For example, 00001110000111 indicates that the 7th temperature data point collected is the onset T_g, while the 14th point collected is the endset

T_g. The fitness function was $3-(R_1^2+ R_2^2+ R_3^2)$, where the three R_i^2 are the R-square value of each section by fitting the data to each solution. The first and third sections of the data curves were fitted to a linear model while the second section was fitted to an exponential model. In addition, punishments were applied during the calculation of fitness value of each 'individual' if they had either of two violations: (1) if less than 8 data points were used to fit the model in any section in the capacitance versus temperature data and (2) if any of the three sections had R-square values less than 0.9 after fitting to the model. If a violation was triggered, the fitness value was set to the maximum so that the individuals that triggered the violation were very likely to be excluded in the next generation.

Other parameters for the GA were: the population size 'n' of each generation was 100, the crossover fraction p_c was 0.6, and the mutation rate p_m was 0.005. The 'Tournament' procedure was used as the selection method to select the 'parents' to produce 'children', that is the next set of solutions. A tournament selects each parent by choosing certain individuals at random; in this study, the size tournament for one time was 4. Among the selected tournament groups, the best individual was picked to be one of the parents. The crossover method for the GA was the 'scatter' procedure. The procedure creates a random binary vector. It then selects the 'genes' where the vector is a 1 from the first parent, and the genes where the vector is a 0 from the second parent, and combines the genes to form the child (a new solution). Also, performance of the algorithm was improved by using 'elitism' with a value of 2. This means that the two best individuals in one generation were bypassed to the next generation. This reduces the chance of reusing previously discovered partial solutions. Each sample's capacitance versus temperature data were processed by the GA 10 times, and the one with the minimum value of the fitness function was chosen as the final result.

2.6 Moisture content

To determine the relationship between T_g and moisture, the moisture content of each sample was determined. Each sample (~ 4g) was dissolved in deionized water at a ratio of candy –to-water weight of ~ 1:2. After allowing the candy to dissolve 18h in a sealed container, the sugar content of the resultant solution was determined by a refractometer (model PR-201, ATAGO CO., LTD). The Brix reading was converted to dry solids content using standard curves generated by the RI-DS software program (Version 4, Corn Refiners Association, Washington DC). The moisture content ($\omega_{\%}$ in g H_2O per 100g sample) was then calculated by:

$$\omega_{\%} = \left(1 - m_s - \frac{m_w}{m_w + m_o}\right) * 100 \quad (3)$$

where m_s is the mass of sugar in solution determined by refractometry, m_o is the initial mass of candy, and m_w the mass of water added.

2.7 Statistical methods

All measurements were repeated at three times on samples prepared in triplicate. The results were displayed as mean of the measurements ± standard deviation. Measurements were compared by one-way ANOVA using SAS 9.3 (SAS Institute Inc., Cary NC). The different methods for determining T_g were the main factors. The level of significance was set at $p \leqslant 0.05$.

3. Results and discussion

3.1 T_g determined by DSC versus moisture content

Values of the onset and endset T_g versus moisture content, as determined by DSC, are shown in Fig. 2. The data were fit to a second-order polynomial of the form:

$$T_g = a*\omega_{\%}^2 + b*\omega_{\%} + c \quad (4)$$

where the derived constants a, b and c are shown in Table 2. The onset T_g values ranged from 28°C at 0.8% moisture to 2°C at 13.5% moisture. As noted in previous studies (Nowakowski, 2000; Roos and Karel, 1991, Noel et al., 1991), a small percent difference in moisture content can cause a large difference in T_g when the moisture content is relatively low (less than 5 %). All candies in this study had a $T_{g,onset} < 35$℃. In our samples, the major constituent of the candy was sucrose (>77%) which has a T_g in the dry state about 62-70℃ (Ergun et al. 2010). As the candies were mixtures of different sweeteners and carbohydrates, low molecular weight molecules including fructose (T_g of 5℃) (>13%) and glucose (T_g of 31℃) may have further reduced the T_g of the candies.

There are several theories to explain the influence of moisture content on T_g. Water can serve as a plasticizer, thus increasing the free volume amongst larger molecules. Thus, these glass forming components have a greater spatial volume in which to move. In addition, the water molecules may help shield attractive forces amongst the larger molecules. While the overall mobility of the system is reduced in the glassy state, small molecules such as water still possess some mobility, and their mobility will increase drastically when temperature increases (Fennema, 1996, Slade and Levine, 1995).

3.2 T_g determined by GA based CTA

Examples of how the measured capacitance varied with temperature during heating are shown in Fig. 2. In all cases, the capacitance was quite low in the glassy state with values below ~10 pF. As the temperature increased, and the system entered the glass transition zone, the capacitance began to increase. The figure, showing curves for hard crack candy (HC) and a commercial hard candy, also demonstrates how the three-section model was applied to determine the T_g values. Thus, the three arrows represent regions of the curve represented by the optimized

fitness function. The GA generates a population of solutions for fitting the curve using a linear, exponential and linear region. From these, individual solutions are selected and serve as "parents" for the "children" of the next generation. That is, solutions with low values of the fitness function are selected, and then subject to random mutations of the bit string, or cross-over of bits with other solutions. Generally, but not always, the new generation of solutions have better fitness than the previous generation. After ten generations, the optimized boundaries of the transition region provide the onset and endset T_g values.

The fitness values of all samples were smaller than 0.1607, indicating that for all samples the GA-fit three-section model had an R^2 value greater than 0.946. The logic of the three-section model is supported by other studies. When the temperature is below the glass transition temperature of a material, generally, the molecules have little if any translational mobility and retain only limited rotational and vibrational mobility (Hancock et al., 1995). In this region, there may be some increase in the rotational and vibrational mobility of the molecules, and perhaps some minor translational movement of water, which cause a small increase in capacitance with temperature. While undergoing a glass transition, Debenedetti and Stillinger (2001) indicated that there is a decoupling between translational and rotational mobility at a temperature around $1.2T_g$. Thus, in our results, the region between the onset and endset T_g may arise from the initiation of translational and rotational mobility, leading to an exponential increase in capacitance. At temperatures above the endset Tg, a full rubbery state is developed. In this stage, the inter-molecular forces are greatly reduced, so that both translational and rotational mobility increase as a function of temperature. This in turn leads to a more dramatic increase in capacitance with temperature.

Components of the candies do have dipole moments. Thus, crystalline sucrose has a dielectric constant of $\varepsilon_s = 3.6$ (Reiser, 1994), while water has a value of $\varepsilon_w = 80$. In the glassy state, there is only limited ability for sugar molecules to rotate and orient with an electric field. Thus, the sample does not create a significant opposing electric field, and capacitance is low. With the transition region, rotational freedom becomes more available allowing molecular dipoles to align with the field, and the capacitance increases. At even higher temperatures, the degrees of motion are even greater and the capacitance continues to rise. At some point, however, excess thermal energy would tend to counter the tendency for field alignment.

Others have used capacitance sensors to study the T_g of carbohydrate solutions containing NaCl (Kilmartin et al., 2004; Kilmartin et al., 2000), although these studies measured transitions from the frozen maximally-freeze concentrated state. Their work showed a large (10,000 x) increase of capacitance when samples underwent a glass transition. For the candy systems, we found only a 5- to 6- fold increase in capacitance. This can be attributed to the relatively low moisture content of the hard candy systems. The mobility of small molecules, especially water, is much greater than larger sucrose and polysaccharides. In the candies, increasing temperature results in a viscous rubbery state, while in the high-moisture system there is a transition to a very mobile system. In addition, in the frozen system ice has a much lower dielectric constant (3.2) as compared to the liquid water (80) that develops with melting (Hallikainen, 1977). Finally, the frozen food model systems also contained NaCl. Once a T_g and incipient melting began, these could become highly mobile and contribute to electrical conductivity.

3.3 Comparison of DSC and GA based CTA

T_g values determined by DSC and GA based CTA are shown in Table 3.3. For samples with relatively low T_g (FB, SC and SC1), there were differences between the onset T_g acquired

by DSC and the GA based CTA. Typically, onset T_g values were 2 to 3 degrees higher when measured by the CTA system compared to the DSC. Some researchers (Kalichevsky et al., 1992; Biliaderis et al., 1999) have concluded that T_g measured by traditional DEA or DSC may have different measured T_g values. The methods measure different physical properties, and couple different structural units (each with particular relaxation times). Thus, the thermal or electrical responses may differ in how they respond with the imposed perturbations, and how these change with temperature.

The factors that cause disparity in the T_g measured by traditional DEA and DSC might also apply to the different T_g values measured by CTA and DSC. However, not every pair of T_g measured by the two methods exhibited a significant difference. Thus, for samples with higher T_g values, the two methods agreed more closely, with difference less than 1°C. Differing heating rates may also cause some disparity in the T_g values. The DSC scans were conducted at 5°C/min, while the heating in the CTA was not controlled by a feedback system. For the CTA system, heating rates were greatest when the cell temperature was relatively low (0 - 5°C). As the temperature of the CTA increased, the heating rate slowed (Fig. 4). For the first few minutes, the heating rate was ~15°C/min, about 3 times greater than that for the DSC. At longer times, the heating rate decreased to ~4°C/min. The relatively faster heating rate may have contributed to the T_g measured by CTA to be higher, if the T_g of the candies were in the temperature range where the heating rate of the CTA was greater than the DSC.

In addition, T_g values are known to vary with frequency. The DSC does not apply oscillatory heating, thus occurs at relatively low rates. However, the CTA system operated at a frequency of 22kHz. Kilmartin et al. (2004) and Kilmartin et al. (2000) found that capacitance

meters employing high frequency (>1000Hz) acquired lower T_g values than at lower frequency (50Hz), the latter which resulted in T_g values closer to those measured by DSC.

4. Conclusion

The GA based CTA introduced in this study was found to be a viable alternative to measuring glass transitions in sugar candies. T_g values found by the CTA method were similar to those determined by DSC, particularly at high T_g values. Onset temperatures varied at most by a few degrees, and in a practical setting the CTA could be calibrated to match DSC values if desired. The advantage of the CTA method is that it is relatively inexpensive and easy to use. This is made possible by using relatively large sample sizes (1-2 ml), a property (capacitance) that is easy to measure, and relying on a simplified heating system. In addition, difficulties incurred because of user interpretation of data is bypassed by using a robust modeling system to determine the transition temperatures. This was based on a genetic algorithm procedure which uses iterative procedures, but which more quickly finds an optimal fit based on evolutionary procedures. The algorithm requires no additional input from the user. In the future, the system may be improved by optimizing sample size and area requirements. In addition, we hope to test the system or other food items that undergo glass transitions.

References

Angell, C. A., 2002. Liquid fragility and the glass transition in water and aqueous solutions. Chem. Rev., *102*(8), 2627-2650.

Bhandari, B. R., & Howes, T., 1999. Implication of glass transition for the drying and stability of dried foods. J. Food Eng., *40*(1), 71-79.

Biliaderis, C. G., Page, C. M., Maurice, T. J., & Juliano, B. O., 1986. Thermal characterization of rice starches: A polymeric approach to phase transitions of granular starch. J. Agric. Food Chem., *34*(1), 6-14.

Biliaderis, C. G., Lazaridou, A., & Arvanitoyannis, I., 1999. Glass transition and physical properties of polyol-plasticised pullulan–starch blends at low moisture. Carbohydr. Polym., *40*(1), 29-47.

Champion, D., Le Meste, M., & Simatos, D., 2000. Towards an improved understanding of glass transition and relaxations in foods: molecular mobility in the glass transition range. Trends. Food Sci. Tech., *11*(2), 41-55.

Cocero, A. M., & Kokini, J. L., 1991. The study of the glass transition of glutenin using small amplitude oscillatory rheological measurements and differential scanning calorimetry. J. Rheol., *35*(2), 257-270.

Debenedetti, P. G., & Stillinger, F. H., 2001. Supercooled liquids and the glass transition. Nature, *410*(6825), 259-267.

Ergun, R., Lietha, R., & Hartel, R. W., 2010. Moisture and shelf life in sugar confections. Crit. Rev. Food Sci. Nutr., *50*(2), 162-192.

Fennema, O. R., 1996. Water and ice. In: *Food* Chemistry (O. R. Fennema, ed. *New York-Marcel Dekker-*, 17-94.

Forssell, P. M., Mikkilä, J. M., Moates, G. K., & Parker, R., 1997. Phase and glass transition behaviour of concentrated barley starch-glycerol-water mixtures, a model for thermoplastic starch. Carbohydr Polym. ,*34*(4), 275-282.

Goldberg, D. E., 1990. A note on Boltzmann tournament selection for genetic algorithms and population-oriented simulated annealing. Complex Syst., *4*(4), 445-460.

Hallikainen, M., 1977. Dielectric properties of sea ice at microwave frequencies. *NASA STI/Recon Technical Report N*, *78*, 11293.

Hartel, R. W., Ergun, R., & Vogel, S., 2011. Phase/State Transitions of Confectionery Sweeteners: Thermodynamic and Kinetic Aspects. Compr. Rev. Food Sci. Food Saf., *10*(1), 17-32.

Hancock, B. C., Shamblin, S. L., & Zografi, G., 1995. Molecular mobility of amorphous pharmaceutical solids below their glass transition temperatures. Pharm Res., *12*(6), 799-806.

Kalichevsky, M. T., Jaroszkiewicz, E. M., & Blanshard, J. M. V., 1992. Glass transition of gluten. 1: Gluten and gluten—sugar mixtures. Int. J. Biol. Macromol., *14*(5), 257-266.

Kasapis, S., Al-Marhoobi, I. M., & Mitchell, J. R., 2003. Testing the validity of comparisons between the rheological and the calorimetric glass transition temperatures. Carb. Res., *338*(8), 787-794.

Kilmartin, P. A., Reid, D. S., & Samson, I., 2000. The measurement of the glass transition temperature of sucrose and maltose solutions with added NaCl. J. Sci. Food Agric. *80*(15), 2196-2202.

Kilmartin, P. A., Reid, D. S., & Samson, I., 2004. Dielectric properties of frozen maltodextrin solutions with added NaCl across the glass transition. J. Sci. Food Agric. *84*(11), 1277-1284.

Kumagai, H., & Kumagai, H., 2002. Analysis of Molecular or Ion Mobility in Glassy and Rubbery Foods by Electric and Proton-NMR Measurements. Food Sci. Technol. Res., *8*(2), 95-105.

Laaksonen, T. J., & Roos, Y. H., 2000. Thermal, dynamic-mechanical, and dielectric analysis of phase and state transitions of frozen wheat doughs. J. Cereal Sci., *32*(3), 281-292.

Labuza, T. P., & Labuza, P. S., 2004. Influence of temperature and relative humidity on the physical states of cotton candy. J. Food Proc. Pres., *28*(4), 274-287.

Liu, Y., Bhandari, B., & Zhou, W., 2006. Glass transition and enthalpy relaxation of amorphous food saccharides: a review. Agric Food Chem., *54*(16), 5701-5717.

Lourdin, D., Coignard, L., Bizot, H., & Colonna, P. 1997. Influence of equilibrium relative humidity and plasticizer concentration on the water content and glass transition of starch materials. Polym., *38*(21), 5401-5406.

Madeka, H., & Kokini, J. L., 1996. Effect of glass transition and cross-linking on rheological properties of zein: development of a preliminary state diagram. Cereal Chem., *73*(4), 433-438.

Moynihan, C. T., Easteal, A. J., Wilder, J., & Tucker., J. 1974. Dependence of the glass transition temperature on heating and cooling rate. J. Phys. Chem., *78*(26), 2673-2677.

Nowakowski, C. M. 2000. *Effect of Corn Syrup on Stability of Amorphous Sugar Products*. University of Wisconsin--Madison.

Noel, T. R., Ring, S. G., & Whittam, M. A. 1990. Glass transitions in low-moisture foods. Trends. Food Sci. Tech., *1*, 62-67.

Räsänen, J., Blanshard, J. M. V., Mitchell, J. R., Derbyshire, W., & Autio, K. 1998. Properties of frozen wheat doughs at subzero temperatures. J. Cereal Sci., *28*(1), 1-14.

Reiser, P. 1994. Sucrose: properties and applications. Berlin: Springer Science & Business Media.

Rotter, G., & Ishida, H. 1992. Dynamic mechanical analysis of the glass transition: curve resolving applied to polymers. Macromolecules, *25*(8), 2170-2176.

Richardson, T. 2003. Sweets: a history of candy. Bloomsbury Publishing USA.

Roos, Y., & Karel, M. 1991. Water and molecular weight effects on glass transitions in amorphous carbohydrates and carbohydrate solutions. J. Food Sci., *56*(6), 1676-1681.

Roos, Y. 1993. Melting and glass transitions of low molecular weight carbohydrates. Carbohydr Res., *238*, 39-48.

Roos, Y., & Karel, M. 1991. Plasticizing effect of water on thermal behavior and crystallization of amorphous food models. J. Food Sci., *56*(1), 38-43.

Roos YH. 1995. Phase transition in Foods. San Diego, Calif.: Academic Press

Ruan, R. R., & Chen, P. L. 1997. Water in foods and biological materials. CRC Press.

Schmidt, S. J., & Lammert, A., 1996. Physical aging of maltose glasses. J. Food Sci., *61*(5), 870-875.

Sivaraj, R., & Ravichandran, T., 2011. A review of selection methods in genetic algorithm. Int. J. Eng Sci and Technol., *3*(5).

Slade, L., & Levine, H., 1995. Glass transitions and water-food structure interactions. Adv. Food Nutr Res*., 38*(2), 103Á179.

Smidova, I., Copikova, J., Maryska, M., & Coimbra, M. A., 2003. Crystals in hard candies. Czech J. Food Sci., *21*(5), 185-191.

Tananuwong, K., & Reid, D. S., 2004. Differential scanning calorimetry study of glass transition in frozen starch gels. J. Agric. Food Chem., *52*(13), 4308-4317.

Van den Berg, O., Sengers, W. G., Jager, W. F., Picken, S. J., & Wübbenhorst, M., 2004. Dielectric and fluorescent probes to investigate glass transition, melt, and crystallization in polyolefins. Macromol., *37*(7), 2460-2470.

Figures

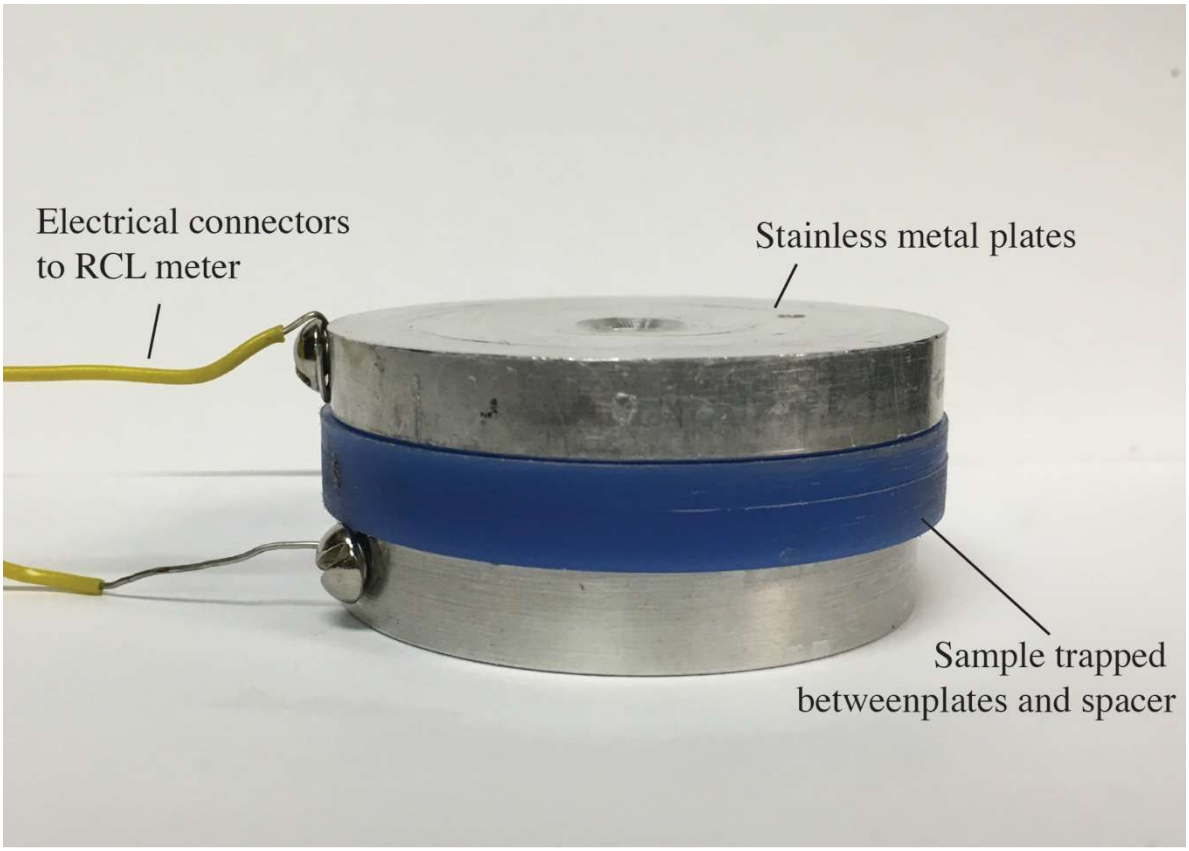

Figure 3.1. Capacitance cell used for measuring T_g values of candies.

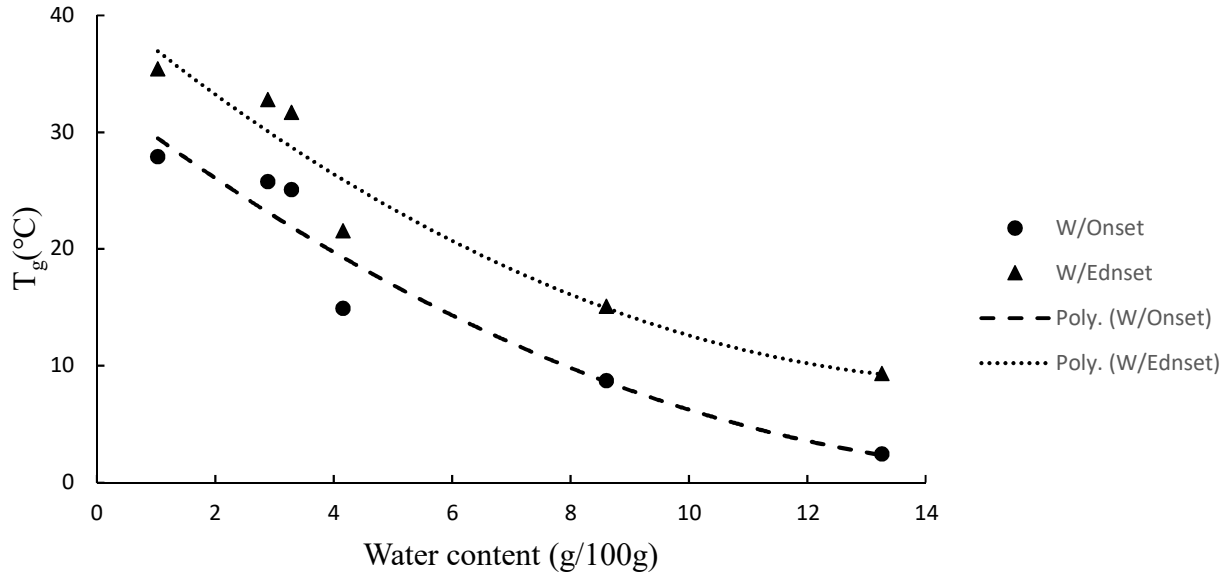

Figure 3.2. Influence of water content on the glass transition temperature as determined by DSC.

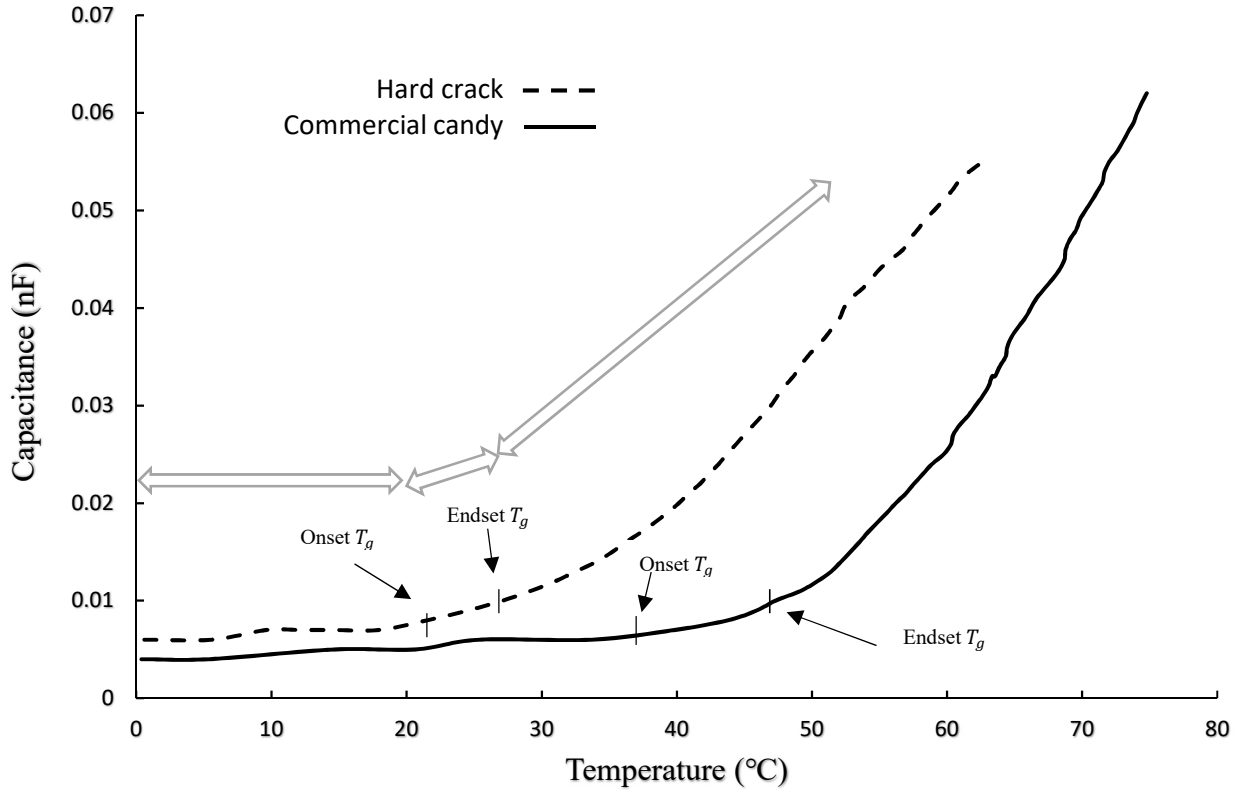

Figure 3.3. Temperature dependence of capacitance for heating candy through the glass transition, analyzed by a three-section genetic algorithm model.

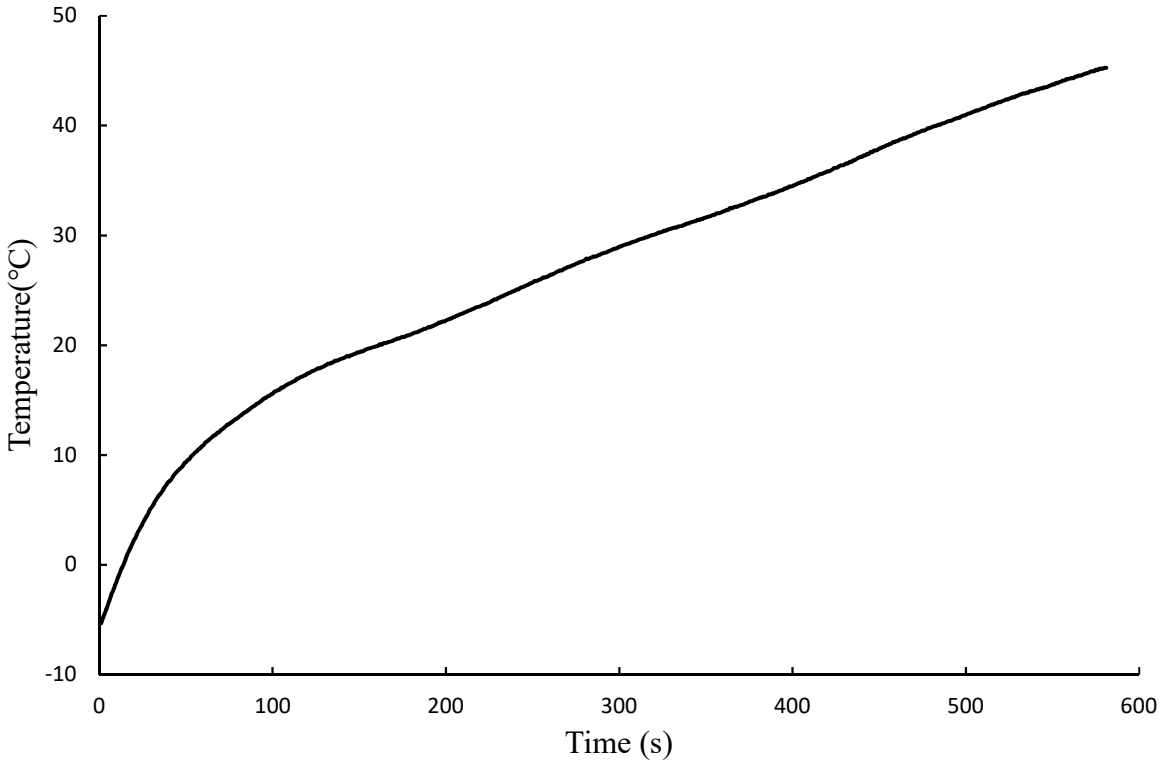

Figure 3.4. Sample temperature versus time during heating of a candy sample in the CTA capacitance cell.

Tables

Table 3.1 Range of candy samples used for study of T_g values.

Label	Texture	Boiling Temperature	Moisture ($gH_2O/100g$)
FB	Firm ball	125℃	13.3
SC	Soft crack	130℃	8.63
SH1		135℃	4.18
SH2		140℃	3.21
SH3		145℃	2.90
HC	Hard crack	150℃	0.92

[1]Hard candies were produced from 450g sucrose, 134g light corn syrup and 100 g deionized water

Table 3.2. Parameters of second-order polynomial model for glass transition temperature versus moisture content.

	a	b	c	R^2
Onset T_g (℃)	0.138	-4.2349	41.154	0.9336
Endset T_g (℃)	0.1143	-3.851	33.321	0.9291

Table 3.3. Glass transition temperature determined by calorimetry (DSC) and GA based capacitance (CTA) methods.

	FB	SC	SH1	SH2	SH3	HC	COM1	COM2
$gH_2O/100g$	13.3	8.63	4.18	3.21	2.90	0.92		
Capacitance based								
Onset T_g (℃)	5.1[b]	11.1[b]	16.4[b]	25.3[a]	26.5[a]	28.4[a]	44.0[a]	46.4[a]
Endset T_g(℃)	8.9[c]	14.8[c]	21.6[c]	31.2[b]	32.1[b]	36.6[c]	56.8[c]	57.2[c]
Fitness	0.1183	0.0563	0.1607	0.0568	0.1083	0.0225	0.1297	0.1547
Calorimetry (DSC)								
Onset T_g (℃)	2.4[a]	8.7[a]	14.9[a]	25.1[a]	25.8[a]	27.9[a]	44.5[a]	46.5[a]
Endset T_g (℃)	9.3[c]	15.0[c]	21.5[c]	31.7[b]	32.8[b]	35.4[b]	54.3[b]	55.6[b]

CHAPTER 4

DETERMINATION OF CHOCOLATE MELTING PROPERTIES BY CAPACITANCE BASED THERMAL ANALYSIS (CTA)[2]

[2] Tan, J. and W.L Kerr. Submitted to *Journal of Food Measurement and Characterization.*

ABSTRACT

Melting properties are important to the quality of manufactured chocolate products. Their measurement is often done by expensive and sophisticated equipment including differential scanning calorimetry, rheological and dielectric thermal techniques. In this study, a capacitance thermal analysis (CTA) was designed and tested for measuring the melting properties of chocolates. Chocolates with different fat content and particle size distribution (PSD) were placed between stainless steel plates, while capacitance and temperature were monitored between 20 to 60°C. The PSD did not influence the T_{onset} (~25°C) and T_{peak} (33°C) measured by DSC. However, samples with finer particles had lower Tend than those with coarser particles (36.59 - 37.28°C). Varying fat content did not result in differences in the DSC melting curves. Samples with smaller particle sizes had lower temperatures at peak capacitance than those with larger particles, with peak temperatures ranging from 30.84 to 39.29°C, while higher peak capacitance values (2.61 - 2.84 10-11 F) were measured by CTA. Samples with higher fat content had lower peak temperatures (range 34.7 to 39.71 °C) but higher peak capacitance values (range 3.29 to 4.3 10-11F). Values from the CTA were correlated with DSC.

Keywords: chocolate; melting properties; capacitance; thermal analysis

1. Introduction

Chocolate is a complex semi-solid suspension of fine particles containing cocoa, sugar, and sometimes dairy ingredients in a continuous fat phase (Afoakwa et al., 2007). Chocolates are categorized as dark, white, or milk chocolate based on the content of cocoa mass, dairy ingredients and cocoa butter. The production of chocolate starts from raw cocoa beans, which are then subjected to fermentation, roasting, milling, winnowing, refining, and tempering. The melting properties of chocolates are critical to their quality because they greatly influence consumer acceptability, appearance and storage stability of the product. Improper processing can lead to undesirable melting temperatures and crystal states, along with loss of glossy appearance or formation of fat bloom during storage (Afoakwa et al., 2009; Stapley et al., 1999; Dhonsi and Stapley 2006).

One important factor that influences melting properties is the crystal form of the fat phase in chocolate. The fat crystals may exhibit polymorphism, that is they may have more than two distinct crystalline forms in the same sample (Afoakwa et al., 2009). At least six polymorphic forms have been identified, designated Forms I through VI in the Roman numeral system (Schenk and Peschar 2004). The forms have different melting temperatures: 16-18°C for Form I, 22-24°C for Form II, 24-26°C for Form III, and 26-28°C for Form IV. Although, the most stable form is VI (m.p 34-36°C), that form is difficult to generate unless the chocolates go through lengthy storage. The preferred polymorph is Form V (m.p 32-34°C) in most cases (Wille and Lutton 1966).

Particle size distribution and fat content of the chocolate are also important factors influencing appearance, consumer acceptance, and processing properties. The influence of these factors on the rheological properties, texture and consumer evaluation of chocolates have been

well studied. Afoakwa et al. (2008) found that higher fat content and smaller particle size decreased the plastic viscosity of molten dark chocolate. Some researchers have noted that relatively large particle size of the cocoa mass can lead to sensations of grittiness or coarseness in the mouth (Servais et al., 2002). Do et al. (2007) studied how fat content and particle distribution of chocolate liquor influence the hardness and heat resistance of solid chocolates. They also found that chocolates with higher fat content need longer heating times to be completely melted. In addition, chocolates with finer particles exhibited relatively long melting times. However, the influence of fat content and particle size distribution on melting temperatures has been barely studied.

Differential scanning calorimetry (DSC) is one of the most commonly used methods to determine the melting properties of chocolates. The DSC compares the relative flow of heat between a sample and empty reference pan during a constantly changing temperature. Large changes in heat flow are indicative of increases in specific heat related to phase transitions (Afoakwa et al., 2008). Often the heat flow change during a phase transition is not a specific point, but associated with a temperature range. Therefore, there are several ways to characterize melting properties. That is, starch gelatinization, fat melting and other first-order transitions can be characterized by an onset temperature (T_{onset}), peak temperature (T_{peak}), ending temperature (T_{end}) and enthalpy of melting (ΔH_{melt}) (Vasanthan and Bhatty 1996).

The melting properties of chocolates have also been studied by dynamic thermal rheology (Glicerina et al., 2013). These instruments measure the storage modulus (G') or loss modulus (G"). As cocoa butter melts, the firm chocolate becomes softer and may begin to flow. Thus, G' is a good indicator to show the beginning and the end of chocolate melting. Generally, G' is on the order of 103 – 104 Pa for the solid and diminishes to 100 – 101 Pa once melted.

Dielectric thermal analysis (DETA) is another method to study phase transitions of food materials. DETA is carried out by a dielectric analyzer, which measures the change of dielectric constant ε' and dielectric loss ε'' of a food material as a function of temperature or AC frequency. The ε' is the ability of a material to store energy in response to an applied electric field. In contrast, ε'' describes the ability of one material to dissipate energy in response to an applied electric field, and that typically results in heat generation (Wang et al., 2003). The dielectric loss of a food material reaches a peak value when it reaches the second-order transition temperature, as with a glass transition. On the other hand, when a food material undergoes a first-order transition such as melting, the dielectric constant will increase greatly (Laaksonen and Roos 2000).

Capacitance is an electrical property dependent upon the dielectric properties of the medium. However, it is an easier property to measure as it does not require determination of both the real and imaginary components of ε*. In addition, many capacitance measuring instruments determine values at discrete frequencies. Thus, they are much simpler to build and less expensive than full-scale network analyzers. In this study, a capacitance based thermal analysis (CTA) system was proposed to study the melting properties of chocolate. The apparatus was constructed at the University of Georgia using metal plates and a relatively inexpensive capacitance meter. Capacitance is the ability of a subject to store electrical charge, and the capacitance of a parallel-plate capacitor can be determined as:

$$C=\varepsilon'\varepsilon_0\frac{A}{d} \quad (1)$$

where ε' is dielectric constant or permittivity of the medium between the parallel-plates, ε_o is the dielectric constant when the medium is air, A is the overlap area (completely and exclusively filled with medium) of the two parallel plates, and d is the distant between the two plates. The

variables related to the dimensions (A and d), as well as ε_0, remain relatively constant over a moderate temperature range. A medium such as food, particularly when undergoing a phase transition, will have an ε' and capacitance that changes substantially with temperature.

A few studies have used capacitance sensors similar to the CTA to study the glass transition and melting temperatures of frozen carbohydrate and NaCl solutions (Kilmartin et al., 2004). They found transition temperatures similar to those measured by differential scanning calorimetry. A similar system has been successful for measuring glass transitions in soft and hard sugar candies (Tan and Kerr 2017). In this study, a system is described to study the melting properties of chocolates with different fat content, particle size distribution and cocoa mass content. DSC and viscoelastic properties were also measured for comparison.

Frozen or glassy aqueous systems containing salts or low molecular weight compounds such as sugars and acids undergo a relatively large change in ε' when transitioning from solid to liquid. In contrast, high fat systems have comparatively smaller differences in ε' between solid and liquid states. Thus, the cell was modified from previous versions (Tan and Kerr 2017) to enhance the measured differences between states. The modified CTA consists of one smaller upper plate and one larger base plate. During a temperature scan, the chocolate sample (with larger area than the upper plate but smaller than the base plate) melts and collapses when the temperature reaches its melting point. The composition of the medium between the parallel plates changes from chocolate only to layers of chocolate and air. The capacitance of the layered medium is given by:

$$C=(\theta(T)\varepsilon'+(1-\theta(T))\varepsilon_0)\varepsilon_0 \frac{A}{d} \quad (2)$$

where $\theta(T)$ is the fraction of chocolate in the medium at different temperature.

The objective of this research was to evaluate the use of a modified CTA system to measure melting transitions in chocolate. In addition, samples with differing cocoa mass particle size and fat content were tested to determine if these had an influence on the measured properties.

2. Materials and Methods

2.1 Materials

Cocoa mass containing 70.4% cocoa solids was purchased from Callebaut (Wieze, Belgium). Raw organic cocoa butter was purchased from Saaqin (Hicksville, New York). Raw cocoa nibs were provided by Cocoatown (Roswell, Atlanta). Commercial chocolates were purchased from a Kroger grocery in Athens, Georgia.

2.2 Preparation of chocolate samples

Chocolate samples with different fat content were produced by mixing raw cocoa butter with cocoa mass in percentages of 10%, 20%, 30%, 40%, and 50% by weight. Each mix was treated in a tempering machine (Model Revolution 2, ChocoVision Corp., Poughkeepsie, New York). The program heating schedule included a gradual rise to 46°C followed by a slow decrease to 27°C. At that point Form V chocolate seed crystals were added followed by an increase in temperature to 31°C with a hold for 5 min. The well-tempered chocolate was poured into to 5cm χ 5cm χ 1.5 cm chocolate molds (Wilton INC. Woodridge, Illinois) and held overnight.

Particle size of the chocolate samples was controlled by varying the grinding time. Raw cocoa butter was mixed with cocoa nibs in a percentage of 10% and processed by a double-conical stone grinding conche (Model ECGC05, Cocoatown, Roswell, Atlanta). About 5 ml cocoa liquid was taken from the mix for particle size analysis every 15 min for the first 2 hours,

and every 1 h thereafter. Five different batches of cocoa butter and mass were processed in the conche for 15 min, 30 min, 1 h, 2 h, 4 h, and 12 h, respectively. The final chocolate liquor from each batch was used to make chocolate samples using the tempering method described above.

2.3 Particle size distribution

The particle size distribution was determined by laser diffraction using a Malvern Mastersizer (Model MSS, Malvern Instruments Ltd., Malvern, England). The presentation was selected as "Custom" with refractive indices of n(CH3)2CHOH = 1.378 and nparticle = 1.590. About 2 g of chocolate sample was melted and dispersed with 30 ml isopropanol in a 50 ml centrifuge tube, then mixed with a vortex mixer for 2 min. The samples were then introduced into the Mastersizer dispersion mixer until an obscuration of 20% was reached. Between samples, the detector and laser were aligned and backgrounds were calibrated. The size distribution was expressed as the relative volume of particles in each size range (Malvern MasterSizer Micro Software v 2.19). Several particle size distribution parameters were determined including largest particle size (d90), mean particle volume (d50), smallest particle size (d10), Sauter mean diameter (d3,2) and volume mean diameter (d4,3).

2.4 Capacitance based thermal analysis (CTA)

The parallel-plate capacitor cell (Figure 4.1) was built at the University of Georgia Instrument Design and Fabrication Shop (Athens, GA). It consisted of one 100 mm diameter stainless base plate, two 60 mm diameter stainless upper plates, one Teflon spacer, one Teflon cap and one stainless screw (12.5 mm in diameter). The base plate had a 4 mm hole drilled into the side to provide connection with a banana or needle plug. A cylinder spacer was made from Teflon with outer diameter 100 mm, inner diameter 80 mm and 100 mm in height. The lower side was fixed to the base plate by a groove on the base plate, while the upper side of the spacer

was fixed with a Teflon plate cap (100 mm in diameter). A stainless screw penetrated the Teflon cap at the center of the cap and both sides of the screw were welded with a stainless upper plate. The upper plate also had a 4 mm hole drilled into the side for connection.

Each chocolate sample was placed on the base plate and the upper plate lowered until it contacted the sample. The base plate was then heated by a Thermolyne Nuova hotplate at constant temperature (80°C). The measurement of capacitance was done with an LCR meter (NI PXI 4072, National Instrument Corporation, Austin, Texas) attached to a PXI chassis (NI PXI 1042, National Instrument Corporation, Austin, Texas). A T-type thermocouple (Probe 1/16'' diameter, OMEGA Engineering, Stamford, Connecticut) penetrated the base plate to just make contact with the sample on one side. Temperature data was collected with a data acquisition board (NI 9219, National Instrument Corporation, Austin, Texas). The virtual instrument interface and data collection were accomplished with LabVIEW software (Version 2015, National Instrument Corporation, Austin, Texas).

2.5 DSC

The melting temperature of each sample was determined by differential scanning calorimetery (Model DSC 1, Mettler-Toledo International Inc., Greifensee, Switzerland). Approximately 12 mg of each sample was sealed into a 40 ul aluminum pan. An empty pan was used as a reference sample. Dry nitrogen gas was used to minimize water condensation in the measuring cell. The temperature was scanned from 0°C to 60 °C at a heating rate of 5°C per minute. The onset temperature (T_{onset}), peak temperature (T_{peak}), end temperature (T_{end}) and enthalpy of melting (ΔH_{melt}) were calculated using the STARe Thermal Analysis Software. The melting index (T_{index}) was computed as (T_{end} -T_{onset}). Each sample was analyzed in triplicate and mean values and standard deviations reported.

2.6 Dynamic rheological analyses

The viscoelastic properties of the samples as a function of temperature were measured with a dynamic rheometer (Model Discovery HR-2, TA Instrument Inc., New Castle DE). Before the tests were initiated, the samples were melted and tempered in the rheometer. Approximately 4g of each chocolate sample was placed on the temperature-controlled stage below a 40 mm cone and plate probe (1.997°), then raised to 48°C at a rate of 5°C/min. The sample was then cooled to 26.7°C at a rate of 2°C /min. After a 5 min rest period, the temperature was raised to 31.6°C at a rate of 2°C/min. After the solid chocolate was formed, the sample was then cooled to 10°C at a rate of 15°C/min. The instrument was run in the small-strain oscillatory mode, with dynamic strains set to 1%. The temperature ramp was set at 10 to 60°C at a rate of 5°C/min.

2.7 Statistical methods

All tests were repeated at least three times and results presented as the mean and standard deviation. The results were compared by one-way ANOVA using SAS 9.3 (SAS Institute Inc., Cary NC) to determine the effects of the fat content and the particle size distribution of the chocolate sample on the melting properties measured by DSC and CTA. Tukey's HSD was used to determine significant differences amongst treatments at the 95% level of confidence.

3. Results and Discussion

3.1 Particle size reduction and particle size distribution

The largest particle size (d90) for a typical cocoa mix (fat and nibs) is shown in Figure 4.2 as a function of grinding time. A compilation of the size and distribution measurements (d10, d50, d90, d32, d4,3) is shown in Table 4.1. Most of the particle size reduction was achieved within the first 2 hours of grinding. The initial d90 was 77 µm, which was reduced to 15.4 µm within 2 h, and finally reached a constant value of ~8 µm (Figure 4.2). As shown in Table 4.1, the d90 and d4,3 were significantly smaller after 15 min, 30 min, 4 h and 8 h. The smallest

diameter particle (d10), however, did not decrease after 15 min. This indicates that the stone grinding is most effective at reducing the size of large particles, but a point is reached at which no further reduction in particle size is achieved.

A few researchers have studied the effects of particle size on the properties of chocolate products. Bolenz and Manske (2013) researched the impact of fat content during grinding on particle size distribution in chocolate milk. Afoakwa et al. (2008b) reviewed the role that particle size distribution and ingredients have in determining rheological and sensory properties of dark chocolate. In these cases, the researchers used a three-roller refiner followed by sifting to control particle size distribution, thus quickly creating fairly uniform particle size distributions with one peak. In our case, particle properties were determined solely by the grinding time. This is more reflective of industry practices, where stone grinding is often used to create small and uniform particle sizes after relatively long grinding times.

Figure 4.3 shows how the full particle size distribution changed during refining. Initially, there is a trimodal distribution with sizes centered around 1 μm, 12 μm and 190 μm. During grinding, the peak with largest particles diminished, and disappeared within 4 h. In conjunction, the middle peak shifted to smaller sizes, with the peak value going from 12 μm to 9 μm. The volume fraction of the medium size particles also increased with time, suggesting that this fraction grew at the expense of the larger particles.

3.2 DSC measurements of chocolate melting

The melting temperatures of chocolate samples measured by DSC are shown as a function of the refining time (Table 4.2) or fat content (Table 4.3). In general, particle size did not greatly affect the melting temperature as measured be either T_{onset} and T_{peak}. Samples with smaller particles had slightly higher T_{onset} and slightly lower Tend (and therefore smaller T_{index}).

The differences were small, however, with Tend ranging from 36.59 to 37.28℃ and T_{index} from 11.13 to 12.68℃. Other researchers have seen similar trends (Afoakwa et al., 2009; Beckett 2000), suggesting that in chocolate, PSD has only a small influence on melting properties. They concluded that chocolates with finer particles would take relatively longer time to melt than their corresponding products with larger particles. There is no particular reason that the lipid phase would have differing properties due to the cocoa mass particles. Thus, any measured differences in melting behavior might be attributed to different crystal sizes or polymorphs, or more likely due to differences in heat transfer rates in samples with different size particles.

Differences in fat content (10 to 50%) resulted in slightly different T_{onset}, T_{peak} and T_{end} values. T_{onset} varied from 25.70 to 26.11°C with increasing fat content, while Tend varied from 36.33 to 37.47°C. Thus, T_{index} (reflective of peak width) increased from 10.22 to 11.77°C. Again, this may reflect differences of heat transfer rates in the samples. In addition, samples with more fat will take longer to melt, and this plays out even as the calorimeter temperature is constantly increasing. Previous studies have shown that the melting properties can be influence by PSD, crystallization form (Svanberg et al., 2013, Loisel et all., 1997), lipid types, additives, and composition (Loisel et al., 1998) of chocolates. Others have suggested that the amount of fat in dark chocolates influences the degree of crystallinity and crystal size distribution (CSD) of the samples (Lonchampt and Hartel 2004).

3.3 Dynamic rheological analyses of chocolate melting

Changes in the dynamic rheological properties during temperature scans of chocolate were best characterized by the storage modulus (G') (Table 4.4). In general, G' in the solid state was ~103 – 104 Pa and decreased over a short temperature range corresponding to melting, to values near 101 Pa in the molten state. The beginning of melting was characterized as T_{onset},

where the gradient of this temperature point is at least 3 times greater than the previous three data points. The end of melting was characterized as T_{end}, where the gradient after T_{end} was less than 10% less than its previous three data points. The T_{index} of each sample was calculated as $T_{end} - T_{onset}$.

As found with the DSC results, increasing fat content resulted in larger T_{index} values, indicating samples with higher fat content had a broader temperature range over which they melted. In addition, the T_{onset} and T_{endset} measured by the rheometer were similar to DSC measurements, but did have slightly greater T_{onset} values. The difference may be attributed to the differing sample sizes (~ 3g vs ~10mg) required by the rheometer and DSC, respectively, and that different physical phenomena are being measured by the two instruments.

However, rheometric measurements did show a greater range in T_{onset} (25.33 to 28.11°C) than measured by DSC, and greater statistical significance amongst values measured for samples with differing fat levels.

3.4 CTA measurements of chocolate melting

Figure 4.4 shows a representative figure of how capacitance changes with temperature for chocolate samples in the CTA device. In general, capacitance values were in the picofarad range for samples in the solid state. As the temperature increased there was a slight increase in the capacitance, followed by a decrease after melting had commenced. The initial increase is likely due to an increase in the dielectric constant ε' as temperature increased, stemming from increased molecular mobility. However, changes would only be slight for molecules in the solid phase. There are different lipid fractions in cocoa butter, and some may begin to melt at lower temperatures. For example, Torbica et al. (2006) showed that cocoa butter had a solid fat content of 82%, 76%, 51% and 8% at temperatures of 20, 25, 30 and 35°C, respectively.

At a critical temperature, the capacitance began to drop. This coincided with melting of the chocolate, and its flow into the outer chamber, which began to reduce the volume of chocolate between the plates. The voids were replaced by air, which has a much lower dielectric constant (1.00059 at 20°C), and thus the measured capacitance began to decrease.

The particle size distribution (PSD) of the samples significantly influenced the temperature at peak capacitance, which ranged from 30.84 to 39.29℃ (Table 4.6), while peak capacitance values ranged from 26.1 to 28.4 pF. That is, finer PSD resulted in lower peak capacitance temperature and greater peak capacitance value. As previously noted, larger cocoa mass particle size can produce chocolate that is more difficult to melt. This likely resulted in higher peak temperatures for the CTA. In addition, and by design, the heating rate in the CTA was not carefully regulated, and this also resulted in slower melting.

It has also been observed that PSD influences the rheological properties of chocolate. Samples with larger PSD yielded lower apparent viscosity and lower yield stress (Afoakwa et al., 2007, Do et al., 2007, Mongia and Ziegler 2000). Changes in such properties may influence how the melted chocolate spreads away from the capacitance plates, and thus affects the measured transition temperature. However, this would be expected to give lower measured transition temperatures. Thus, the influence of particle size on heat transfer and the resulting rate of melting are likely to be the predominant factors.

Table 4.7 shows how the peak capacitance temperature varied with fat content in the chocolate. Samples with greater fat content resulted in lower peak capacitance temperature (range 34.7 to 39.71 ℃). This may be attributed to the fact that chocolates with greater fat content have lower apparent viscosity and yield stress, again making them easier to flow (Yanes et al., 2002, Sokmen and Gunes 2006). These observations concurred with results from the

dynamic rheology, which also indicated that higher fat content in chocolate samples produced lower T_{onset}.

Overall, samples with finer particles or lower fat content had lower peak capacitance values than those with larger particles and more fat. One of the critical factors that influences capacitance is the dielectric constant ε' of the medium. The ε' of cocoa butter (ε'~2.5) is higher than cocoa mass (ε'~1.5), so that higher fat content in chocolate samples will lead to higher absolute capacitance values. The way in which particles influence the dielectric properties of inhomogeneous media is complex. Several models have attempted to predict the complex permittivity of such media (Kiley et al., 2012). These models typically incorporate the ε' and ε" values for each phase, the volume fraction (α), and in some cases the shape or size factors of suspended media. In general, increasing the volume fraction would tend to emphasize the properties of the suspended phase. Experimental studies suggest that these models perform better at lower α, and fail at some critical value at which percolation behavior becomes dominant. This critical value is thought to be dependent on particle size and shape.

3.5 Comparison of CTA, DSC and rheological data

DSC and dynamic thermal rheological techniques have been widely used to study melting behavior. The former measures changes in specific heat during warming, the latter changes in mechanical relaxation for samples subject to oscillating shear stresses. Both require significant capital investments and user training to obtain useful results. The CTA device was proposed as a relatively inexpensive alternative for measuring melting behavior, and which requires minimal user skill.

The fat content and particles size had only a limited influence on melting temperatures as measured by DSC. Only the T_{index} provided some information as to the fat content and PSD of the samples. In contrast, CTA measurements were more sensitive to variations in fat content and

PSD. Rheological assessments of melting behavior were also more dependent on fat content and PSD. These observations reflect that melting has a thermodynamic component as well as a time-dependent element dependent on rates of heat transfer. Thus, the rheometer and CTA both require samples of greater mass as compared to that for DSC. Thus, DSC might be expected to give transition temperatures with greater precision, but may not totally reflect melting behavior as experienced by real world users of a product.

The transition temperatures measured by CTA were generally greater than those measured by DSC or rheometric techniques. This indicates that a sudden change in capacitance did not occur immediately upon reaching the Tm. As noted, the major change in capacitance probably did not occur until flow away from the plate had manifested. However, a correlation between CTA values and the other methods could be achieved. Both a linear model ($z=P_0+P_xX+P_yY$) and second order polynomial model ($z=P_0+P_xX+P_yY+ P_{xx}X_2+ P_{xy}XY$) were applied, with results shown in Table 4.8 for comparisons of the CTA and rheology data. The results showed that there were strong correlations ($R2>0.95$ and $SSE< 0.025$) between measurements from the CTA and rheometer.

4. Conclusions

The CTA device introduced in this study could measure melting temperatures in chocolate with good repeatability. The device also showed some sensitivity to the effects of cocoa particle size and fat content on melting behavior. The instrument was relatively inexpensive as it was built from metal plates connected to a capacitance meter, and did not require precise control of temperature ramping as used with DSC or dynamic thermal rheometers. While the measured temperatures were not identical to those from DSC or rheometric techniques, they could be easily correlated with those values if required.

References

Afoakwa, E. O., Paterson, A., & Fowler, M., 2007. Factors influencing rheological and textural qualities in chocolate–a review. Trends. Food Sci. Tech. 18(6), 290-298.

Afoakwa, E. O., Paterson, A., & Fowler, M., 2008a. Effects of particle size distribution and composition on rheological properties of dark chocolate. Eur Food Res. Technol. 226(6), 1259-1268.

Afoakwa, E. O., Paterson, A., Fowler, M., & Vieira, J., 2008b. Characterization of melting properties in dark chocolates from varying particle size distribution and composition using differential scanning calorimetry. Food Res Int. 41(7), 751-757.

Afoakwa, E. O., Paterson, A., Fowler, M., & Vieira, J., 2009. Influence of tempering and fat crystallization behaviours on microstructural and melting properties in dark chocolate systems. Food Res. Int. 42(1), 200-209.

Beckett, S. T. (2000). The science of chocolate (Vol. 22). Royal Society of Chemistry.

Bolenz, S., & Manske, A., 2013. Impact of fat content during grinding on particle size distribution and flow properties of milk chocolate. Eur Food Res. Technol. 236(5), 863-872.

Dhonsi, D., & Stapley, A. G. F., 2006. The effect of shear rate, temperature, sugar and emulsifier on the tempering of cocoa butter. J. Food Eng. 77(4), 936-942.

Do, T. A., Hargreaves, J. M., Wolf, B., Hort, J., & Mitchell, J. R., 2007. Impact of particle size distribution on rheological and textural properties of chocolate models with reduced fat content. J. Food Sci. 72(9), E541-E552.

Kilmartin, P. A., Reid, D. S., & Samson, I., 2004. Dielectric properties of frozen maltodextrin solutions with added NaCl across the glass transition. J. Sci. Food Agric. 84(11), 1277-1284.

Laaksonen, T. J., & Roos, Y. H., 2000. Thermal, dynamic-mechanical, and dielectric analysis of phase and state transitions offrozen wheat doughs. J. Cereal Sci. 32(3), 281-292.

Loisel, C., Keller, G., Lecq, G., Launay, B., & Ollivon, M., 1997. Tempering of chocolate in a scraped surface heat exchanger. J. Food Sci. 62(4), 773-780.

Loisel, C., Lecq, G., Keller, G., & Ollivon, M., 1998. Dynamic crystallization of dark chocolate as affected by temperature and lipid additives. J. Food Sci. 63(1), 73-79.

Lonchampt, P. and Hartel, R.W., 2004. Fat bloom in chocolate and compound coatings. European Journal of Lipid Science and Technology,106(4), pp.241-274.

Mongia, G., & Ziegler, G. R., 2000. The role of particle size distribution of suspended solids in defining the flow properties of milk chocolate. Int. J. Food Prop. 3(1), 137-147.

Servais, C., Jones, R., & Roberts, I., 2002. The influence of particle size distribution on the processing of food. J. Food Eng. 51(3), 201-208.

Schenk, H., & Peschar, R., 2004. Understanding the structure of chocolate. Radiat Phys. Chem. 71(3), 829-835.

Svanberg, L., Ahrné, L., Lorén, N., & Windhab, E., 2013. Impact of pre-crystallization process on structure and product properties in dark chocolate. J. Food Eng. 114(1), 90-98.

Sokmen, A., & Gunes, G., 2006. Influence of some bulk sweeteners on rheological properties of chocolate. LWT Food Sci. Technol. 39(10), 1053-1058.

Wille, R. L., & Lutton, E. S., 1966. Polymorphism of cocoa butter. J. Am Oil Chem Soc. 43(8), 491-496.

Stapley, A. G., Tewkesbury, H., & Fryer, P. J., 1999. The effects of shear and temperature history on the crystallization of chocolate. J. Am Oil Chem Soc. 76(6), 677-685.

Torbica, A., Jovanovic, O., & Pajin, B. 2006. The advantages of solid fat content determination in cocoa butter and cocoa butter equivalents by the Karlshamns method. Eur. J. Food Res. Tech. 222(3-4), 385-391.

Yanes, M., Durán, L., & Costell, E., 2002. Rheological and optical properties of commercial chocolate milk beverages. J. Food Eng. 51(3), 229-234.

Vasanthan, T., & Bhatty, R. S., 1996. Physicochemical properties of small-and large-granule starches of waxy, regular, and high-amylose barleys. Cereal Chem. 73(2), 199-207.

Wang, Y., Wig, T. D., Tang, J., & Hallberg, L. M., 2003. Dielectric properties of foods relevant to RF and microwave pasteurization and sterilization. J. Food Eng. 57(3), 257-268.

Figures

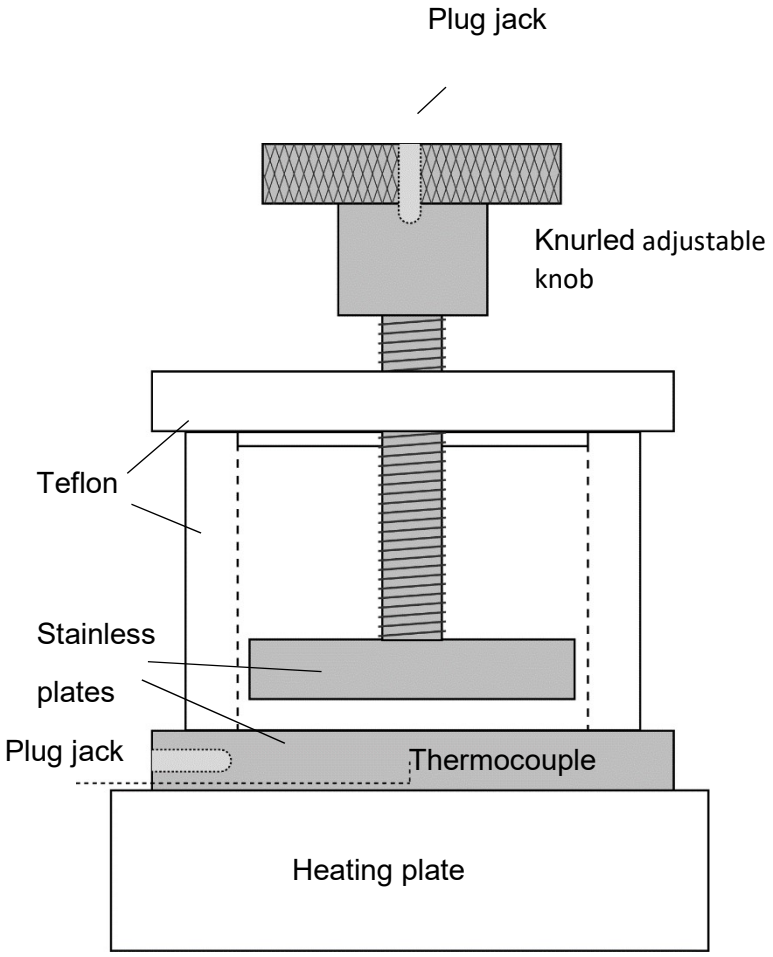

Figure 4.1. Configuration parellel-plate capacitor cell for CTA.

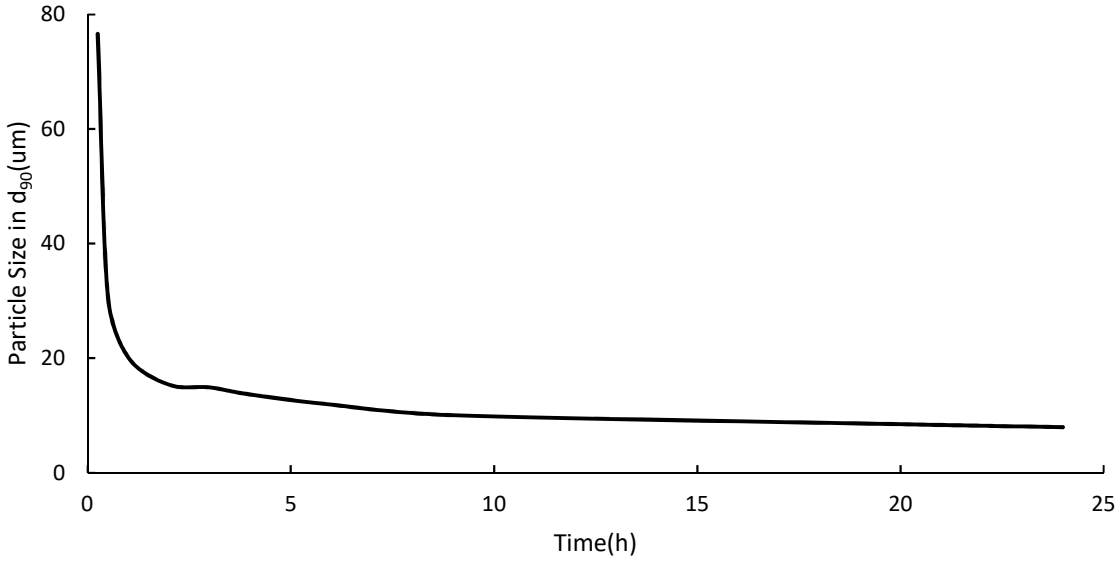

Figure 4.2. Particle size of chocolate mix (mass and butter) over time during conching.

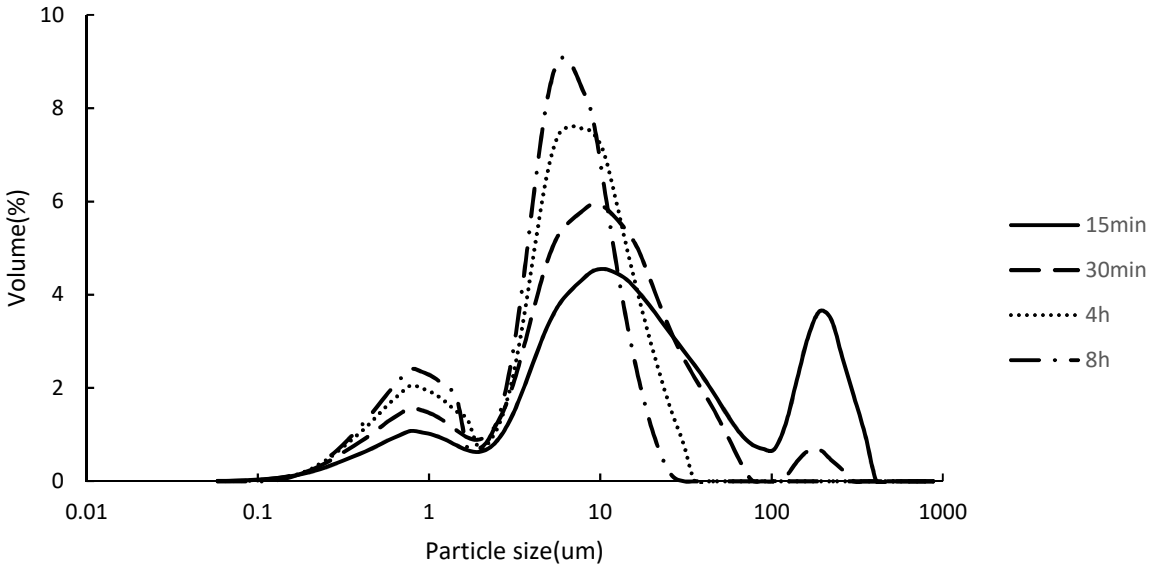

Figure 4.3. Particle size distribution of sample processed by different conching time.

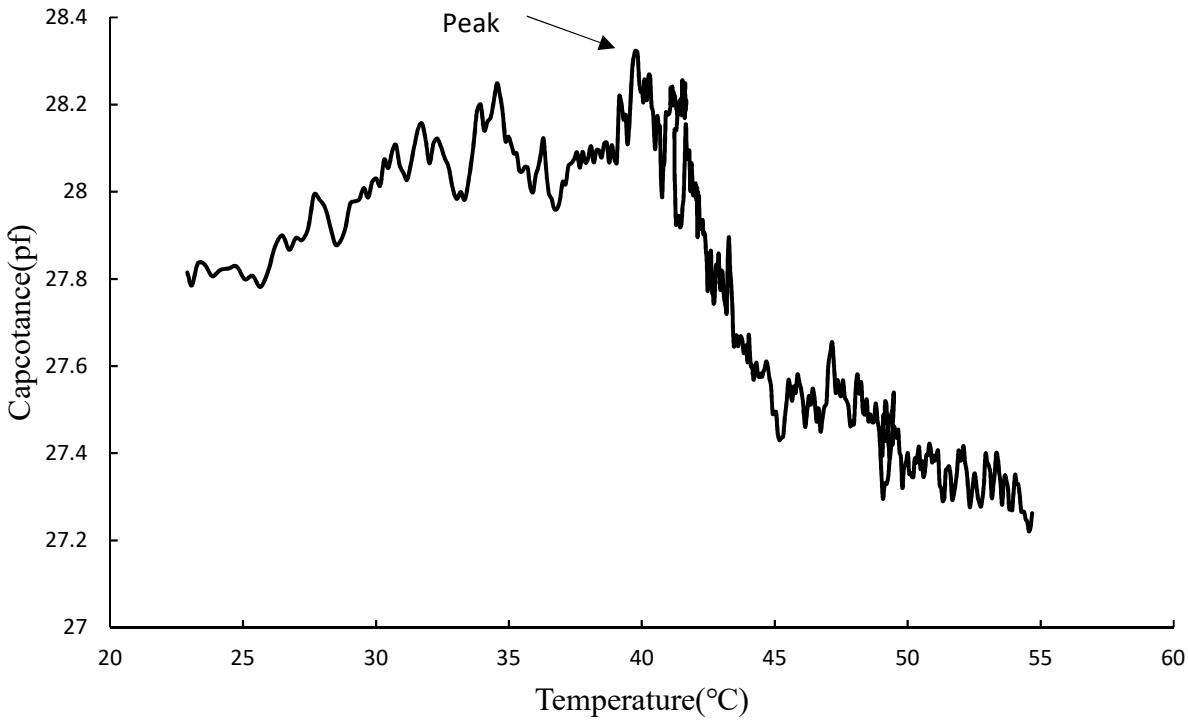

Figure 4.4. Capacitance change of capacitor cell as a function of temperature.

Table 4.1. Particle size distribution of samples as a function of conching time.

	d_{10}(um)	d_{50}(um)	d_{90}(um)	$d_{(3,2)}$ (um)	$d_{(4,3)}$ (um)
15 min	1.13^{b}	11.63^{c}	146.41^{d}	2.94^{b}	39.46^{d}
30 min	0.84^{a}	7.64^{b}	30.67^{c}	2.73^{b}	15.98^{c}
4 h	0.71^{a}	5.93^{a}	15.50^{b}	2.06^{a}	7.25^{b}
8 h	0.68^{a}	5.16^{a}	11.75^{a}	1.95^{a}	5.85^{a}

Table 4.2. DSC melting temperatures as a function of conching time.

	T_{onset}	T_{end}	T_{peak}	T_{index}
15min	24.60^{a}	37.28^{b}	32.97^{a}	12.68^{b}
30min	25.04^{ab}	37.05^{b}	32.86^{a}	12.01^{b}
4h	25.50^{b}	36.62^{ab}	32.94^{a}	11.12^{a}
8h	25.46^{b}	36.59^{a}	32.83^{a}	11.13^{a}

Table 4.3. DSC melting temperatures of samples with different fat content.

Fat content (%)	T_{onset}	T_{end}	T_{peak}	T_{index}
10	26.11^{b}	36.33^{a}	33.19^{a}	10.22^{a}
20	25.90^{ab}	37.02^{b}	33.40^{a}	11.12^{b}
30	25.68^{a}	37.19^{b}	33.80^{a}	11.51^{c}
40	25.61^{a}	37.23^{b}	33.57^{a}	11.62^{cd}
50	25.70^{a}	37.47^{b}	34.28^{a}	11.77^{d}

Table 4.4. Melting temperatures as a function of conching time as measured by dynamic rheometry.

	T_{onset}	T_{end}	T_{index}
15min	28.39^{d}	37.12^{a}	9.08^{a}
30min	26.17^{c}	37.96^{ab}	11.79^{b}
4h	25.56^{ab}	38.31^{b}	12.75^{c}
8h	25.11^{a}	38.93^{c}	13.82^{d}

Table 4.5. Melting properties of samples with different fat content determined by dynamic rheometry.

Fat content (%)	T_{onset}	T_{end}	T_{index}
10	28.11^{d}	37.19^{a}	9.08^{a}
20	27.19^{c}	37.66^{ab}	10.47^{b}
30	26.23^{bc}	37.91^{b}	11.68^{c}
40	26.11^{b}	38.23^{c}	12.12^{d}
50	25.33^{a}	38.91^{d}	13.58^{e}

Table 4.6. CTA transitions as a function conching time.

	Capacitance peak temperature (℃)	Peak capacitance (10^{-11}F)
15min	39.29^{d}	2.84^{d}
30min	36.14^{c}	2.75^{c}
4h	32.45^{b}	2.66^{b}
8h	30.84^{a}	2.61^{a}

Table 4.7. CTA transitions for samples with different fat content.

Fat content (%)	Capacitance peak temperature (℃)	Peak capacitance (10^{-11}F)
10	39.71[c]	3.29[a]
20	37.46[b]	3.70[b]
30	36.45[b]	4.11[c]
40	35.49[ab]	4.16[c]
50	34.70[a]	4.30[d]

Table 4.8. Correlation modeling between CTA and rheometric data.

	P_0	P_x	P_y	P_{x2}	P_{xy}	SSE	R^2
Linear							
x_1,y_1 vs z_1	14.97	-2.596	0.3373	0	0	0.1215	0.974
x_1,y_1 vs z_2	34.58	4.663	0.05447	0	0	0.0485	0.971
x_2,y_2 vs z_3	44.41	0.923	-0.1836	0	0	0.0820	0.952
x_2,y_2 vs z_4	5.54	0.2432	0.5765	0	0	0.2651	0.958
Polynomial							
x_1,y_1 vs z_1	-13.52	835.4	1.172	-160	-21.88	5.98×10^{-27}	1
x_1,y_1 vs z_2	63.87	-199.8	-0.6764	50.22	4.949	5.05×10^{-28}	1

x_1: added fat content, y_1: T_m of samples with different fat content measured by CTA, z_1: endset T_m of samples with different fat content measured by Rheometer, z_2: onset T_m of samples with different fat content measured by Rheometer, x_2: grinding time (min), y_2: T_g of samples with different grinding time measured by CTA, z_3: endset T_m of samples with different grinding time measured by Rheometer, z_4: onset T_m of samples with different grinding time measured by Rheometer

CHAPTER 5

PARTICLE SIZE MEASUREMENTS AND SCANNING ELECTRON MICROSCOPY (SEM) OF COCOA PARTICLES REFINED/CONCHED BY CONICAL AND CYLINDRICAL ROLLER STONE MELANGERS[3]

[3] Tan, J. and, B.M. Balasubramanian. Accepted by *Journal of Food Engineering*.
Reprinted here with permission of the publisher.

ABSTRACT

The particle size distribution (PSD) and the microstructure of the non-fat particles in chocolates are very important to the appearance, mouth feel and texture of the chocolate. Refining/conching is critical to chocolate processing because most particle size reduction is made and the microstructure of the particles is developed in this process. Currently, the commonly used comprehensive measurement method for chocolate products is using a laser scattering particle size analyzer, which is relatively expensive for small manufacturers. In this study, three potential alternative methods (micrometer, light microscopy image analysis and Hegman gauge) for the laser scattering method were used to measure the size of cocoa particles at different stages of refining/conching. Also, the influences of the sample weights of cocoa and melanger configuration (conical roller and cylindrical roller) on the efficiency of refining/conching were studied. The performances of the two melangers were similar, however, cylindrical roller stones tend to generate thin and flat particles during the first 4 h of refining. Varying sample weights only influenced particle size reduction at early stages of refining. From the SEM images, a decreasing trend in the number of large spherical particles and an increasing trend in the number of small flat irregularly shaped particles were observed. The particle size measurements by the micrometer of cocoa particles refined for 0.5 h was greater than all other methods. However, the particle size measurements by the micrometer of particles refined for 2 h, 4 h, and 24 h were smaller than the measurements made by any other methods. Except for cocoa being refined for 0.5 h, the particle size measurements tested by light microscopy image analysis for all cocoa samples were much greater than other measurement methods.

Keywords: cocoa; PSD; refining/conching; microstructure

1. Introduction

Cocoa originated in Central America over 1000 years ago, but its popularity and production has spread all over the world (Grivetti and Shapiro 2011). Chocolate is a complex suspension system of solid particles (cocoa, sugar, milk components, additives) in a continuous fat phase which consists of cocoa butter, milk fat and emulsifiers (Afoakwa et al., 2008a, Beckett 2000, Chetana et al., 2013). Chocolate can be a snack, special treat, or delicacy to be tested and evaluated much like wine to some people. For many people around the world, chocolate is an important industry. By 2016, the global chocolate market worth $98.3 billion (Worldatlas 2016).

The manufacture of chocolate generally includes procedures such as fermentation, roasting, cracking, winnowing, grinding, refining, conching, tempering, transporting and storing. Each procedure greatly influences the final quality of the chocolate. Refining and conching are very important because they determine the particle size distribution (PSD), suspension consistency and viscosity of chocolates, to yield specific textural and sensory qualities (Afoakwa et al., 2007). Refining is a step following grinding, where the particle size of chocolate is greatly reduced, producing an extremely smooth texture in which no grit can be detected by the tongue (Lucisano et al., 2006). Conching is a long process of continuous mixing, agitating, and aerating the heated chocolate liquid. During this process, undesirable flavors and bitter substances, along with water vapor evaporate away from the chocolate liquid (Capodieci 1993). In many cases, refining and conching were combined into one process. For example, when using a melanger to process raw cocoa nibs, the cocoa nibs were crushed and sheared along with mixing and agitating.

The PSD and the microstructure of the non-fat particles in chocolates are two very important factors that influence the flow behavior (Fischer, 1994; Mongia and Ziegler 2000) and

sensory quality of the chocolate (Ziegler et al., 2001). Inhomogeneous particles tend to give a pasty chocolate that is harder to manipulate in the mouth (Beckett, 1994). It has been hypothesized that the finer the chocolate, the sweeter the taste, because small crystals dissolve faster than larger crystals. However, there was no published systematic research on the effect of particle fineness on the flavor of chocolate (Ziegler and Hogg, 2009).

The measurements of the PSD and microstructure of chocolate particles are conducted by relatively expensive equipment, such as laser particle size analyzers (Glicerina et al., 2014; Bolenz et al.,2014; Hahn et al., 2015; Toker et al., 2016) and scanning electron microscopy (SEM) image analysis (Luo et al., 2013; Börjesson et al., 2014). However, small/medium chocolate manufacturers have limited access to this type of equipment. In addition, the usage and maintenance of the equipment is costly and complicated. Therefore, developing fast and inexpensive methods for measuring PSD is very critical for small/medium chocolate manufacturers. A previous study (Meghwal and Goswami, 2013) used a sieve to determine the PSD of black pepper, however, the sieve is not applicable to paste-like samples, such as cocoa paste, because of the high viscosity of the paste.

In this study, three particle size measurement methods using a micrometer, Hegman gauge, and light microscopy image analysis were developed. The measurement methods were used to monitor the PSD profile of cocoa during the refining/conching process and compared to measurements conducted by a laser scattering particle size analyzer.

The refining and conching procedure usually takes about 12-24 h before reducing the particle size to around 20 ums (Afoakwa et al 2007). The time needed for these processes depends mainly on the amount of material being refined and the configuration of the refining/conching equipment. The efficiency of refining and conching is very critical for

chocolate manufacturers, because the energy cost and time expended may influence the profit of the manufacturers. In this study, two configurations of grinding roller stones (conical and cylindrical) were tested with different sample weights (1 kg, 1.5 kg and 2 kg) and the particle size profiles of the materials were monitored as a function of time.

As mentioned before, the shape of the cocoa particles in chocolate products is a very important factor for the texture of the products. In this study, SEM images of the cocoa samples were used to study the change in shape of the particles during the refining/conching process with different grinding roller stones.

2. Materials and methods

2.1 Sample preparation

Raw cocoa beans (*Frastero*) were roasted by a mini drum roaster (Model SS, CocoaTown, Roswell, Georgia, USA) (30 min roasting per kg batch of cocoa beans). 50 kg roasted cocoa beans were prepared. The roasted beans were immediately chilled by a tray cooler (CocoaTown, Roswell, Georgia, USA) after roasting and then cracked by a manual mini cracker (CocoaTown, Roswell, Georgia, USA). A mini vacuum winnower separated the husk and nibs (CocoaTown, Roswell, Georgia, USA).

The refining and conching was done by feeding cocoa nibs into a melanger (Model ECGC-12SL, CocoaTown, Roswell, Georgia, USA) and refining for 24 hours. The melanger was equipped with either a double conical roller stone or a double cylindrical roller stone to crush and refine the cocoa nibs. Both of the cylindrical stones were 10 ± 0.5% cm in diameter and 5 ± 0.5% cm in height. Both of the conical stones were 2 ± 0.5% cm and 12 ± 0.5% cm in diameter on each side respectively, and the height was 10 ± 0.5% cm. In this study, cocoa samples with three different sample weights were processed by the melanger equipped with each configuration

respectively. During the refining/conching process, about 5 ml cocoa paste was taken from the melanger after the process began for 15 min, 30 min, 1 h, 1.5 h, 2 h, 4 h, 6 h, 8 h and 24 h.

2.2 PSD analysis by micrometer and Hegman gauge

Cocoa paste samples were first mixed with vegetable oil at a ratio 1:1. Then, one drop of the mix was transferred to the anvil face of a digital micrometer (model: H-2780, Mitutoyo America Cooperation, Aurora, IL, USA). Next, the spindle was lowered until a 'click' sound indicated the measurement was finished.

One Hegman gauge (Model: PB-40, Precision Gage & Tool Co., Dayton, OH, USA) was also used to measure the particle size of the cocoa paste samples. The Hegman gauge measurements were conducted according to the standard method described by ASTM (2005).

2.3 PSD analysis by light microscopy image analysis

Samples were melted by a hair dryer and mixed with isopropanol alcohol (99% pure) into a suspension solution with a ratio of 1:20 in a 20ml glass tube. The mixture was then homogenized by a vortex mixer (Fisher Scientific, Hampton, NH, USA). Two drops of the mixture were transferred to a glass slide by a transfer pipette and covered with a cover glass. The slide was then observed under a 40X-2500X LED digital trinocular lab compound microscope (OMAX, Kent, WA, USA). The microscope was coupled with a 5MP camera (OMAX, Kent, WA, USA) and the magnification of the objective lens was 10x. Five pictures were taken at different locations randomly for each sample.

ImageJ (Version 1.47) was used to process the light microscopy images according to the following steps. First, the picture was loaded into the software. Then the ratio of the real distance versus unit distance on the picture was provided. Next, thresholding was conducted to highlight

the objects from the background and erosion was conducted, followed by dilation to eliminate noise. Finally, segmentation was performed to separate particles from each other and calculate the area of each detected particle. The diameter of each detected particle was calculated from the its area by taking each particle as a perfect circle. Parameters including d_{10}, d_{50}, d_{90} and d_{mean} for each sample were calculated, where d_{xx} indicated xx% of the particle size (in diameter) was smaller than d_{xx}.

2.4 PSD measurement by laser scattering

The PSD of all samples was measured by a Malvern Mastersizer (Model MSS, Malvern Instruments Ltd., Malvern, England) as a reference. The presentation was selected as "Custom" and set $n_{(CH3)2CHOH} = 1.378$, $n_{particle} = 1.590$). About 2 g of cocoa paste sample was melted and dispersed with 30ml isopropanol in a 50ml centrifuge pipe, stirring by an analog vortex mixer for 2 min. Then, samples were introduced into a stirred tank filled with isopropanol until an obscuration of 20% was reached. Between each measurement, the detector and laser were aligned and the background was calibrated. Size distribution was quantified as the relative volume of particles in size bands presented as size distribution curves (Malvern MasterSizer Micro Software v 2.19). PSD parameters obtained included largest particle size (d_{90}), mean particle volume (d_{50}), smallest particle size (d_{10}), Sauter mean diameter $d_{(3,2)}$ and volume mean diameter $d_{(4,3)}$.

2.5 SEM image analysis

SEM was used to obtain information about the surface morphology of the cocoa particles. The sample preparation for the SEM followed the method suggested by Chatana et al (2013) with some modifications. The cocoa paste sample was first defatted with isopropanol and then the isopropanol was removed by vacuum filtration. The remaining cocoa solids were placed on

the sample holder with the help of double scotch tape and then, the powder was sputter-coated with gold/palladium (2 min, 2 mBar) where it was observed at 15 kV, and examined with the SEM (model:1450 EP, Carl Zeiss MicroImaging Inc, Thornwood, NY, USA). At least 5 pictures for each sample were taken at randomly selected locations.

2.6 Statistical method

All tests were repeated at least three times and results were displayed as mean of the measurements ± standard deviation. Measurements were compared by one-way ANOVA using SAS 9.3 (SAS Institute Inc., Cary NC) to determine the effect of the fat content and the particle size distribution of the chocolate sample on their melting properties measured by DSC and contact based CTA. Tukey multiple comparisons at 95% significance determined differences between factor levels.

3. Results and discussion

3.1 Particle size measurements of cocoa conducted by laser scattering method and the influences of the melanger configuration

One of the main aims of the refining/conching process was to reduce the particle size of cocoa solids so that the final particles are small enough to not be detected on the tongue. Refining/conching also reduce unpleasant flavors and develops chocolate aroma by a mechanism combining particle size reduction, heating, and shearing (Beckett 2009). The diagram or configuration of the refining equipment has great influences on the physical properties of the chocolate products and the efficiency of the refining/conching process. The most predominant configuration of melangers that chocolate manufacturers are currently using is cylindrical roller stones (Lucisano et al., 2006; Bolenz et al., 2003), while some manufacturers also select conical roller stones for refining. Many studies provided the performance of different types of mills

during the grinding process of food materials. For example, Meghwal and Goswami (2014) provided comprehensive studies comparing particle size reduction of black pepper and fenugreek conducted by hammer, pin, rotor and ball mill.

Figure 5.1 shows the change of particle size (d_{90} measured by laser scattering method) of cocoa solids as a function of time in cylindrical and conical roller stone melangers. The particle size reduction made by the melanger equipped with conical roller stones was greater than the melanger equipped with cylindrical roller stones for the first 4 hours of refining. However, after 4 hours of refining, the reductions made by the two melangers were not significantly different. This was because big cocoa particles were much more likely being crushed and sheared by the roller stones than small particles at the beginning stage of refining. At the later stages, small particles (<20 um) prevailed and they were missed by the roller stones because of relatively small size of the particles, and the particle size reduction made by shearing was relatively slow compared to crushing. The measurements conducted by laser scattering methods were based on the volumes of the particles. Therefore, at the beginning stage, conical roller stones tend to make smaller particle clusters than cylindrical roller stones. As many previous studies (Imai et al., 1995; Servais et al., 2002; Afoakwa et al., 2008b; Carvalho-da-Silva et al., 2013) indicated, well refined smooth chocolates should have particle size, in terms of d_{90}, less than 20 ums. In this case, it took both melangers more than 8 hours to reach that goal, which implied that although greater particle size reduction can be made by the melanger equipped with conical roller stones, the efficiency for finishing the refining/conching process was the same for the two melangers.

The particle size profiles of cocoa samples with different initial sample weights were shown in Figure 5.2. The profiles indicated that the particle size reductions of samples with different sample weights were similar after 2.5 hours of refining, which implied that as long as

the sample weight of cocoa nibs did not overfill the drum of the melanger, the times needed for finishing the refining/conching process, in terms of matching particle size requirement, were not significantly different.

3.2 SEM image analysis

In Figure 5.3, the images show cocoa particles observed by SEM microscope. Many large spherical particles with diameters greater than 200 um, along with many small shards can be seen in the images of the 30 min refined cocoa sample. From the images of the cocoa samples refined for 2 hours and 4 hours, fewer large spherical particles can be observed compared to the images of the 30 min refined sample. In addition, the diameters of the large spherical particles were decreased to ~120 um for 2 h refined particles and ~100 um for 4 h refined particles. Except for the large spherical particles, most of the particles observed were flat irregular small pieces of cocoa solids and their clusters. The size of the flat irregular small pieces was around 10 um and the quantity of these particles increased as a function of refining time. After 24 h of refining, the flat irregular small pieces of cocoa solids predominated. Barely any spherical particles were observed. The formation of the flat irregular pieces was due to the repeated crushing and shearing by the roller stones. When refining was ongoing, the roller stones spanned at fast speed (120 rpm), smashing and rolling over the cocoa particles, thus, creating great crushing and shearing force on the particles. The speed gradient between cocoa paste at different locations of the melanger, however, also resulted in shearing force between the cocoa particles. The influences of the shearing force on the microstructure of particles had two side, it tore the particles into small piece, on the other hand, it pushed the particles to form clusters due to steric hindrance between particles.

Some previous studies (Hoskin and Dimick 1980; Beckett 1995) also observed the phenomena that refining made spherical cocoa particles into small flat pieces. For most chocolate products, texture is very important. The desired texture gives a smooth mouth feel when chocolate melts on the tongue. This smooth mouth feel is created by many factors including the shape, size and homogeneity of chocolate particles (Viaene and Januszewska 1999; Engelen et al 2005., Do et al., 2007). Kilcast and Clegg (2002) directly related thickness of cocoa particles to the smoothness of the chocolate. The flat irregular small particles created by refining and observed by SEM microscopy in this study were similar to the cocoa particles described by previous studies for making high quality chocolate.

3.3 Comparison of the PSD measurement methods

Figure 5.4 shows the particle size of the same samples described in 3.1, but the measurements were conducted by the micrometer. The essential element of measuring instruments operating on the micrometer principle is amplifying small distances into large rotations of the screw that are big enough to read from a scale. The screw of the micrometer is integrated with the measuring spindle, whose face establishes the measuring contact with the object. The distance of that contact face from a fixed datum constitutes the measuring length, which is then displayed by the scale graduations of the micrometer (Lanz and Molina 1820).

By Comparing the trendlines in Figure 5.4 to the measurements in Figure 5.1 and Figure 5.2, similar conclusions as in 3.1, about the influences of the sample weight of cocoa on the particle size reduction profiles can be drawn. Varying the sample weights only resulted in different amounts of particle size reduction at the first 2.5 hours of refining. After 2.5 hours of refining, there were no significant differences between samples with different sample weights in terms of particle size. However, based on the measurements conducted by the micrometer, the

conclusion of the influences of the configurations of the melangers on the particle size reduction of cocoa was different from the conclusion based on the measurements conducted by the laser scattering method. The particle size reduction achieved by the cylindrical roller stones melanger was greater than the reduction made by the melanger equipped with conical roller stones for the first 4 hours of refining. However, after 4 hours of refining, the particle size of the samples processed by the two melangers were not significantly different.

Unlike measuring the diameters of the particles based on their two-dimensional areas or volumes, the micrometer measured the thickness of the particles and the particle clusters. In Figure 5.5, the linear speed gradients of cocoa paste in different melangers were displayed. With rollers running at constant rotational speed, the linear speed of the cocoa paste at the outer edge of the cylindrical roller stones was much faster than the linear speed of the paste at the inner edge of the roller stones due to the difference in the distances between the two edges of the stones to the center of the drum. Therefore, there was a great linear speed gradient between the cocoa paste at the center and the cocoa paste at outer space of the drum. As mentioned in 3.2, the gradient introduced shearing force between particles and generated particle clusters. The clusters had greater volume than single particles and they were more likely being crushed by the roller stone. Therefore, the thickness of the particles was decreased by repeating crushing. In addition, the shearing force also tore the particles into small pieces, which also decreased the size of the particles. . On the other hand, the linear speed gradients created by conical roller stones at different locations of the drum were much smaller than the one made by cylindrical roller stones. The shearing force introduced by conical roller stones to the cocoa particles was much smaller than the shearing force introduced by cylindrical roller stone. Therefore, it took more time for the conical roller stone than the cylindrical roller to tear the particles into small particles by shearing

force. In addition, weak shearing force introduced by conical roller stones took more time to form clusters which can be crushed by roller stones. This theory explained why the measurements conducted by the micrometer were different from the measurements using the laser scattering method.

The particle size of samples refined by the melanger equipped with double conical roller stones at 4 different stages (30 min, 2 h, 4 h and 24 h) of refining was measured by 4 different methods (laser scattering, micrometer, Hegman gauge and light microscopy image analysis) and the measurements were summarized in Table 5.1. The particle size measurement conducted by the micrometer for 30 min refined cocoa particles was greater than the measurements made by using all other method, because the micrometer measured the size of the biggest particles in the sample. However, other methods measured the d_{90} of the particles, which is not necessarily the size of the biggest particle in the sample. The particle size measurements conducted by the micrometer for cocoa particles refined for 2 h, 4 h, and 24 h were smaller than the measurements provided by any other methods. The SEM image analysis for cocoa particles indicated that as cocoa particles were refined for more time, more small flat particles were created. The measurements conducted by the micrometer were actually measuring the thickness of the clusters of small flat particles, rather than the two-dimensional diameter of the biggest particle in the samples, while most of the spherical particles were deformed to flat particles. Therefore, the measurements produced by the micrometer were much smaller than measurements produced by other methods for samples from later stages of refining/conching.

Figure 5.6 shows how raw images from the light microscope processed by ImageJ and how the particle size of cocoa solids was calculated. From Table 5.1, generally, except for measurements of 30 min refined cocoa sample, the measurements conducted by light microscopy

image analysis for all other samples were much larger than the measurements made by other methods. One theory to explain this phenomenon would be that the light illuminated the small thin particles (<10 um) and partially penetrated the thin small particles, which decreased the intensity of the pixels that represented the small particles in the images. In addition, the number of particles that can be detected from the images should be great enough (>80 particles) that the particle size distribution of the samples can be calculated. Thus, the magnification of the objective lens should not be greater than 10 x. With 10 x magnification objective lens, the size of small particles shown in images were relatively small. Therefore, some of the small particles were very likely to be filtered out along with background noise during image thresholding and erosion. In addition, the number of particles that could be captured by the camera in one image was ~100, which is relatively small compared the number of particles captured by using laser scattering. With the number of small particles greatly decreased, the values of d_{90} were closer to the size of the bigger particles.

The measurements conducted by Hegman gauge were presented as the size of the smallest particle - the biggest particle in the samples and the measurements were shown in Table 5.1. The gauge consists of a steel block with a series of very small parallel grooves machined into it. The grooves decrease in depth from one end of the block to the other, according to a scale stamped next to them (McKay 1994). Generally, the measurements tested by Hegman gauge were not meaningful in this study, because cocoa samples were cocoa solids in continuous fat phase and the viscosity was very high. Therefore, the small particles can still fill the deep groove on the gauge by accumulation, which increased the ceiling of the particle size range of the samples. In addition, the fat phase of the paste also filled up the shallow side of the groove, which decrease the threshold of the particle size range.

4. Conclusion

Based on the measurements conducted by laser scattering methods, the efficiency of refining by using the melanger equipped with double conical roller stones was higher than using the cylindrical roller stone melanger at the beginning stage of refining. However, at later stages (>4 h), both melangers showed similar efficiency in terms of particle size reduction. Based on the measurements conducted by the micrometer, the cylindrical roller stone melanger had higher efficiency than the conical roller stone melanger at the beginning stage. Similarly, the sample weight only influenced the particle size reduction at the beginning stage. Therefore, the sample weight and the type of melanger were not critical to the efficiency of refining since refining usually takes more than 12 hours. Both the micrometer and light microscopy image analysis methods can be used to monitor the particle size of cocoa solids during refining. However, the Hegman gauge failed to provide meaningful information due to the incorrect measurements of the boundary values of the particle size. Although, the micrometer and light microscopy image analysis methods did not provide as comprehensive information of PSD as the laser scattering method, they provided useful information from different angles, concerning how the particle size of cocoa solids changed over time during the refining/conching process. The measurements provided by the two methods can serve as a good alternative to the particle size measurements provided by the laser scattering method.

References

Afoakwa, E.O., Paterson, A. and Fowler, M., 2007. Factors influencing rheological and textural qualities in chocolate–a review. Trends Food Sci. Technol. 18(6), pp.290-298.

Afoakwa, E.O., Paterson, A. and Fowler, M., 2008. Effects of particle size distribution and composition on rheological properties of dark chocolate. Eur. Food Res. Technol. 226(6), pp.1259-1268.

Afoakwa, E.O., Paterson, A., Fowler, M. and Vieira, J., 2008. Particle size distribution and compositional effects on textural properties and appearance of dark chocolates. J. Food Eng., 87(2), pp.181-190.

ASTM Standard D01, 2005, " Physical Properties of Liquid Paints and Paint Materials," ASTM International, West Conshohocken, PA, 2003, DOI: 10.1520/C0033-03, www.astm.org.

Beckett, S.T., 1994. Control of particle size reduction during chocolate grinding. Manufacturing Confectioner, 74, pp.80-80.

Beckett, S.T., Nestec SA, 1995. Chocolate shape retention. U.S. Patent 5,445,843.

Beckett, S., 2000. The science of chocolate (Vol. 22). Royal Society of Chemistry.

Beckett, S.T., 2009. Conching. Industrial Chocolate Manufacture and Use, Fourth Edition, pp.192-223.

Bolenz, S., Thiessenhusen, T. and Schäpe, R., 2003. Fast conching for milk chocolate. Eur. Food Res. Technol. 218(1), pp.62-67.

Bolenz, S., Manske, A. and Langer, M., 2014. Improvement of process parameters and evaluation of milk chocolates made by the new coarse conching process. Eur. Food Res. Technol. 238(5), pp.863-874.

Börjesson, E., Innings, F., Trägårdh, C., Bergenståhl, B. and Paulsson, M., 2014. Evaluation of particle measures relevant for powder bed porosity—A study of spray dried dairy powders. Powder Technol. 253, pp.453-463.

Capodieci, R.A., Mars, Incorporated, 1993. Chocolate conching. U.S. Patent 5,200,220.

Carvalho-da-Silva, A.M., Van Damme, I., Taylor, W., Hort, J. and Wolf, B., 2013. Oral processing of two milk chocolate samples. Food & function, 4(3), pp.461-469.

Chetana, R., Reddy, S.R.Y. and Negi, P.S., 2013. Preparation and properties of probiotic chocolates using yoghurt powder. Food Nutr. Sci.4(3), p.276.

Do, T.A., Hargreaves, J.M., Wolf, B., Hort, J. and Mitchell, J.R., 2007. Impact of particle size distribution on rheological and textural properties of chocolate models with reduced fat content. J. Food Sci. 72(9), pp.E541-E552.

Engelen, L., de Wijk, R.A., van der Bilt, A., Prinz, J.F., Janssen, A.M. and Bosman, F., 2005. Relating particles and texture perception. Physiology & behavior, 86(1), pp.111-117.

Fischer, B.J., 1994. Particle Size Distribution Effects on Rheology of Molten Dark Chocolate.

Glicerina, V., Balestra, F., Rosa, M.D., Bergenhstål, B., Tornberg, E. and Romani, S., 2014. The Influence of Different Processing Stages on Particle Size, Microstructure, and Appearance of Dark Chocolate. J. Food Sci. 79(7), pp.E1359-E1365.

Grivetti, L.E. and Shapiro, H.Y., 2011. *Chocolate: history, culture, and heritage*. John Wiley & Sons.

Hahn, C., Nöbel, S., Maisch, R., Rösingh, W., Weiss, J. and Hinrichs, J., 2015. Adjusting rheological properties of concentrated microgel suspensions by particle size distribution. Food Hydrocolloids, 49, pp.183-191.

Hoskin, J.M. and Dimick, P.S., 1980. Observations of chocolate during conching by scanning electron microscopy and viscometry. J. Food Sci. 45(6), pp.1541-1545.

Imai, E., Hatae, K. and Shimada, A., 1995. Oral perception of grittiness: effect of particle size and concentration of the dispersed particles and the dispersion medium. J. Texture Stud. 26(5), pp.561-576.

Kilcast, D. and Clegg, S., 2002. Sensory perception of creaminess and its relationship with food structure. Food Quality and Preference, 13(7), pp.609-623.

Lanz, P.L. and y Molina, A.D.B., 1820. Analytical Essay on the Construction of Machines. J. Diggens for R. Ackermann.

Lucisano, M., Casiraghi, E. and Mariotti, M., 2006. Influence of formulation and processing variables on ball mill refining of milk chocolate. Eur. Food Res. Technol. 223(6), pp.797-802.

Luo, P., Morrison, I., Dudkiewicz, A., Tiede, K., Boyes, E., O'TOOLE, P., Park, S. and Boxall, A.B., 2013. Visualization and characterization of engineered nanoparticles in complex environmental and food matrices using atmospheric scanning electron microscopy. J. Microsc. 250(1), pp.32-41.

Meghwal, M. and Goswami, T.K., 2014. Comparative study on ambient and cryogenic grinding of fenugreek and black pepper seeds using rotor, ball, hammer and Pin mill. Powder Technol. 267, pp.245-255.

Meghwal, M. and Goswami, T.K., 2013. Evaluation of size reduction and power requirement in ambient and cryogenically ground fenugreek powder. Adv. Powder Technol. 24(1), pp.427-43.

McKay, R.B. ed., 1994. Technological applications of dispersions (Vol. 52). CRC Press.

Mongia, G. and Ziegler, G.R., 2000. The role of particle size distribution of suspended solids in defining the flow properties of milk chocolate. Int. J. Food Prop. 3(1), pp.137-147.

Servais, C., Jones, R. and Roberts, I., 2002. The influence of particle size distribution on the processing of food. J. Food Eng. 51(3), pp.201-208.

Toker, O.S., Sagdic, O., Şener, D., Konar, N., Zorlucan, T. and Dağlıoğlu, O., 2016. The influence of particle size on some physicochemical, rheological and melting properties and volatile compound profile of compound chocolate and cocolin samples. Eur. Food Res. Technol. pp.1-14.

Viaene, J. and Januszewska, R., 1999. Quality function deployment in the chocolate industry. Food Quality and Preference, 10(4), pp.377-385.

Worldatlas. "Top 10 Cocoa Producing Countries." WorldAtlas. WorldAtlas, 22 July 2016. Web. 25 Nov. 2016.

Ziegler, G.R., Mongia, G. and Hollender, R., 2001. The role of particle size distribution of suspended solids in defining the sensory properties of milk chocolate. Int. J. Food Prop. 4(2), pp.353-370.

Ziegler, G.R. and Hogg, R., 2009. Particle size reduction. Industrial Chocolate Manufacture and Use, Fourth Edition, pp.142-168.

Figures

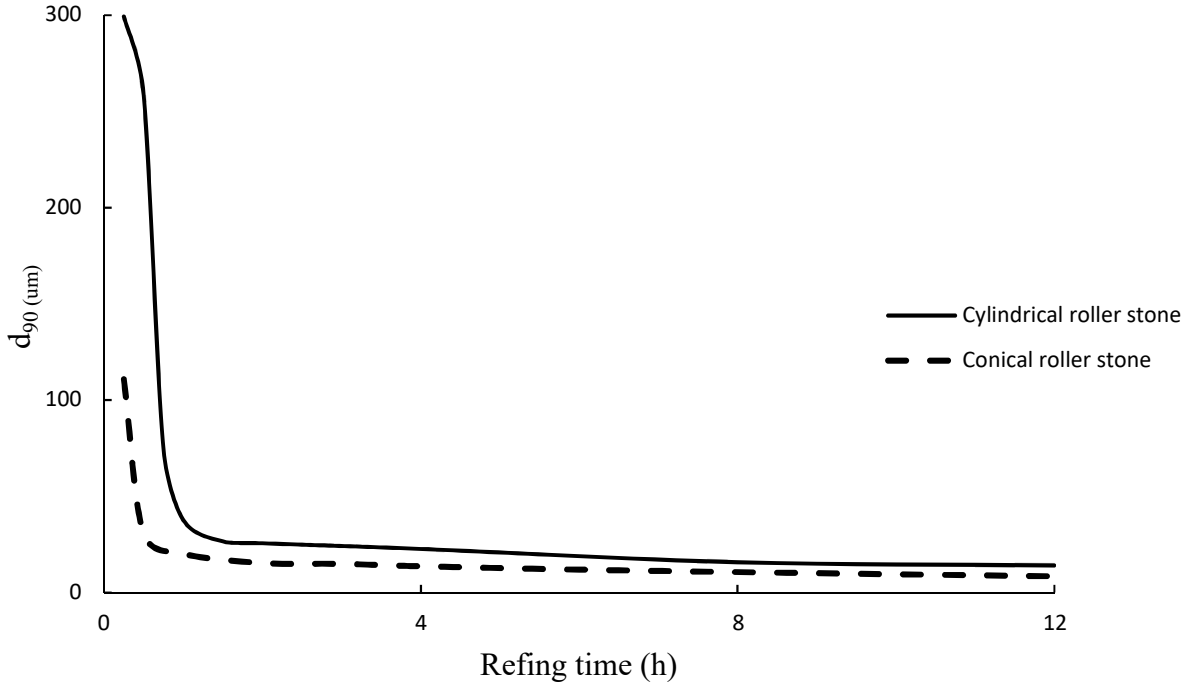

Figure 5.1. Particle size of cocoa solids refined by different melanger as a function of time.

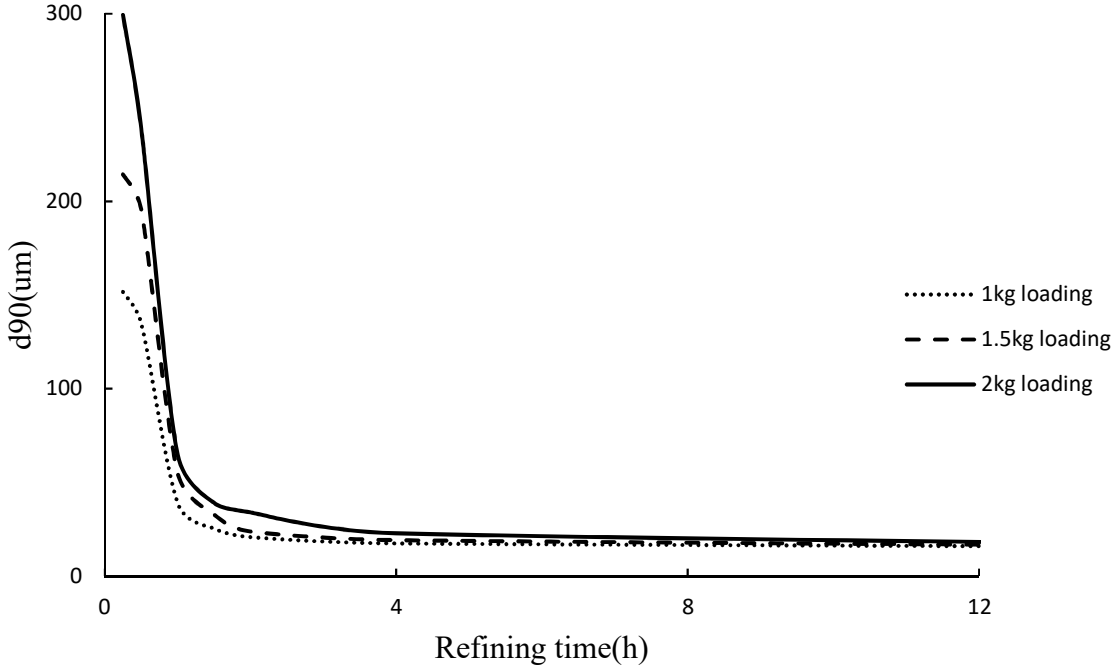

Figure 5.2. Particle size of cocoa solids with different initial weights as a function of time.

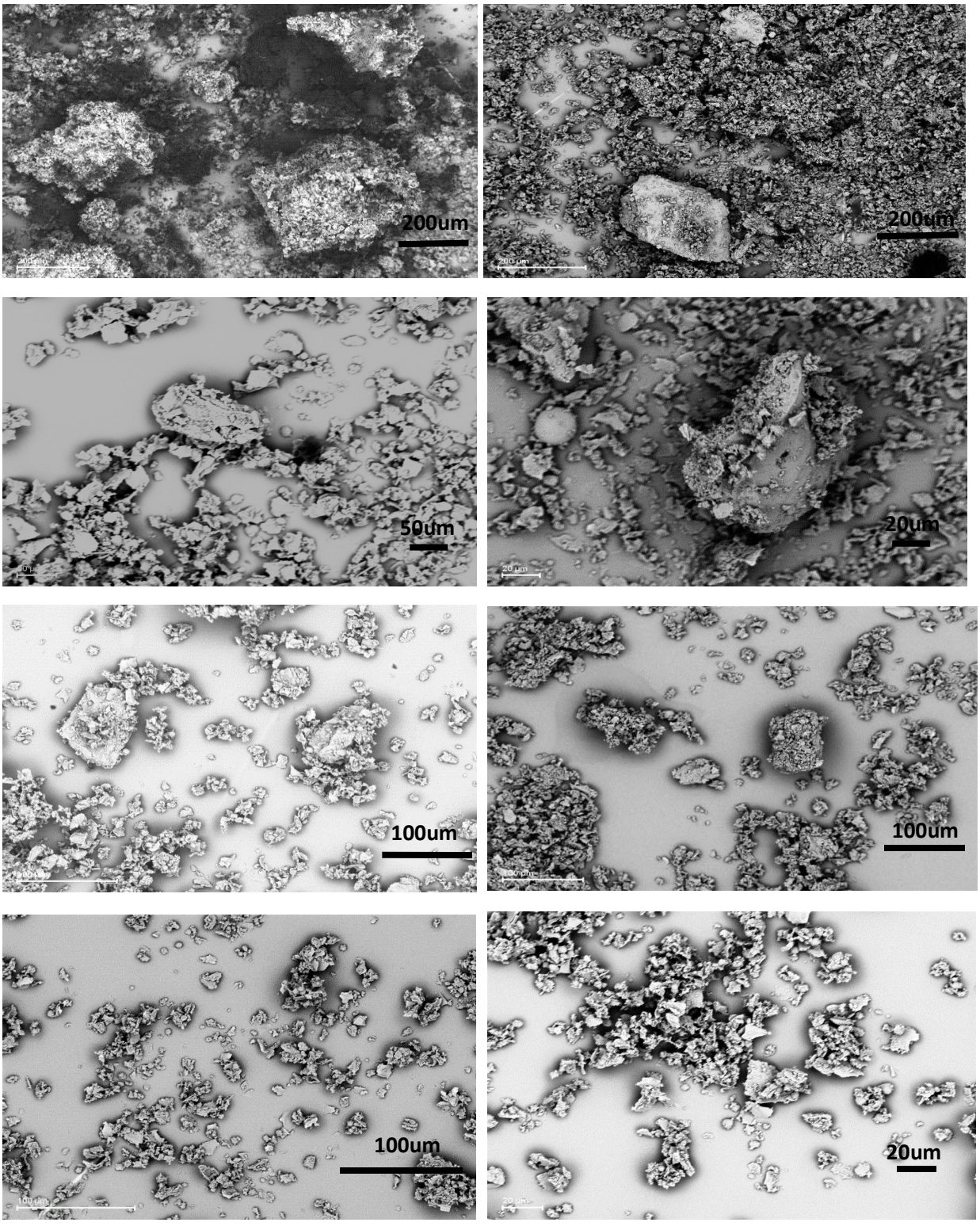

Figure 5.3. SEM images of 0.5 h, 2 h, 4 h and 24 h refined cocoa solids (from up to bottom) by different refiner (left: by conical roller stone, right: by cylindrical stone).

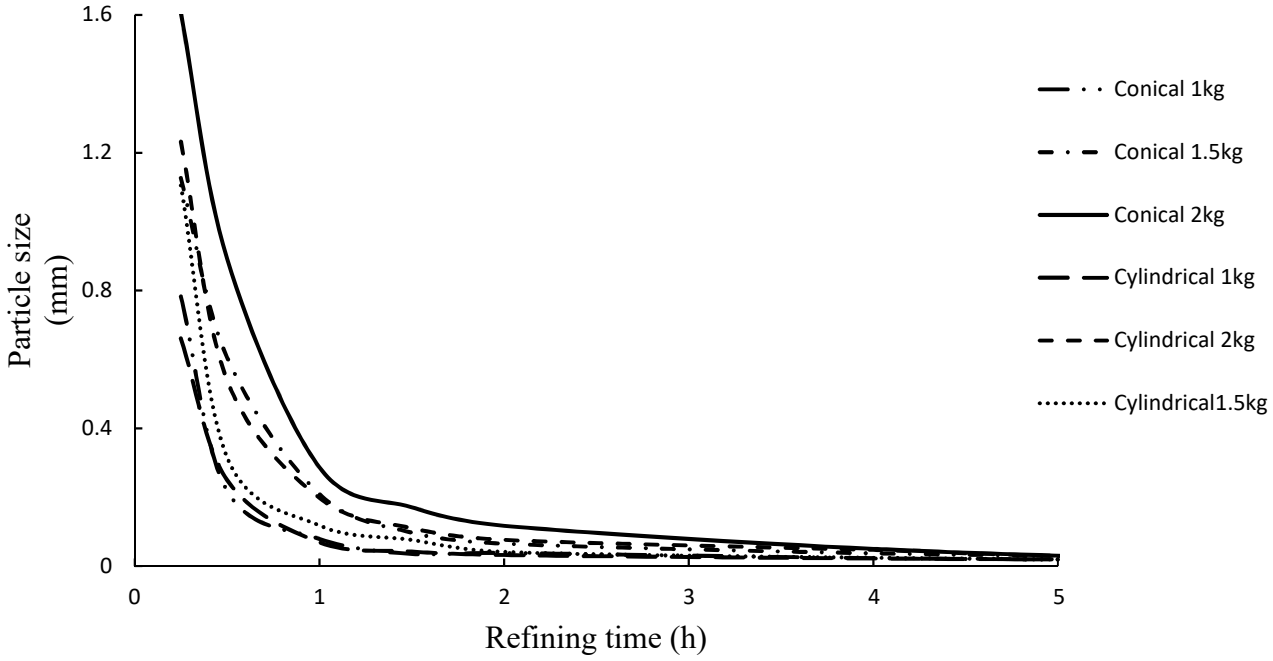

Figure 5.4. Measurements conducted by micrometer for particle size of cocoa solids with different initial weights and processed by different melanger as a function of time.

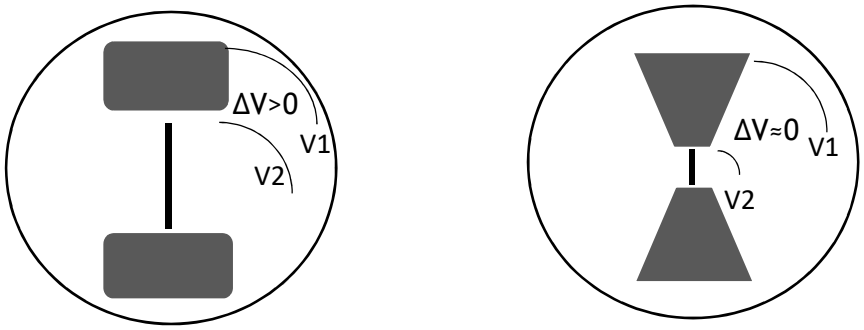

Figure 5.5. Gradients of linear speed of cocoa paste in melangers equipped with cylindrical roller stone and conical roller stone.

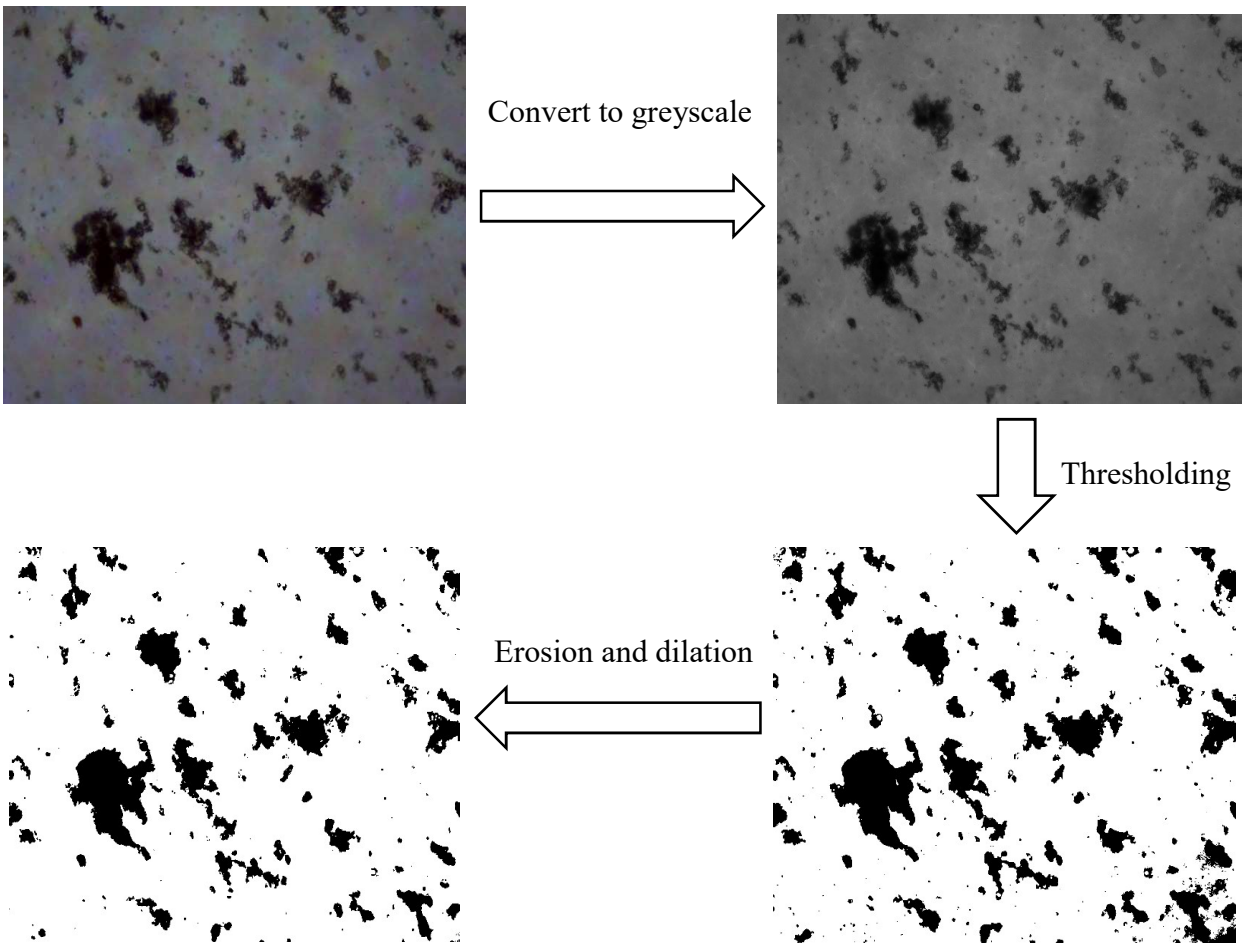

Figure 5.6. Light microscopy image processing by ImageJ.

Table 5.1. The particles size measurements done by 4 different methods at after cocoa solids being refined for 0.5h, 2h, 4h and 24h.

	0.5h (um)	2h (um)	4h (um)	24h (um)
Laser scattering	134.90[a]	39.01[a]	25.35[a]	20.83[b]
Micrometer	219[c]	38[a]	23[a]	6[a]
Light microscopy image analysis	206.61[b]	184.12[b]	133.66[b]	51.48[b]
Hegman gauge	21-190	15-172	15-166	11-120

CHAPTER 6

DETERMINING DEGREE OF ROASTING IN COCOA BEANS BY ARTIFICIAL NEURAL NETWORK (ANN) BASED ELECTRONIC NOSE SYSTEM AND GAS CHROMATOGRAPHY/MASS SPECTROMETRY (GC/MS)[4]

[4] Tan, J. and W. L. Kerr. Submitted to *LWT-Food Science and Technology*

ABSTRACT

Roasting is a critical step in chocolate processing, where moisture content is decreased and unique flavors and texture are developed. The determination of the degree of roasting in cocoa beans is important to ensure the quality of chocolate and helps determine the commercial value of cocoa beans collected from cocoa farmers. Determining the degree of roasting relies on human specialists or sophisticated chemical analysis that are inaccessible to small manufacturers and farmers. In this study, an electronic nose system was constructed consisting of an array of gas sensors and used to detect volatiles emanating from cocoa beans roasted at 0, 20, 30, and 40min. The several signals were used to train a three-layer artificial neural network (ANN). Headspace samples were also analyzed by GC-MS with 23 select volatiles used to train a separate ANN. Both ANNs were used to predict the degree of roasting of cocoa beans. The electronic nose had a prediction accuracy of 94.4% using signals from TGS 813, 826, 820, 880, 830, 2620, 2602 and 2610 sensors. In comparison, the GC-MS predicted the degree of roasting with an accuracy of 95.8%. Roasting is an essential step in the conversion of cocoa beans into chocolate, but there are no simple techniques for processors to determine the extent of flavor development. This work shows how relatively inexpensive gas sensors can be used to monitor roasting, with a computer program used to correlate the several sensors output with the extent of roasting. The electronic nose system is able to predict the extent of roasting as well as a more sophisticated approach using gas chromatography-mass spectrometry.

Keywords: cocoa beans, roasting, electronic nose, neural network

1. Introduction

Cocoa belongs to the family of *Sterculiaceae* and the genus *Theobroma*, and originated in Central and Southern America (Nair, 2010). It is the key raw material of chocolate, the basis of confections that are popular around the world. In addition, cocoa exporting has become an important part of the economy in several countries, including Ghana, Togo and Cote d'Ivoire (Afoakwa et al., 2011; Krähmer et al., 2015). In 2016, the global chocolate market produced 4,400,000 tons of cocoa beans worth $98.3 billion. The seeds of the cocoa, known as cocoa beans, are collected from the pods. There are typically 30-40 seeds imbedded in a mucilaginous pulp (Lima et al., 2010; Schwan and Wheals, 2004). The seeds must be subject to several post-harvest processing steps to make them suitable for chocolate, including fermentation, roasting, winnowing and conching.

Although there are many indicators used to judge the quality of cocoa beans, the most important factor is the volatile flavor profile (Magi et al., 2011). The flavors and flavor precursors that develop depend on the processing steps. With total polyphenolic content about 6% to 8% by weight of dried fermented cocoa beans, using unroasted cocoa beans to make chocolate will lead to unpleasant bitterness and astringency. The predominant polyphenolic compounds in unroasted cocoa beans are flavanols, which significantly decrease during roasting because they are heat labile (Crozier et al., 2011). Moreover, the procedure of roasting can also greatly reduce the moisture content in cocoa beans, which helps prevent blooming during chocolate storage (Kothe et al., 2013).

Roasting of cocoa is also essential for the formation of the typical chocolate aroma from the precursor compounds formed during fermentation (Arlorio et al., 2008). The flavor developed during roasting results from some 400-500 compounds including thiazoles, phenols,

ketones, alcohols, pyrazines, aldehydes, ethers, furans and esters. The major compounds formed during roasting are aldehydes and pyrazines. Most are formed by the Maillard reaction and Strecker degradation of amino acids and sugars at high heat (Dimick and Hoskin, 1981; Heinzler and Eichner, 1992). Some studies (Ramli et al., 2006) have revealed that there are significant differences in flavor compounds formed due to different roasting times and temperatures. Major flavor components include aliphatic and alicyclic groups such as 3-methylbutanal and phenylacetaldehyde, and heterocyclic groups such as 2,3-diethyl-5-methylpyrazine. Some researchers have suggested that compounds such as trimethylpyrazine, tetramethylpyrazine and 5-methyl-2-phenyl-2-hexanal are useful indicators to evaluate how well beans have been roasted.

Determining the appropriate extent of fermentation or roasting is usually accomplished by sensory tests or empirical methods conducted by trained personnel (Emmanuel et al., 2012; Hamid and Lopez, 2000). The initial grading may be done by a "cut" test, in which the percentage of good and defective beans is assessed. Determining the appropriate endpoint for roasting is complicated as the development of flavor compounds depends on the variety, type of roaster, and time and temperatures used for roasting. In research settings, the extent of roasting of cocoa beans has been determined by GC-MS (gas chromatography mass spectrometry) and near infrared spectrometry (Bonvehí, 2005; Pätzold and Brückner, 2006; Frauendorfer and Schieberle, 2008; Schenker et al., 2002). However, instruments such as GC-MS are generally expensive and complicated to operate, leaving them outside the purview of many small/medium chocolate manufacturers and cocoa bean producers.

An electronic nose or "e-nose" is an instrument consisting of an array of weakly specific or broad-spectrum chemical sensors that mimic the human olfactory system, by converting sensor signals to digital data which are then analyzed by appropriate software (Gardner and

Bartlett, 1994; Keller, 1995). There are many types of gas sensors available including metal oxide semiconductors (MOS), metal oxide semiconductor field effect transistors (MOSFET), conducting organic polymers (CP), and bulk acoustic wave (BAW) devices. The most popular are the MOS-type gas sensor because of its high sensitivity and low cost (Wilson and Baietto, 2009). MOS sensors consist of a round or flat ceramic substrate heated by a wire and coated with a metal oxide semiconducting film. The metal oxide coating may be either of the *n*-type, such as zinc oxide, tin dioxide, or titanium dioxide which respond to oxidizing compounds, or of the *p*-type (mainly nickel oxide or cobalt oxide) which respond to reducing compounds. These reactions may change the resistance of the gas sensors, and therefore influence the output voltages of the circuits with the gas sensors (Mielle, 1996).

Currently, the food industry is the biggest market for the implementation of electronic nose systems. Researchers have studied the application of e-noses to tomato shelf-life (Gómez et al., 2008), wine quality (García et al., 2006), coffee analysis (Pardo and Sberveglieri, 2002), honey discrimination (Escriche et al., 2012) and pecan quality (Xu et al., 2017). Olunloyo et al., (2012) used an electronic nose to distinguish good from bad cocoa beans. Hashim and Plumas (1999) showed that gas phase sensors would respond to aromas emanating from cocoa beans roasted at different temperatures. Radi et al. (2016) used an electronic nose system to predict the degree of coffee been roasting but were not able to distinguish between light, medium, and dark roasted beans. However, little has been done to develop simple methods to detect and analyze changes in cocoa bean volatiles during roasting.

One challenge is that e-noses generate several time-varying voltage signals which must be analyzed and interpreted to provide useful information. One approach to such complex data problems is artificial neural network (ANN) analyses, which is based on the cognitive process of

the human brain. Mathematical functions, the “neurons”, are linked together to build a network that mimics the human nervous system (Persaud and Pelosi, 1992). A weight is randomly assigned to each neuron and then adjusted by means of an iterative or ‘learning’ process such as error back-propagation until an optimized output is achieved. The resultant set of weights and functions is then saved as a ‘neural network’.

In this study, an electronic nose system was developed and tested to see if it could monitor changes in volatile compounds during roasting of cocoa beans. Cocoa beans were roasted to different levels, and the gas phase sampled using nine gas sensors. Outputs from the sensors were analyzed by statistical methods and with an artificial neural network in conjunction with data collected by GC-MS. This allowed us to understand chemical changes in the beans as they were roasted, which and how many of the e-nose sensors were needed to make a successful model, and whether an ANN trained e-nose could perform as well as a GC/MS-based system.

2. Materials and Method

2.1 Sample preparation

Dried and fermented ‘Forastero’ cocoa beans (*Theobroma* cacao) were obtained from Scharffen Berger (San Francisco, CA). Three batches of cocoa beans were roasted in 1 kg batches using a drum roaster (Model CocoaT Junior Roaster CS, CocoaTown, Roswell, Georgia, USA). The beans were tumbled in a rotating chamber at ~3 times per second, and heated at 135°C for 20, 30 or 40 min respectively. The roasted beans were immediately chilled by a tray cooler (CocoaTown, Roswell, Georgia, USA) after roasting. Chilled samples were packaged in heat sealed aluminum laminated pouches (10.2 x 15.2 x 6.35cm) and stored at -40℃ prior to subsequent testing.

2.2 Electronic nose system

The diagram of the e-nose system is shown in Figure 6.1. The system consisted of three major components, including a gas injector (syringe pump and syringe), e-nose (gas sensors and chamber), and data collection boards. The e-nose chamber was built from a 10cm x 10cm x 5cm nylon box with a 1.5cm thick Teflon top. The sensor sockets were inserted into the outer top of the chamber, while the gas sensors were inserted into the sockets from inside the chamber. The sensor array had nine gas sensors purchased from Figaro USA, INC (Arlington Heights, IL) including the TGS 821, TGS 813, TGS 822, TGS 830, TGS 823, TGS 826, TGS 2602, TGS 2610, and TGS 2620. The target gasses for each type of sensor is summarized in Table 1.

For testing, the roasted cocoa beans (15 g) were preheated to 70℃ in an incubator for 5min, and then quickly loaded into an air-tight 60 ml syringe equipped with a Luer-Lock mechanism. The beans were held for 30 s to let the volatile compounds fill the space of the syringe. The syringe pump (Model 200 series, Kd Scientific INC, Holliston, MA) then injected the gas in the syringe into the e-nose chamber (constant temperature of 27.5℃) at 3 ml/s for 10 s. The injected gas reacted with the gas sensors and the signals (output voltage as a function of time) were collected by two data acquisition boards (Model NI9219, National Instruments, Austin, TX). A program was developed using LabView software (Version 2014, National Instruments, Austin, TX) to collect data from the DAQ boards and to provide a visual representation of voltage versus time for each channel.

The peak value minus the baseline values of each sensor were calculated and defined as the relative peak. The ‘relaxation time’ of each sensor was defined as the time that the output voltage decreased from the peak value to 10% of the relative peak value. Both the relative peak values and the relaxation time of each sensor were used as input data for ANN training. There

were 60 repetitions at each level of roasting, of which 30 repetitions were used for training the ANN while the rest were used for prediction validation.

2.3 GC-MS analysis

The GC-MS system used to analyze the volatile compounds of cocoa bean samples consisted of a Clarus 680 gas chromatograph (PerkinElmer, Waltham, MA) and a Clarus SQ8T mass spectrometer (PerkinElmer, Waltham, MA). The roasted cocoa beans were ground and 2 g transferred into a capped glass vial. An internal standard of 4-picoline was applied to the cocoa liquor. A polydimethylsyloxane divinylbenzene (PDMS-DVB) SPME fiber was used for extraction of volatile compounds. The fiber was inserted through a rubber septum and exposed to the contents of the vial for 30 min, while the vial was kept at a constant 60°C. The fiber was transferred to the GC injection port fitted with an SPL-1 splitless injector. The compounds were analyzed on a Rtx5 cross-bond diphenyl dimethyl polysiloxane capillary column, using a helium carrier gas at 30 ml/min. The injector temperature was maintained at 250 ℃ and the column programmed from 40 ℃ (5 min) to 200 ℃ at 5 ℃ /min for 5 min, following the method described by Hashim et al. (1998). The chromatographic peaks were identified based on their molecular ion patterns, using the Autobuild software. The quantity of each compound was calculated by dividing the peak area by the sum of the peak areas of all identified compounds. These relative peak areas of the identified compounds were used to train the ANN. The extractions and GC/MS runs were repeated 24 times for samples at each degree of roasting, of which 14 repetitions were used for training the ANN while the rest of 10 repetitions were used for prediction validation.

2.4 ANN training and prediction validation

The training and predictive models of the ANN were constructed using the MATLAB (Version R2015b, MathWorks, Natick, MA) neural network toolbox. During the training

process, the signals (relative peak values and relaxation times) collected from each sensor were scaled and used as input data. The target data were then scaled for the degree of roasting with 0, 0.5,0.75, and 1 representing roasting times of 0, 20, 30, and 40 min respectively. The network was a feed-forward type with back propagation. Performance of the network was judged by the MSE and R values. During training, initial weights between 0 to 1 were randomly assigned. Training was done using a backpropagation function, which updates weight and bias values according to the Levenberg-Marquardt optimization. Settings for the routine are shown in Table 2. The parameter "mu" is part of the training function and is used to tune how roots of differentiable equations are determined. The values of "mu-dec" or "mu-inc" specify how this factor can be decreased or increased, allowing it to be adjusted to most quickly reach an optimized solution. Hyperbolic tangent sigmoid ("tansig") functions were used for hidden layers and output layers. The "validation check" parameter allows the training to be stopped early if the network performance fails to improve. After the training was finished, 36 sets of new signals (9 sets for each degree of roasting) were used to validate the trained ANN. The accuracy of the trained ANN was calculated by the number of correct predictions over the number of all predictions. A similar procedure was used to develop an ANN trained with values obtained from the normalized peaks of volatile compounds detected by GC-MS.

2.5 Statistical methods

Principal component analysis (PCA) was used to identify the major volatile compounds and sensor responses related to the degree of roasting. Scores obtained from each PCA were analyzed by a one-way analysis of variance (ANOVA) to test for significant differences between samples. All the statistical analyses were performed by Matlab (Version R2015b, MathWorks, Natick, MA).

3. Results and discussion

3.1 Volatile composition and PCA analysis of cocoa beans

Some 43 volatile compounds were identified by GC-MS from the SPME headspace extraction of the roasted cocoa beans. In comparison, Frauendorfer and Schieberle (2008) observed 42 "odor-active" volatile compounds in both roasted and unroasted Criollo cocoa beans using aroma extract dilution analysis (AEDA**),** combined with GC-olfactory analyses. Ducki et al. (2008) also found 43 volatile compounds in cocoa and chocolate powders by GC-MS after extraction with SPME. Other researchers observed more volatile compounds, however. For example, Jinap et al. (1998) identified 53 volatile compounds in *Theobroma* nibs using a steam distillation procedure. Rodriguez-Campos et al. (2012) found 58 compounds in 'Forastero' beans using solid phase micro-extraction in the headspace (SPME-HS). Bonhevi (2005) showed there are 9 compounds common to cocoa powders regardless of their geographic origin.

Table 6.3 shows 24 volatile compounds found in this study, and as reported by others, to be good indicators of cocoa roasting (Ramli et al., 2008, Bonvehí and Coll, 2002, Krist et al., 2004; Hernández and Rutledge, 1994). The table also shows how the relative concentrations of these compounds changed during roasting. Some compounds, such as acetic acid and 3-methyl-1-butanol acetate decreased over time, while others such as 2-ethyl-6-methyl-pyrazine increased with roasting.

Principal component analysis (PCA) was used to determine the effects of roasting time on the composition of volatile compounds in cocoa beans and showed that the first two components explained 49.1 and 14.8% of the variance, respectively. The PCA loading plots are shown in Figure 6.2. Clusters of those compounds with loading factors (LF) greater than 0.2 are highlighted and are those that explained the greatest variance due to roasting time. In general,

those compounds that had an LF > 0.2 were those that increased during the roasting process (see also Table 3). These included 2-ethyl-6-methylpyrazine; dimethyl disulfide; 2,3-diethyl-5-methylpyrazine; trimethylpyrazine and 3-ethyl-2,5-dimethylpyrazine. Compounds with LF < -0.2 were those that decreased during roasting and included acetic acid and benzaldehyde.

Researchers such as Hashim and Chaveron (1994) have identified a variety of compounds formed during roasting. These include monomethyl-; 2,3-dimethyl-; 2,5-dimethyl-; 2,6-dimethyl-; trimethyl- and tetramethylpyrazine. Some of these are present in small amounts in unroasted, fermented beans and develop to greater levels during roasting. This is particularly true for fermented beans, as the fermentation process helps develop reducing sugars. Some pyrazines can form during fermentation through conversion by lactobacilli. Others develop in the process of Maillard reactions between proteins and reducing sugars, a reaction enhanced by the high temperatures and intermediate moistures incurred in roasting. Compounds such as benzaldehyde are present in the raw bean and contribute to a beany almond-like aroma. Acetic acid develops during the fermentation of the beans. Both of these volatile compounds are gassed out from the beans during roasting.

A few compounds had high LF along the negative PC2 axes. These included 2-heptanol acetate and 3-methyl butanoic acid. These are compounds that were present in the unroasted beans, decreased slightly during intermediate roasting, then increased slightly at 40 min of roasting. Several compounds had low LF values and thus contributed little to the variance. This included compounds such as 2-heptanone and 2-nonanone. Some aldehydes and ketones are formed as part of the Strecker reaction. These may be volatilized in roasting or become part of reactions leading to the formation of pyrazines. Interestingly, tetramethyl-pyrazine was present at relatively high levels in the unroasted beans, then decreased by only small amounts during

roasting. Others have noted that this compound is present in relatively high levels in both unroasted and roasted cocoa beans (Hashim and Chaveron, 1994).

3.2 PCA analysis of gas sensors

Examples of how each sensor responded to the gasses generated by cocoa beans with different roasting times are shown in Figure 6.4, with details of the responses (peak values and relaxation times) summarized in Table 6.4 and 6.5. Generally, varying the roasting time of cocoa beans did not significantly change the relative peak values of TGS sensors 821, 830 or 2610. As shown in Table 6.1, these sensors were targeted towards hydrogen, halocarbons and butane/propane. However, the roasting time significantly influenced the relative peak values of the five other sensors. With regards to relaxation time, all sensors showed significant changes due to roasting time. This indicates that both measured responses can be used as indicators for the degree of roasting.

PCA was also used to determine the effect of roasting time of cocoa beans on the response signals (relative peak value and relaxation time) generated by gas sensors (Figure 6.3a-b). PC1 explained 41.62% of the total variation of the sensor signals listed in Table 6.1, PC2 24.17% and PC3 10.20%. The positive side of the PC1 axis was influenced by peak values and relaxation time of TGS sensor 823, 830 and 2620, while the positive side of PC2 was influenced by the sensors 822, 813, 821 and 2602. PC3 was mostly influenced by sensor 2610.

The relative peak values and relaxation times formed two major clusters in the loading plots. This suggests that each group of sensors has overlapping sensitivities to a particular class of aromatic compounds. Thus, TGS sensors 823, 830 and 2620 are more sensitive to alcohols, alkyls, ketones and related organic solvents. These are either volatile compounds generated by

roasted/unroasted cocoa beans or products of those compounds and oxygen that develop during roasting. TGS sensors 822, 813, 821 and 2602 are more sensitive to combustible and low molecular weight gasses such as hydrogen, methane, ammonia and sulfide gasses.

3.3 ANN training and prediction

Table 6.6 shows the performance parameters of the two neural networks as trained by e-nose signals or GC-MS detected volatile compounds. Overall, the ANN trained by e-nose had a slightly lower accuracy (94.4%) as compared to that trained by the GC-MS volatiles (95.8%). Both models had 100% prediction at 0 or 20 min roasting time. At 30 min, the e-nose system accurately predicted 8 out of 9 cases, the GC/MS system 6 out of 6. The two systems are not expected to behave identically, however. While the GC-MS is able to detect and discriminate many volatile compounds, the e-nose sensors are sensitive to particular classes of compounds and may have overlapping detection on more than one sensor. For example, TGS sensors 823 and 822 responded to 3-ethyl-2,5-dimethyl-pyrazine; 2,3-diethyl-5-methyl-pyrazine and tetramethylpyrazine similarly. In addition, the GC/MS created substantially more data points at a given roasting time, namely the concentrations of 24 compounds, while the e-nose system relied on signals from 8 sensors providing 2 measurements (peak and relaxation times). In general, a system with more inputs can be better fit by an ANN, although over-fitting can sometimes be a concern.

Both systems did predict the extent of roasting with reasonable accuracy. The e-nose system does offer several advantages. First, the sample preparation was less complicated and less time consuming than GC-MS based system. In the e-nose system, the cocoa beans were just pre-heated prior to injection into the sensor chamber, and the readings were taken within 5-10 min. The GC-MS requires substantial grinding and extraction of volatile compounds by the SPME

fiber. Second, the cost of building an e-nose system is much less than purchasing a GC-MS based system. The materials cost of the e-nose system can be confined to a few hundred dollars while GC-MS instruments may cost $60,000 or more. Third, the detection and analysis for the e-nose based system were much faster and less complicated. Typically, 15 min was required for the e-nose system and only two parameters for each sensor was required to be collected. However, the GC-MS takes ~1h for sample preparation, an additional 30-60 min to run and additional extra time to identify and analyze many peaks. It should also be noted that, while not attempted in this study, the e-nose lends itself to on-line applications.

4. Conclusion

Both GC-MS and e-nose systems could be trained by ANN to predict the stage of roasting of cocoa beans. Both systems work as the volatile components emanating from the samples are continuously changing. The former senses these as several specific compounds, the latter senses these as categories of volatile compounds. As noted, the e-nose system is a much simpler and inexpensive system to use. While not attempted in this study, it is anticipated that the e-nose could be adapted to collect and analyze gases on-line and in real time.

The volatile composition originating from cocoa beans can be an indicator of the quality of cocoa beans and products. Thus, the combination of an e-nose system with ANN might be useful for determining whether beans are rotten or not, the grade of the beans, the degree of fermentation and the degree of roasting. Future studies will be focused on these applications.

Acknowledgement

We would like to thank Dr. M. Balu and the CocoaTown Company in Atlanta, Georgia for their help with funding and acquisition of supplies.

References

Afoakwa, E. O., Quao, J., Budu, A. S., Takrama, J. and Saalia, F. K., 2011. Effect of pulp preconditioning on acidification, proteolysis, sugars and free fatty acids concentration during fermentation of cocoa (Theobroma cacao) beans. Int. J. Food Sci. Nutr., *62*(7), pp.755-764.

Arlorio, M., Locatelli, M., Travaglia, F., Coïsson, J. D., Del Grosso, E., Minassi, A., Appendino, G. and Martelli, A., 2008. Roasting impact on the contents of clovamide (N-caffeoyl-L-DOPA) and the antioxidant activity of cocoa beans (Theobroma cacao L.). Food Chem., *106*(3), pp.967-975.

Bonvehí, J. S., 2005. Investigation of aromatic compounds in roasted cocoa powder. Eur. Food Res. Technol., *221*(1-2), pp.19-29.

Serra Bonvehí, J. and Ventura Coll, F., 2002. Factors affecting the formation of alkylpyrazines during roasting treatment in natural and alkalinized cocoa powder. J. Agric. Food Chem., *50*(13), pp.3743-3750.

Crozier, S. J., Preston, A. G., Hurst, J. W., Payne, M. J., Mann, J., Hainly, L. and Miller, D. L., 2011. Cacao seeds are a" Super Fruit": A comparative analysis of various fruit powders and products. Chem. Cent. J., *5*(1), p.5.

J.Ducki, S., Miralles-Garcia, J., Zumbé, A., Tornero, A. and Storey, D. M., 2008. Evaluation of solid-phase micro-extraction coupled to gas chromatography-mass spectrometry for the headspace analysis of volatile compounds in cocoa products. Talanta, *74*(5), pp.1166-1174.

Emmanuel, O. A., Jennifer, Q., Agnes, S. B., Jemmy, S. T. and Firibu, K. S., 2012. Influence of pulp-preconditioning and fermentation on fermentative quality and appearance of Ghanaian cocoa (Theobroma cacao) beans. Int. Food Res. J., *19*(1).

J.Escriche, I., Kadar, M., Domenech, E. and Gil-Sánchez, L., 2012. A potentiometric electronic tongue for the discrimination of honey according to the botanical origin. Comparison with traditional methodologies: Physicochemical parameters and volatile profile. J. Food Eng., *109*(3), pp.449-456.

Frauendorfer, F. and Schieberle, P., 2008. Changes in key aroma compounds of Criollo cocoa beans during roasting. J. Agric. Food Chem., *56*(21), pp.10244-10251.

García, M., Aleixandre, M., Gutiérrez, J. and Horrillo, M. C., 2006. Electronic nose for wine discrimination. Sens. Actuators, B, *113*(2), pp.911-916.Gardner, J. W. and Bartlett, P. N., 1994. A brief history of electronic noses. Sens. Actuators, B, *18*(1-3), pp.210-211.

Gomez, A. H., Wang, J., Hu, G. and Pereira, A. G., 2008. Monitoring storage shelf life of tomato using electronic nose technique. J. Food Eng., *85*(4), pp.625-631.

Asimah, H. and Lopez, S. A., 2000. Quality and weight changes in cocoa beans stored under two warehouses' conditions in East Malaysia. Planter, *76*(895), pp.619-637.

Hashim, P., Selamat, J., Muhammad, S., Kharidah, S. and Ali, A., 1998. Changes in free amino acid, peptide-N, sugar and pyrazine concentration during cocoa fermentation. J. Sci. Food Agric., *78*(4), pp.535-542.

Hashim, L. and Plumas, B., 1999. Electronic nose for monitoring cocoa beans aroma. Electronic noses and sensor array based systems-design and applications, Technomic Publishing Co., Inc. Lancaster, pp.296-307.

Hashim, L. and Chaveron, H., 1994. Extraction and determination of methylpyrazines in cocoa beans using coupled steam distillation-microdistillator. Food Res. Int., *27*(6), pp.537-544.

Hernández, C. V. and Rutledge, D. N., 1994. Multivariate statistical analysis of gas chromatograms to differentiate cocoa masses by geographical origin and roasting conditions. Analyst, *119*(6), pp.1171-1176.

Heinzler, M. and Eichner, K., 1992. The role of amodori compounds during cocoa processing–formation of aroma compounds under roasting conditions. Z. Lebensm.-Unters.-Forsch, *21*, pp.445-450.

Jinap, S., Wan Rosli, W. I., Russly, A. R. and Nordin, L. M., 1998. Effect of roasting time and temperature on volatile component profiles during nib roasting of cocoa beans (Theobroma cacao). J. Sci. Food Agric., *77*, pp.441-448.

Keller, P. E., 1995, October. Electronic noses and their applications. In Northcon 95. IEEE Technical Applications Conference and Workshops Northcon95 (p. 116). IEEE.

Kothe, L., Zimmermann, B. F. and Galensa, R., 2013. Temperature influences epimerization and composition of flavanol monomers, dimers and trimers during cocoa bean roasting. Food Chem., *141*(4), pp.3656-3663.

Krähmer, A., Engel, A., Kadow, D., Ali, N., Umaharan, P., Kroh, L. W. and Schulz, H., 2015. Fast and neat-Determination of biochemical quality parameters in cocoa using near infrared spectroscopy. Food Chem., *181*, pp.152-159.

Krist, S., Unterweger, H., Bandion, F. and Buchbauer, G., 2004. Volatile compound analysis of SPME headspace and extract samples from roasted Italian chestnuts (Castanea sativa Mill.) using GC-MS. Eur. Food Res. Technol., *219*(5), pp.470-473.

Kothe, L., Zimmermann, B. F. and Galensa, R., 2013. Temperature influences epimerization and composition of flavanol monomers, dimers and trimers during cocoa bean roasting. Food Chem., *141*(4), pp.3656-3663.

Lima, L. J., Almeida, M. H., Nout, M. R. and Zwietering, M. H., 2011. Theobroma cacao L.,"The food of the Gods": quality determinants of commercial cocoa beans, with particular reference to the impact of fermentation. Crit. Rev. Food Sci. Nutr., *51*(8), pp.731-761.

Magi, E., Bono, L. and Di Carro, M., 2012. Characterization of cocoa liquors by GC-MS and LC-MS/MS: focus on alkylpyrazines and flavanols. J. Mass Spectrom., *47*(9), pp.1191-1197.

Mielle, P., 1996. 'Electronic noses': Towards the objective instrumental characterization of food aroma. Trends Food Sci. Technol., *7*(12), pp.432-438.

Olunloyo, V. O., Ibidapo, T. A. and Dinrifo, R. R., 2012. Neural network-based electronic nose for cocoa beans quality assessment. Agric. Eng. Int.: CIGR Journal, *13*(4).

Pardo, M. and Sberveglieri, G., 2002. Coffee analysis with an electronic nose. IEEE Trans. Instrum. Meas., *51*(6), pp.1334-1339.

Pätzold, R. and Brückner, H., 2006. Gas chromatographic determination and mechanism of formation of D-amino acids occurring in fermented and roasted cocoa beans, cocoa powder, chocolate and cocoa shell. Amino acids, *31*(1), pp.63-72.

Persaud, K. C. and Pelosi, P., 1992. Sensor arrays using conducting polymers for an artificial nose. In Sensors and sensory systems for an electronic nose (pp. 237-256). Springer.

Netherlands.Nair, K. P., 2010. The agronomy and economy of important tree crops of the developing world.

Elsevier.Radi, Rivai, M. and Purnomo, M. H., 2016. Study on Electronic-Nose-Based Quality Monitoring System for Coffee Under Roasting. J. Circuit Syst Comp, *25*(10), p.1650116.

Ramli, N., Hassan, O., Said, M., Samsudin, W. and Idris, N. A., 2006. Influence of roasting conditions on volatile flavor of roasted Malaysian cocoa beans. J. Food Process. Preserv., *30*(3), pp.280-298.

Preserv.Rodriguez-Campos, J., Escalona-Buendía, H. B., Contreras-Ramos, S. M., Orozco-Avila, I., Jaramillo-Flores, E. and Lugo-Cervantes, E., 2012. Effect of fermentation time and drying temperature on volatile compounds in cocoa. Food Chem., *132*(1), pp.277-288.

Schenker, S., Heinemann, C., Huber, M., Pompizzi, R., Perren, R. and Escher, R., 2002. Impact of roasting conditions on the formation of aroma compounds in coffee beans. J. Food Sci., *67*(1), pp.60-66.

Schwan, R. F. and Wheals, A. E., 2004. The microbiology of cocoa fermentation and its role in chocolate quality. Crit. Rev. Food Sci. Nutr., *44*(4), pp.205-221.

Wilson, A. D. and Baietto, M., 2009. Applications and advances in electronic-nose technologies. Sensors, *9*(7), pp.5099-5148.

Winquist, F., Hornsten, E. G., Sundgren, H. and Lundstrom, I., 1993. Performance of an electronic nose for quality estimation of ground meat. Meas. Sci. Technol., *4*(12), p.1493.

Xu, K., Wang, J., Wei, Z., Deng, F., Wang, Y. and Cheng, S., 2017. An Optimization of the MOS electronic nose sensor array for the detection of Chinese pecan quality. J. Food Eng., *203*, pp.25-31.

Figures

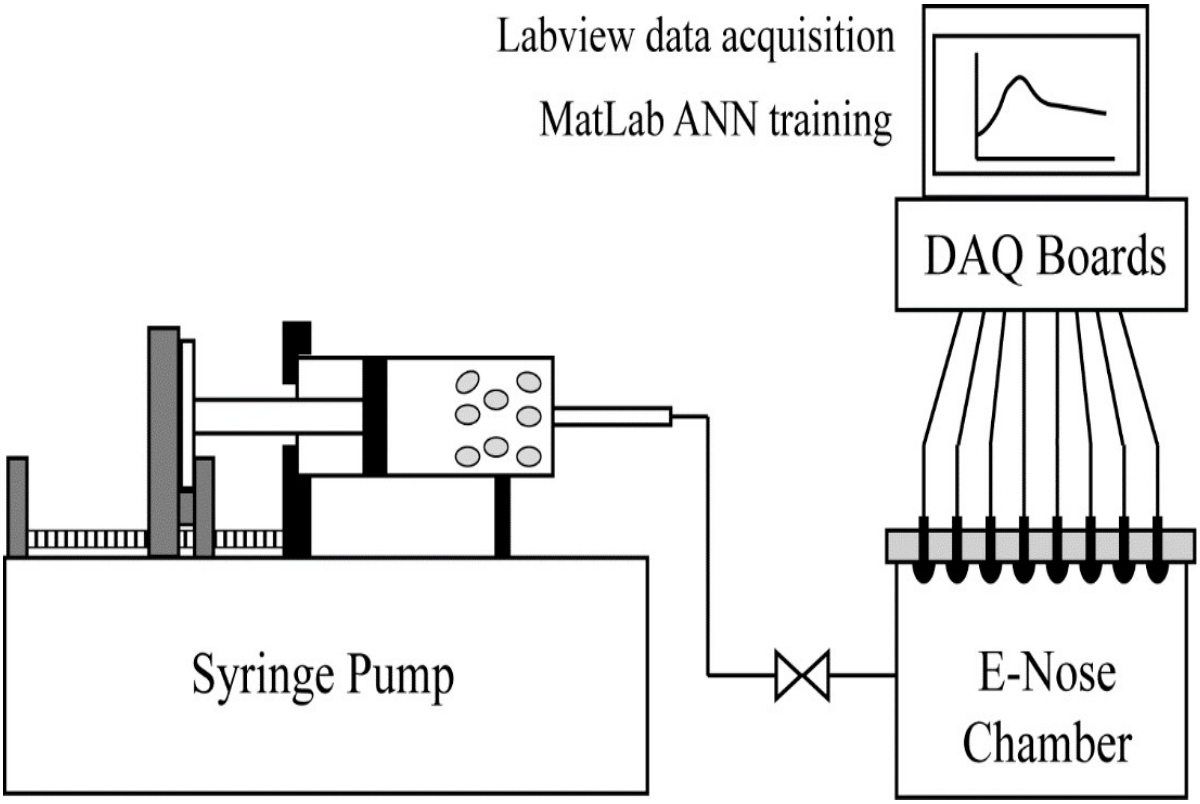

Figure 6.1. Diagram of the electronic nose system for sampling roasted cocoa beans.

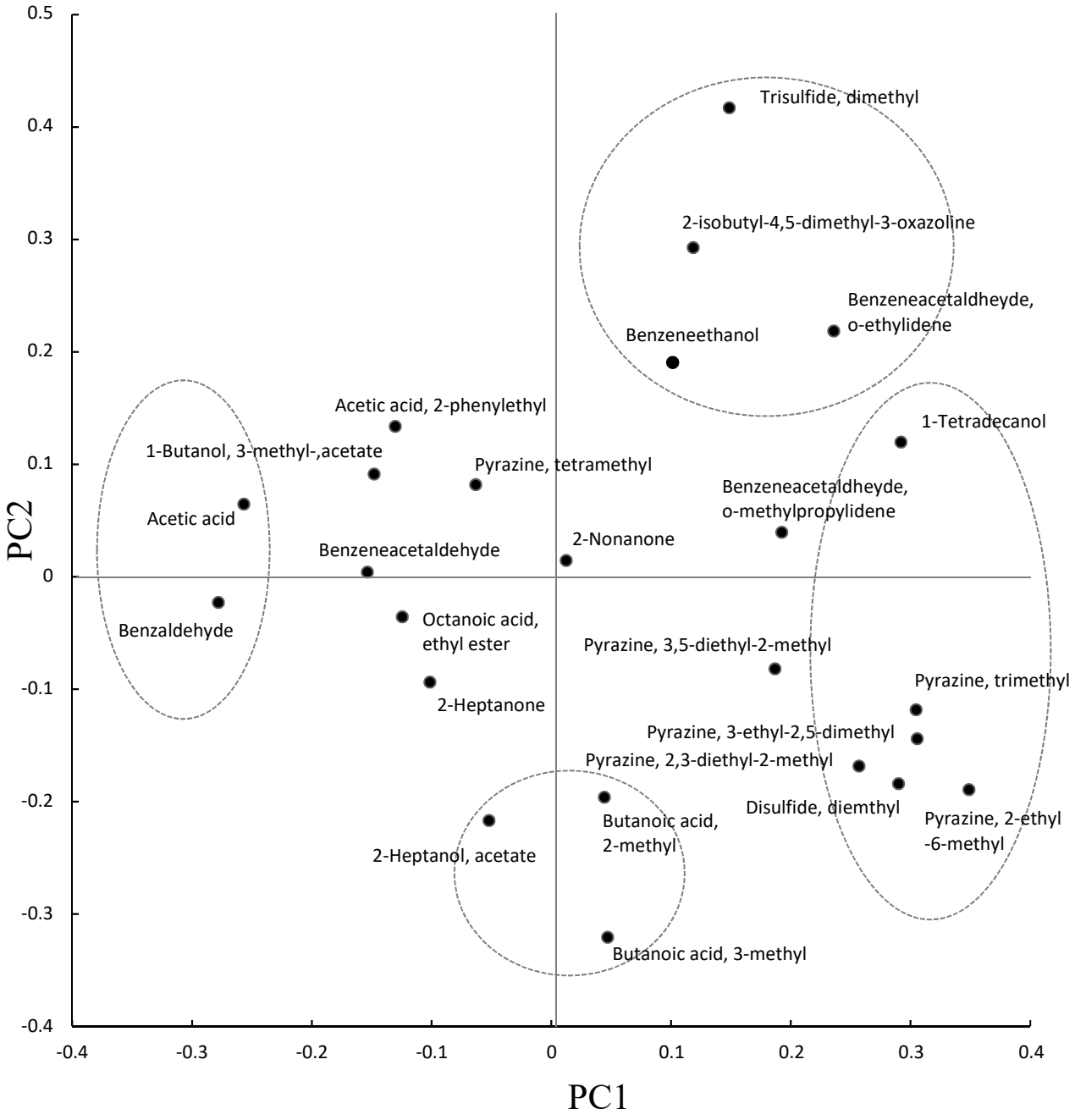

Figure 6.2. Principal component analysis loading plots for select volatile compounds: PC1 and PC2 components.

(a)

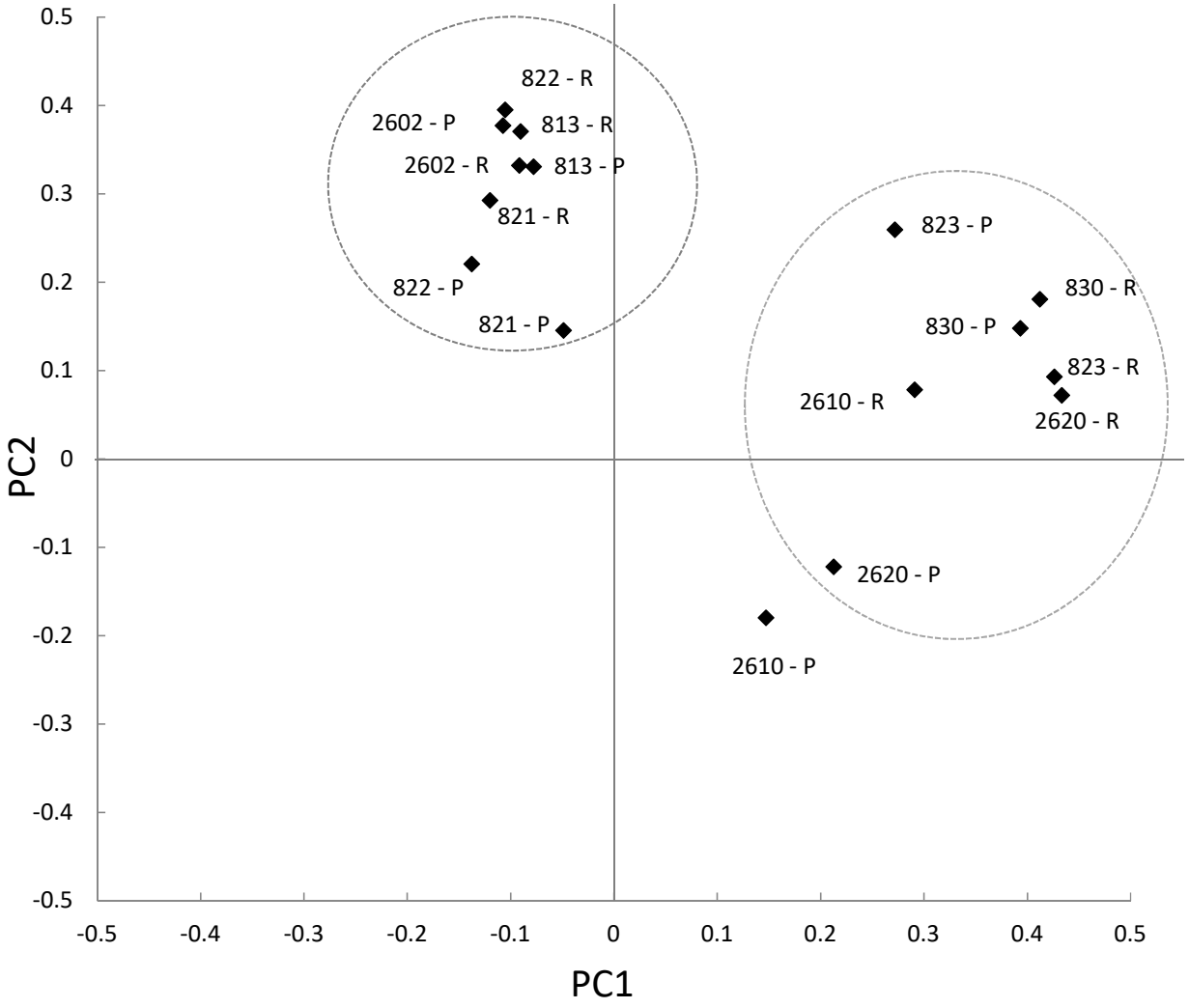
0.5
0.4
0.3
0.2
0.1
0
-0.1
-0.2
-0.3
-0.4
-0.5
PC2
-0.5
-0.4
-0.3
-0.2
-0.1
0
0.1
0.2
0.3
0.4
0.5
PC1
822 - R
2602 - P
813 - R
2602 - R
813 - P
821 - R
822 - P
821 - P
823 - P
830 - R
830 - P
823 - R
2610 - R
2620 - R
2620 - P
2610 - P

(b)

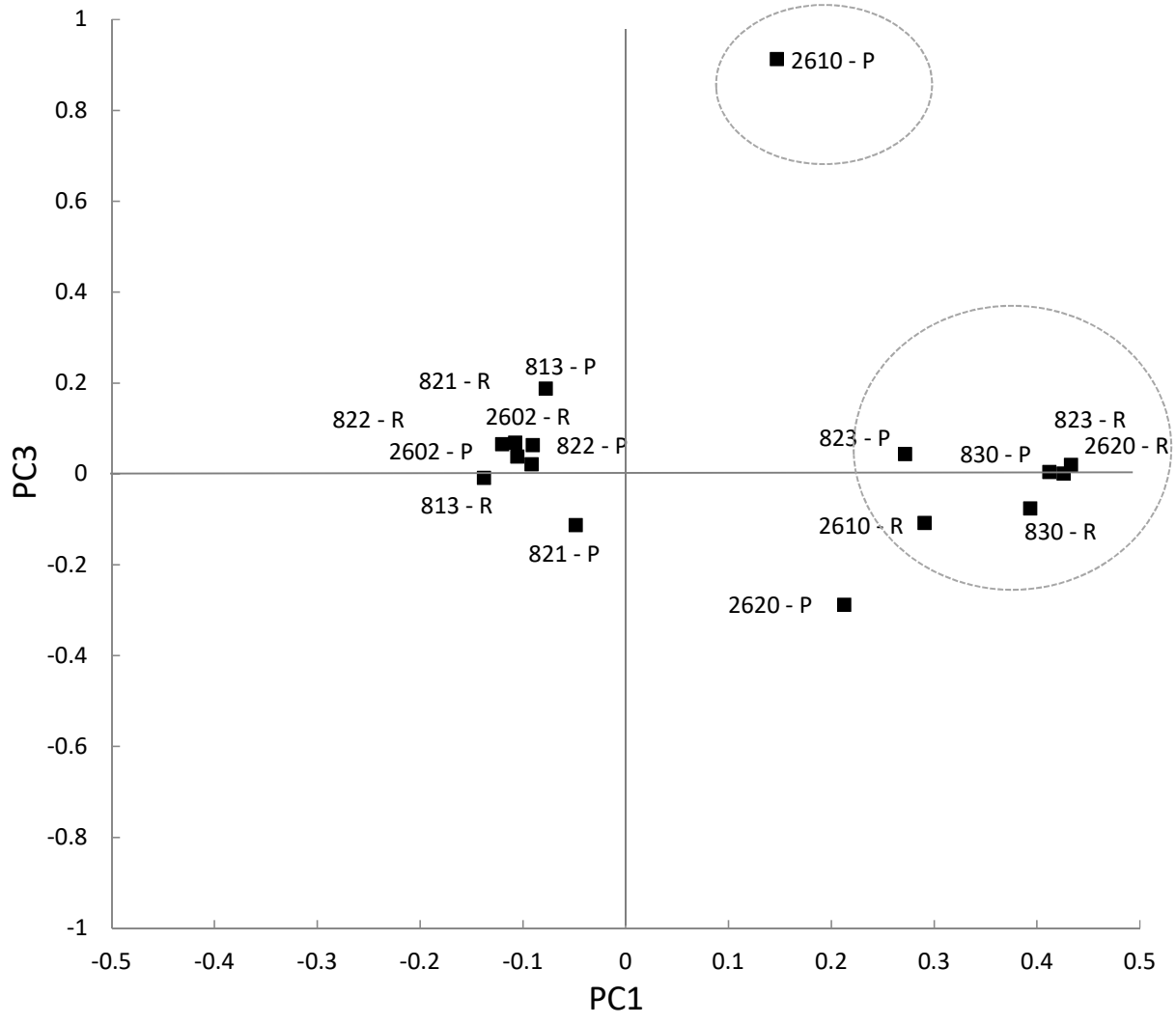

Figure 6.3. Principal component analysis loading plots for gas sensor data (R: Relaxation time, P: Peak voltage value): (a) PC1 and PC2 components and (b) PC1 and PC3 components.

(a)

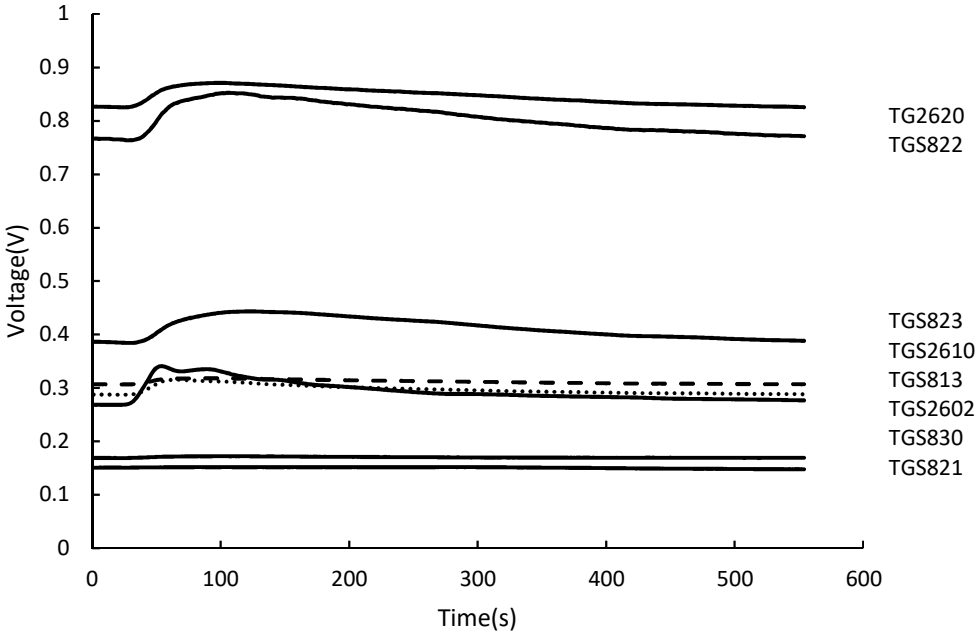
1
0.9
0.8
0.7
0.6
0.5
0.4
0.3
0.2
0.1
0
Voltage(V)
0
100
200
300
400
500
600
Time(s)
TG2620
TGS822
TGS823
TGS2610
TGS813
TGS2602
TGS830
TGS821

(b)

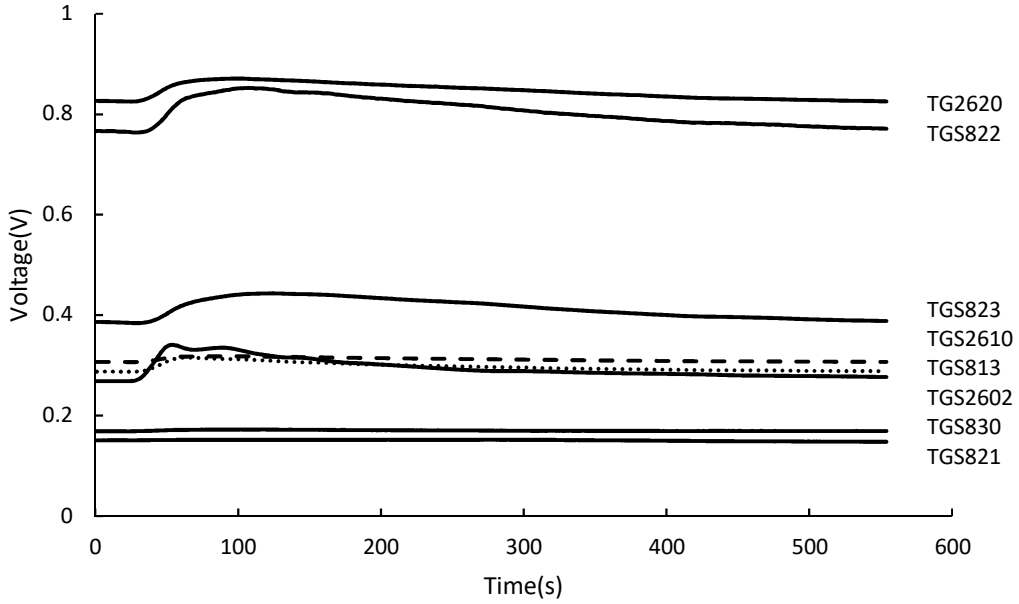
1
0.8
0.6
0.4
0.2
0
Voltage(V)
0
100
200
300
400
500
600
Time(s)
TG2620
TGS822
TGS823
TGS2610
TGS813
TGS2602
TGS830
TGS821

(c)

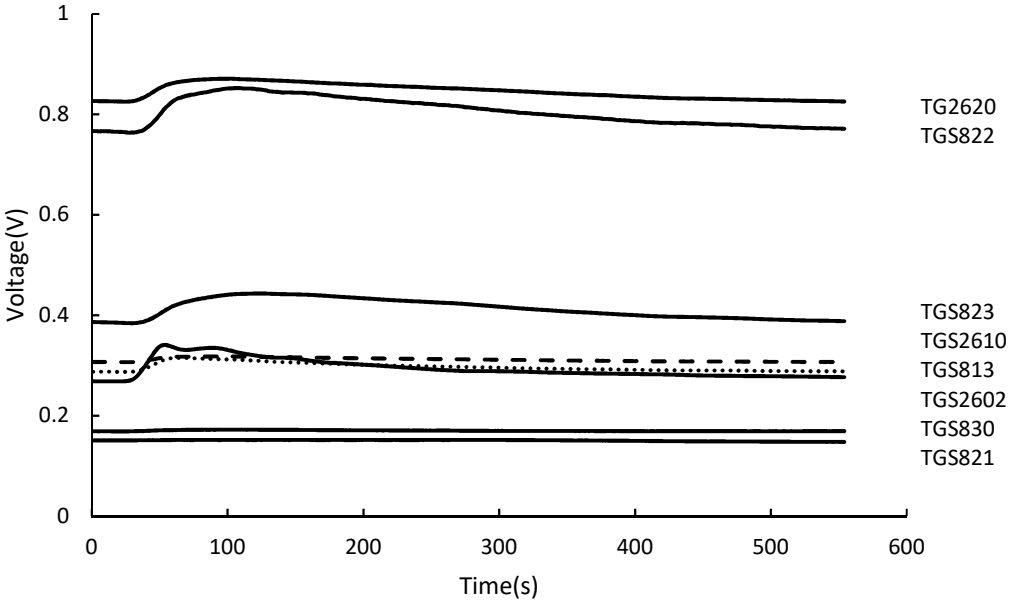

(d)

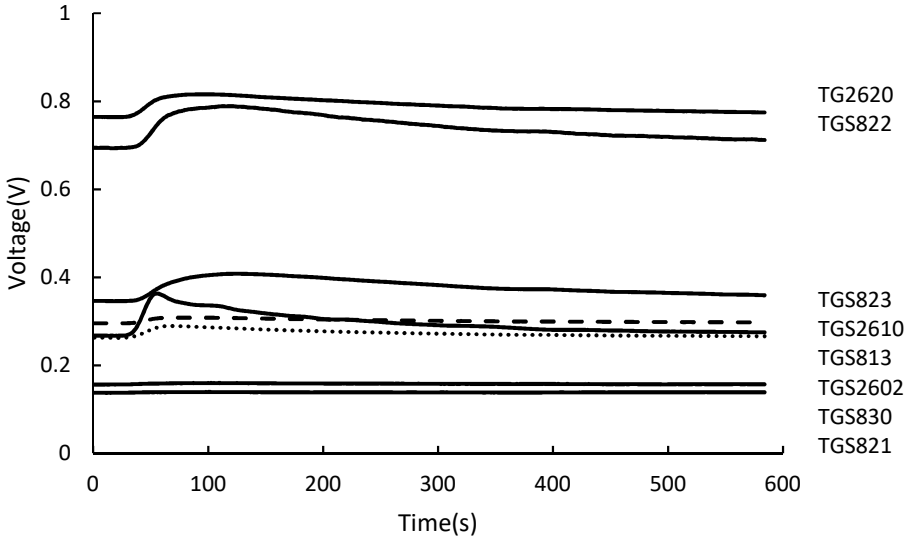

Figure 6.4. Individual gas sensor response when exposed to volatile compounds from cocoa beans roasted for (a) 0, (b) 20, (c) 30 and (d) 40 min.

Table 6.1. Sensitivity of the gas sensors used in the electronic nose system.

Sensors	Target gas
TGS821	Hydrogen
TGS813	Methane, propane, butane
TGS2602	VOCs, NH_3, H_2S
TGS822	Organic solvent, alcohols
TGS2610	Butane, propane
TGS2620	Alcohol, solvent vapors
TGS830	R11, R113, other halocarbons
TGS823	Organic solvent, methane, hexane

Table 6.2. Initial settings for training the artificial neural network (ANN)

Mu	Mu-dec	Mu-inc	Iterations	Validation check
0.001	0.1	0.1	1000	5000

Table 6.3. Relative concentrations of select volatile compounds from cocoa beans roasted at 135°C for 0 to 40 min.

Volatile compound	Relative concentration (%)			
	0 min	20 min	30 min	40 min
Acetic Acid	23.65^{d}	24.64^{c}	10.98^{b}	6.99^{a}
Disulfide, dimethyl	0.00^{c}	0.00^{c}	0.55^{b}	0.99^{a}
1-Butanol, 3-methyl-, acetate	1.39^{c}	1.28^{bc}	1.03^{b}	0.70^{a}
2-Heptanone	1.23^{b}	1.33^{b}	0.85^{a}	0.96^{ab}
Butanoic acid, 3-methyl-	7.64^{b}	6.77^{a}	6.92^{a}	8.37^{c}
Butanoic acid, 2-methyl-	4.33^{ab}	4.02^{a}	4.56^{b}	4.61^{c}
Trisulfide, dimethyl-	0.00^{a}	0.77^{c}	1.46^{d}	0.46^{b}
Benzaldehyde	3.37^{d}	2.85^{c}	0.80^{b}	0.60^{a}
Pyrazine, 2-ethyl-6-methyl-	0.00^{a}	0.04^{a}	0.69^{b}	1.20^{c}
Pyrazine, trimethyl-	0.00^{a}	0.98^{b}	3.23^{c}	5.21^{d}
2-Heptanol, acetate	0.65^{b}	0.56^{ab}	0.41^{a}	0.57^{ab}
Benzeneacetaldehyde	1.68^{b}	1.60^{b}	0.60^{b}	0.35^{a}
2-Isobutyl-4,5-dimethyl-3-oxazoline	0.00^{a}	1.01^{c}	2.15^{d}	0.43^{b}
Pyrazine, 3-ethyl-2,5-dimethyl-	0.00^{a}	0.48^{b}	2.81^{c}	4.54^{d}
Pyrazine, tetramethyl-	17.13^{c}	14.20^{b}	14.38^{b}	13.54^{a}
2-Nonanone	5.01^{b}	4.72^{a}	4.91^{ab}	5.03^{b}
Benzeneethanol	4.68^{a}	5.18^{ab}	7.76^{c}	5.98^{b}
Pyrazine, 2,3-diethyl-5-methyl-	0.00^{a}	0.00^{a}	0.20^{b}	0.42^{c}
Pyrazine, 3,5-diethyl-2-methyl-	1.46^{a}	1.66^{a}	2.48^{b}	2.99^{c}
Octanoic acid, ethyl ester	2.47^{c}	1.53^{b}	1.43^{b}	1.16^{a}
Acetic acid, 2-phenylethyl ester	3.38^{b}	3.38^{b}	2.98^{ab}	2.54^{a}
Benzeneacetaldehyde, α-ethylidene-	0.00^{a}	2.47^{b}	2.86^{b}	3.00^{c}
1-Tetradecanol	0.00^{a}	0.08^{b}	2.09^{d}	1.36^{c}
Benzeneacetaldehyde, α-(2-methylpropylidene)-	0.52^{a}	0.76^{b}	1.87^{c}	1.95^{c}

Table 6.4. Peak values of gas sensor responses to volatile compounds from cocoa beans roasted from 0 to 40 min.

	TGS821	TGS813	TGS2602	TGS822	TGS2610	TGS2620	TGS830	TGS823
0	0.002^{a}	0.029^{b}	0.110^{c}	0.089^{a}	0.012^{a}	0.048^{ab}	0.004^{a}	0.060^{b}
20 min	0.001^{a}	0.024^{a}	0.084^{b}	0.082^{a}	0.011^{a}	0.042^{a}	0.003^{a}	0.052^{a}
30 min	0.004^{ab}	0.029^{b}	0.105^{c}	0.101^{b}	0.014^{b}	0.055^{b}	0.004^{a}	0.066^{c}
40min	0.005^{b}	0.026^{ab}	0.068^{a}	0.087^{a}	0.012^{a}	0.046^{a}	0.003^{a}	0.057^{b}

Table 6.5. Relaxation time of gas sensor responses to volatile compounds from cocoa beans roasted from 0 to 40 min.

	TGS821	TGS813	TGS2602	TGS822	TGS2610	TGS2620	TGS830	TGS823
0	104.6^{ab}	70.1^{a}	33.6^{ab}	145.1^{b}	114.0^{a}	140.6^{ab}	91.6^{a}	153.8^{a}
20 min	145.3^{c}	137.4^{c}	50.3^{c}	287.2^{c}	211.0^{b}	253.2^{c}	144.7^{c}	309.4^{b}
30 min	130.1^{b}	73.4^{a}	28.6^{a}	145.4^{b}	119.9^{a}	145.3^{ab}	86.8^{a}	158.6^{a}
40 min	89.4^{a}	84.1^{b}	38.1^{b}	129.2^{a}	114.9^{a}	134.4^{a}	98.0^{b}	143.7^{a}

Table 6.6. Performance of E-nose trained ANN and Volatile compounds trained ANN.

	E-nose trained ANN		Volatile compounds trained ANN	
Roasting time (min)	Correct prediction	False prediction	Correct prediction	False prediction
0	9	0	6	0
20	9	0	6	0
30	8	1	6	0
40	8	1	5	1
Overall Accuracy	94.44%		95.83%	

CHAPTER 7

CHARACTERIZING COCOA CONCHING AND REFINING PROCESSES BY KERNEL DISTRIBUTION MODEL (KERNEL MD) BASED ELECTRONIC NOSE[5]

[5] Tan, J. and W. L. Kerr. To be submitted to *Journal of Food Engineering*

ABSTRACT

Refining and conching are two important processes for chocolate manufacturing. It is believed that refining/conching process contributes to the improvement of flavor and texture of chocolates. However, the traditional analytical methods, such as gas chromatography-mass spectrometry (GC-MS), for volatile compounds mapping are relative expensive and time consuming. In this study, one electronic nose was built and placed in the headspace of cocoa samples, monitoring the volatile compounds profiles during refining/conching process. The responses of the e-nose were characterized by trained Kernel DM models and three parameters, P_{area}, P_{peak} and P_{width}. The three parameters were able to detect the overall influence of roasting and sample weight on the volatile compound profile of cocoa, however, they failed to characterize the influences introduced by single factor. On the other hand, the trained Kernel DM models were able to characterize the total volatile compounds profiles of samples with different treatment. Classification and discrimination based on volatile compounds profiles were correctly conducted by trained Kernel DM models.

Keywords: cocoa, refining/conching, e-nose, Kernel DM

1. Introduction

The history of chocolate started approximately one thousand years ago in Central America and since then, chocolate was mainly consumed as drinks and medicines up until 1800s when solid chocolate became more popular than liquid chocolate (Grivetti and Shapiro 2011). Today, chocolate is almost everywhere in this world. Chocolate production has increased exponentially since 1990. This grows in chocolate production is driven by growing demands from developing countries in Asia, Africa and Latin America. In 2000, the consumption of chocolate confectionary was 5.6 million tons and the value of the chocolates was $51.314.5 million. The consumption of chocolate confectionary increased to 7.15 million tons in 2013 and the values of the chocolates doubled to $109,991.5 million (Squicciarini and Swinnen 2016; Afoakwa 2016).

The chocolate processing typically includes the following steps: harvesting, drying, fermentation, roasting, cracking, winnowing, refining, conching, tempering, molding, packaging, transportation and storage (Saltini et al., 2013, Afoakwa 2010). Each step in the processing plays important role in determining the final qualities of the chocolate products. The refining or grinding of chocolate usually is defined as one process where ingredients such as cocoa nibs, sugars, and proteins together are mixed and agitated by repeating crushing and shearing, delivering smooth fluid paste with uniform and small particle sizes (< 30um) (Carvallo et al., 2001). And chocolate conching is one procedure that the post-refining ingredients are evenly agitated and heated for certain time (varied from several hours to days) to yield well homogenized liquid chocolate. In this process, the flavor of the chocolate is developed, along with many changes in physical and chemical properties, such as, the viscosity, the moisture content and the morphology of chocolate particles (Beckett 2011, Fryer and Pinschower 2000).

Beckett (2000) divided the chocolate conching process into two distinct stages that take place in the same conching machine. In the first stage, some undesirable flavor compounds such as acetic acids are greatly removed and the flavor compounds and precursors which developed by roasting and fermentation are further developed to bring pleasant taste. The second stage turns the thick or flaky chocolate paste into smooth liquid paste by evenly distribute the fat to coat the solid cocoa particles so that chocolate particles can slide pass each other.

The refining and conching processes are considered two individual processes or one combined process depending on what kind of the equipment is being used to conducts the processes. Many manufacturers use a multi-roller mill to refine the ingredients first and then use a conche to proceed the conching process (Owusu et al 2012). Some manufacturers are using melangers to conduct refining and conching at the same time (Prawira and Barringer 2009). As mentioned above, the time needed for finishing conching varies from several hours to days depending on the equipment being used and the demands of the manufacturers, for example, many chocolate manufacturers leave the conching process ongoing for days just to ensure the undesirable flavors were removed and the texture of the chocolate paste become smooth and liquid like. However, by letting the conching process ongoing for days, the energy cost increase greatly and the equipment are more likely to be damaged due to the wearing of their parts. In some cases, it is not necessary to trade days of conching just for small improvement in the texture and flavor of the products. Also, the conching process can also decrease the concentrations of desirable flavor compounds which developed from fermentation and roasting, vary by bean varies (Beckett 2009, Jolly et al., 2003). It is very important for many manufacturers, who wish to keep the special flavors in their products, to control the time for

conching process. Therefore, tracking the changing of the overall flavor compounds and predict the volatile compounds profiles in ongoing refining/conching process are potentially useful.

The analytical method that can provide comprehensive information about the volatile compounds profile of cocoa product is using a GC-MS system coupled with corresponding flavor extraction methods. Many researchers (Ducki et al., 2008, Rodriguez-Campos et al., 2011, Bonvehí 2005, Jinap et al., 1998, Schnermann and Schieberle 1997) have studied the influence of roasting time, drying condition, variety, fermentation condition, and formulation on the volatile compounds profile of cocoa beans, chocolates, and cocoa power. Owusu et al. (2012) have studied how the conching conditions influence the volatile compounds of chocolate and Counet et al. (2002) have compared the volatile compounds in chocolate with and without conching. However, no previous research have been done to characterize the volatile compounds profiles of chocolates in the refining/conching process. The reason for the lack of information is manifold. Firstly, it requires analyzing at least hundreds of samples from one ongoing conching process at different time before characterizing the profiles of volatile compounds because one refining/conching process typically runs for more than 12 hours. Secondly, the volatile compounds analysis conducted by GC-MS for one sample takes about an hour and the extraction for volatile compounds in cocoa paste is relatively complicated and time consuming. In addition, the GC-MS analysis provides the concentrations of tens of volatile compounds which makes it even more complicated to select the right compounds as indicators to characterize the profiles. Therefore, the traditional method is unable to provide fast measurements for volatile compounds and construct the overall volatile compounds profile of a lengthy continuous process such as chocolate refining/conching.

Electronic nose (E-nose) is an array of gas sensors which give fingerprint responses to a given odors, and the responses are used to perform odor identification and discrimination (Arshak et al., 2004). One of the most widely used type of gas sensor is metal oxide semiconductor (MOS) gas sensor due to its inexpensive price, lightweight, high sensitivity, and fast response (Fine et al., 2010). When target odors interact with the surface of a metal oxide film (generally through surface adsorbed oxygen ions), and it results in a change in charge carrier concentration of the material. The conductivity of the material, however, is depending on the its carrier concentration. The change of conductivity of the sensor is reflected by the change of output voltage of the sensor and the characteristics of the voltage response is used for determining the concentrations and categories of target gases (Pearce et al., 2006, Harsányi, 2000).

There are many researchers have conducted comprehensive studies to implement the e-nose for food quality determination. García et al. (2006), Lozano et al. (2005) and Buratti et al. (2007) have used e-nose to evaluate the quality of wines based the aroma profile of wines. Labreche et al. (2005) have used e-nose to monitor the shelf life of milk. Eklöv et al. (1998) have implemented e-nose to monitor the fermentation of sausages. However, few researches have developed a e-nose system that is suitable for characterizing the chocolate conching process or other continuous process. In this study, one e-nose system was constructed and attached to a melanger, measuring the overall volatile compounds profiles in the headspace of the samples undergoing refining/conching process. The responses of the e-nose were used to characterize the overall volatile compounds profiles of the complete refining/conching processes.

One challenge of using e-nose to monitor the volatile compounds profile of a continuous refining/conching process is gas distribution in real environment is influenced by turbulent

advection introduced by the grinder or conche and such influences are random. The turbulent happens randomly and the turbulent flow creates packets of gas that follow chaotic trajectories (Shraiman and Siggia 2000). In addition, other factors include temperature variation and random flow of winds in the environment can also influence the distribution of the odors. Although make an exact description of turbulent flow is difficult at this moment, it is possible to describe turbulent gas distribution on average under the assumptions that each measurement from the gas sensor is a random variable. By doing that, strong assumption such as perfect environment can be avoided (Hinze 1975). In this study, the Kernel Distribution Model (Kernel DM) was proposed to characterize the volatile compounds profile in process of refining/conching of cocoa based on the responses of the gas sensors (e-nose).

Kernel DM is a statistical model that treats every measurement as a random variable and there are no assumptions about one certain functional form of the model, which indicates that it does not assume certain environmental conditions such as a uniform airflow (Lilienthal et al., 2009). The responds of the e-nose were used to train the Kernel DM model, and the learned model characterize the distribution mean of overall volatile compounds as a function of time.

There were several parameters such as kernel width (σ), which may influence the performance of the model. The parameter selection was done by Genetic Algorithm (GA) which tried to minimize the error of the learned model. GA is an adaptive heuristic search algorithm based on the evolutionary theory of natural selection and genetics. They represent an intelligent exploitation of a random search used to solve optimization problems (Sivaraj et al., 2011). The key idea of the selection operator is to give preference to better individuals (those that are nearer to the solution) by allowing them to pass on their genes to the next generation and prohibit the entrance of worst fit individuals into the next generations. The selection operator mainly works

at the level of chromosomes and the performance of each individual depends on its fitness. The fitness value may be determined by an objective function or by a subjective judgment specific to the problem. As the generations pass, the members of the population should get fitter and fitter. (Goldberg, 1990)

2. Materials and methods

2.1 Sample preparation

Two batch (20kg for each batch) cocoa beans (*Frastero*) were roasted by a mini drum roaster (Model SS, CocoaTown, Roswell, Georgia, USA) for 30 min (well roasting) and 40min (dark roasting) respectively. The roasted beans were immediately chilled by a tray cooler (CocoaTown, Roswell, Georgia, USA) after roasting. Chilled samples were packaged in heat sealed alumina pouches and the pouches were stored in a -40℃ freezer before the tests.

2.2 Experimental design and electronic nose system

The refining/conching processes were conducted by one chocolate melanger (Model: ECGC12SL CocoaTown, Roswell, Georgia, USA). For each refining/conching process, 700g or 1000g of well roasted (30 min roasted) or dark roasted (40 min roasted) sample was added into the drum of the melanger and two double conical roller stones crushed, sheared and stirred the samples for 24 hours. The cocoa samples were transformed from raw cocoa ribs into smooth fine cocoa liquid during the refining/conching process. Each combination of different sample weight and roasting degree were replicated for 6 time.

The diagram of the e-nose system was shown in Figure 7.1. Six gas sensors (TGS 821, TGS 822, TGS 823, TGS 2602, TGS 2610, TGS 2620) were fixed on a teflon bar (20cm*6cm*1cm) and the Teflon bar was fixed above the drum of the melanger, exposing the

gas sensors to the volatile compounds released from the drum during refining/conching. The responses of the gas sensors were collected by two data acquisition boards (Model NI9219, National Instruments, Austin, TX) at a sample rate of 6 second / point. The software being used for interface between DAQ boards was Labviews (Version 2014, National Instruments, Austin, TX). Also, one thermal couple wire was fixed about 1 cm above the bottom of the drum and the temperature of the samples during refining/conching were recorded by a thermal couple DAQ module ((Model NI9211, National Instruments, Austin, TX).

2.3 Data processing and parameters determination

Unlike many previous studies (Olunloyo et al., 2012; Markom et al., 2009; Bleibaum et al., 2002) which used electronic nose to do single measurement for each sample at a time, the electronic nose system did continuous measurement on the overall volatile compounds profile of cocoa in the whole process of refining/conching. The responses of the gas sensors depended on the concentrations of target volatile compounds around the gas sensors and the volatility of the cocoa samples determined the concentration of the volatile compounds. Volatility is directly related to a substance's vapor pressure. The vapor pressure is a measure of the amount of vapor above a liquid. At constant atmospheric pressure, vapor pressure increases with temperature (Shoemaker et al., 1962). During the process of refining/conching, temperature was not constant because the grinding and shearing generated heat throughout the whole process. Vapor pressure (P) of the samples as a function of temperature (T) is given by Clausius-Clapeyron equation below:

$$P=Ae^{\left(\frac{-\Delta H_{vap}}{RT}\right)}$$

where ΔH_{vap} is the enthalpy of vaporization of the sample, and R is the gas constant, R = 8.314 J K^{-1} mol^{-1}. A is unknow constant. In this study, the ΔH_{vap} was set to 50.12 kJ/mol and A was set to 1.0. The responds of the gas sensors were divided by their corresponding vapor pressures calculated by following the Clausius-Clapeyron equation mentioned above, therefore, eliminated the influence of temperature variation to get adjusted 'raw' data R_i. Then parameters that characterized R_i were extracted. Theses parameters included the relative peak value R_{peak}, which was the maximum R_i over the baseline (the minimum value amount R_i), R_{area}, the area between the baseline and the R_i for 1 h, 2 h,3 h,4 h,5 h, and 6 h since the refining/conching process began, R_{width}, the time length that R_i was above a certain value (20%, 30%, 40%, 50%, and 60% of the R_{peak} value).

2.4 Kernel DM model

The basic principle of the Kernel DM model is trying to predict the respond (R) of the gas sensor at time t during one refining/conching process based on the responds ($R_{1:n}$) of the same gas sensor at adjacent time points ($t_{1:n}$) or, in another word, time points that close to t, from several other refining/conching processes with same treatments combination.

$$p(R|t, R_{1:n}, t_{1:n})$$

In this study, refining/conching process with same treatments were replicated for 6 time, and three of the repetitions were used to construct or, in another word, train the Kernel MD model, while the rest three repetitions were used for validation. In the rest of the paper, 'training data' was used to represents the data being used to train the models, and 'validation data' referred to the data being used for evaluating the performances of the models. And the samples provided training data were called 'training group' and samples provided validation data were called 'validation group'.

Before constructing the model, the adjusted 'raw' data R_i from both training and validating data were first scaled to $r_i \in [0, 1]$ to compensate for drift issues and individual variations between different gas sensors. The scale function was shown below:

$$r_i = \frac{R_i - \min(\{R_i\})}{\max(\{R_i\}) - \min(\{R_i\})}$$

then an uni-variate Gaussian weighting function N was used to assign the importance of each responds r_i at different time point t_i in grind cell k. The number of k is equal to the number of the data point from the refining/conching process for training. Two parameters, $\Omega^{(k)}$, the sum of the weights and $R^{(k)}$, the sum of the weighted responds in cell k, was calculated as

$$\Omega^{(k)} = \sum_{i=1}^{n} N(|t_i - t^k|, \sigma)$$

$$R^{(k)} = \sum_{i=1}^{n} N\left(|t_i - t^k|, \sigma\right) \times r_i$$

where t_k was the time point for the predicted respond, n is the number of the time points being included in cell k, σ was the parameter for Gaussian weighting function. Then the prediction ($r^{(k)}$) for the respond of the sensor at t^k is calculated by:

$$r^{(k)} = \frac{R^{(k)}}{\Omega^{(k)}}$$

Four Kernel MD models trained by sensor data (from training group) collected during refining/conching processes with different treatment combinations (700g/1000g beans with well/dark roasted) respectively. Data from validation group were used to check the performance of the trained model by calculating the root mean absolute error (RMAE) of the model:

$$RMAE = \sum_{i=1}^{n} \sqrt{\frac{|r_i^{(k)} - r_i|}{n}}$$

where $r_i^{(k)}$ was the predicted respond of the gas sensor at t_i, r_i was the respond of the same sensor at ti from validation group.

2.5 Genetic algorithm setting

The choice for the value for parameters n, σ were determined by Genetic algorithm (GA) to ensure the Kernel MD model yield good performance. One trained model (trained by data collected at 700g/well roasted condition). The range for n and σ were 5 to 30 and 0.1 to 1 respectively. n was integer and σ a multiple of 0.1. The fitness function is the RMAE of the model and the goal was trying to minimization the fitness value. The initial value of n and σ were randomly given. Each gene only had two units to represent the value of n and σ respectively. No crossover for the GA. The mutation of gene followed the following rules: All the gene from the initial population had to mutate. From the second generation, if the fitness of the gene is better than previous generation, then mutation rates for both n and σ were

$$P_m = 1 - \frac{|f_n - f_{n-1}|}{f_{n-1}}$$

and if any of n and σ was decided to mutate, the value of n and σ was added or deduced by 1 or 0.2 respectively at equal possibility. If the fitness of the gene is no better than previous generation, then the gene had to mutate by following the same methods just mentioned. The population size p was 100 and the GA stopped when 200 generation were created. The GA process was executed on Matlab (Version R2015b, MathWorks, Natick, MA).

2.6 Statistics

All tests were repeated at least three times and results presented as the mean and standard deviation. The results were compared by one-way ANOVA using SAS 9.3 (SAS Institute Inc., Cary NC) to determine the effects of the fat content and the particle size distribution of the

chocolate sample on the melting properties measured by DSC and CTA. Tukey's HSD was used to determine significant differences amongst treatments at the 95% level of confidence.

3. Results and discussion

3.1 Analysis of volatile compounds profile of cocoa refining/conching

Figure 7.1 shows one example of how the trendlines of the responds of three of the selected gas sensors as a function of time in a refining/conching process. Three parameters ($P_{area,}$ $P_{peak,}$ P_{width}) were exacted to characterize the responds of gas sensors in refining/conching processes. The parameters for refining/conching processes with different samples were shown in Table 7.1-3. Some of the gas sensors only had negligible responds during the process because the sensors were not sensitive to the volatile compounds released by cocoa. Therefore, the parameters shown in the tables were extracted from the trendlines of the two gas sensors that had shown strongest responds.

P_{area} can be considered as the amount of volatile compounds being released during a refining/conching process, since the headspace of samples were exposed to the environment. The amount of volatile compounds can be released in a refining/conching process were greatly influenced by the amount volatile compounds that the sample contains. Therefore, it was reasonable to see that the increase of the weight of the samples resulted in increase of P_{area}. Table 7.1 also indicated that dark roasted samples resulted in higher P_{area} values than well roasted samples did if the sample weights were the same. Previous research (de Brito et al., 2001) indicated that roasting increased the number of damaged and disrupted cells, and reduced the amount of cytoplasmic material. Also, the level of phenolic compounds decreased markedly. The damaged and disrupted cells release volatiles compounds easier because the cell structure to keep the compounds were broken. Therefore, damaged and disrupted cells due to roasted may be one

factor that resulted in more volatile compounds were released from dark roasted cocoa samples than well roasted samples.

In addition, many other researches (Diab et al., 2014, Bailey et al., 1962, Cambrai et al., 2010, Frauendorfer and Schieberle 2008) reported that during roasting, Maillard reaction takes place. Therefore, the reaction between reducing sugars and amino acids plays important roles. Typical Maillard reaction produce products include dicarbonyls (e.g., diacetyl), heterocyclic compounds such as pyrazines, pyroles, pyridines, furans and thiazoles), aldehydes (e.g., phenylacetaldehyde and benzaldehyde), ketones, esters, and alcohols. In the meantime, Maillard reaction significantly reduce the concentration of free amino acids and reducing sugars. The volatile compounds generated by Millard reaction and Strecker degradation during roasting may also contributed to the increased concentrations of sensor detectable volatiles compounds.

Table 7.2 shows the P_{peak} values of the cocoa samples during refining/conhcing process. The P_{peak} can be interpreted as the highest concentration of volatile compounds in the headspace in a refining/conhcing process. The concentrations of volatile compounds in the sample headspace was determined by the volatility of the sample. The volatility of the samples strongly relies on the surface area of the samples, the temperature, and the amount of the compounds that the samples contained. This theory concurred with the observations shown in Table 7.2, which imply that more sample weight and linger roasting time significantly increased the P_{peak} value of tested samples. Roasting increased the amount of volatile compounds in the samples, while greater sample weight increased both surface area and the amount of volatile compounds in the samples. In addition, another observation from Table 7.2 was the increase of sample weight from 700g to 1000g resulted in the P_{peak} value of the samples increased from 0.170 to 0.187 for well roasted samples, 0.196 to 0.215 for dark roasted sample. On the other hand, the difference

between P_{peak} values of dark roasted samples and well roasted samples were 0.026 for 700g samples, 0.028 for 1000g samples. These observations indicated that roasting may played greater role than sample weight in influence the P_{peak} value.

The P_{width} values of samples shown in Table 7.3 may interpreted as the time length volatile compounds released by the samples kept the responds of the gas sensors greater than a threshold value. Three threshold values (20%, 40% and 60% of the peak value) were selected in this study. Both increasing sample weight and increasing roasting degree resulting in greater P_{width} values of all samples, no matter which threshold valued were applied. However, unlike P_{area} and P_{peak} values, P_{width} values of all samples were influenced greater by sample weight than by roasting time. This observation implied that roasting increased the amount of volatile compounds in cocoa samples, however, it made it easier for volatile compounds to be released during refining/conching process. As mentioned above, roasting could destroy the structure inside cocoa and increased the number of damaged and disrupted cells, thus, decrease the ability for the cells to 'trap' the volatile compounds.

The three parameters, P_{area}, P_{width} and P_{peak} may have shown the overall influences introduced by sample weight and roasting time on the sensor responds in refining/conching processes, however, the three parameters were not able to differentiate the influence of single factors. Therefore, it is difficult to use the three parameters to characterize the responds of gas sensors and it is also unrealistic to fingerprint the samples based on the three parameters.

3.2 Kernel MD model analysis

After running GA for 10 times, the selected setting for Kernel MD were $n = 22$, $\sigma = 0.3$. Validation data were used to evaluate the performance of the Kernel MD model trained by sensor responses collected during the refining/conching process of 700g well roasted beans and

the results were shown in Figure 7.3 as an example. It indicated that if the validation data was provided by samples with same conditions (sample weight and roasting degree) as samples being used to trained the model, then the RMAE value of the model were much smaller than the RMAE values of using validation data collected from samples had at least one condition was not the same as samples from training group. The figure also implied that for validation the model, if the samples from validation group only have one condition varied from the training samples, then the validation samples had different roasting time yielded great RMAE values than validation sample had different sample weight. Furthermore, if validation samples had both conditions differed from the training samples were used to validate the trained model, then the RMAE values was greater than any of the RMAE value achieved by other samples from validation group. RMAE value can be interpreted as the difference between the trained model and the validation data, or in another word, how the validation data fit the model. From Figure 7.3, based on the RMAE values, the trained model can be used to do classification and discrimination, determining which validation sample had most similar or different condition as training samples.

Figure 7.4 also shows, at different stage of refining/conching, the ratios (ratio1, ratio 2, and ratio3) between the RMAE yielded by validation samples who had the same condition as training samples, to RMAE values achieved by validation samples had different in sample weight, roasting degree and both respectively. Smaller ratio value implied that the validation data was less likely to fit the trained model. For better discrimination and classification, small ratio values were desirable. From Figure 7.3, it shown that smallest value of ratios shown up at around using the first 2h of training data to train the model. Also, from Figure 7.2, it roughly shows that most of the differences between the responds of the gas sensor that monitoring different samples

being refined and conched appeared at the first two hours of the refining/conching process. Therefore, for the performance of other trained model, the evaluations were based on the data collected from the first 2h of reefing/conchig process.

Table 7.4 shown the performances of Kernel MD models trained by different training data from training group. Generally, the smallest RMAE values were produced when the training group and validation group are same type of samples. If the validation group and training group use samples varied in one condition, then differing the roasting made the model produce higher RMAE values than using sample varied in sample weight. Furthermore, if the training data are from well roasted samples, flip both conditions yielded highest RMAE values. Therefore, the models did good job in recognizing samples that had same conditions as training group, also the model also provided good discrimination of samples had different conditions.

4. Conclusion

Although the overall influences introduced by roasting and sample weight on volatile compounds profile were able to be detected by using P_{area}, P_{width} and P_{peak}, they failed to characterize the influence introduced by single factor. On the other hand, the trained Kernel DM models were able to characterize the total volatile compounds profiles generated by samples with same or different treatment. Classification and discrimination for different volatile compounds profiles were correctly conducted by trained Kernel DM models. The Kernel DM method is an inexpensive and in-line models that can be implemented to chocolate manufacturing, monitoring the flavor development during refinling/conching process. Based on the model, chocolate manufacturers can make prediction about the time needed for refinling/conching, in addition, they can find the affinity between one unknow sample between one known sample.

References

Afoakwa, E. O., 2016. Chocolate science and technology. John Wiley & Sons.

Afoakwa, E. O., 2010. Chocolate production and consumption patterns. Chocolate Science and Technology, pp.1-11.

Arshak, K., Moore, E., Lyons, G. M., Harris, J. and Clifford, S., 2004. A review of gas sensors employed in electronic nose applications. Sens. Rev., *24*(2), pp.181-198.

Bailey, S. D., Mitchell, D. G., Bazinet, M. L. and Weurman, C., 1962. Studies on the volatile components of different varieties of cocoa beans. J. Food Sci., *27*(2), pp.165-170.

Beckett, S. T. ed., 2011. Industrial chocolate manufacture and use. John Wiley & Sons.

Beckett, S. T., 2009. Conching. Industrial Chocolate Manufacture and Use, Fourth Edition, pp.19

Beckett, S., 2000. The science of chocolate (Vol. 22). Royal Society of Chemistry.

Bleibaum, R. N., Stone, H., Tan, T., Labreche, S., Saint-Martin, E. and Isz, S., 2002. Comparison of sensory and consumer results with electronic nose and tongue sensors for apple juices. Food Qual Prefer, *13*(6), pp.409-422.

Bonvehí, J. S., 2005. Investigation of aromatic compounds in roasted cocoa powder. Eur. Food Res. Technol., *221*(1-2), pp.19-29.

Buratti, S., Ballabio, D., Benedetti, S. and Cosio, M. S., 2007. Prediction of Italian red wine sensorial descriptors from electronic nose, electronic tongue and spectrophotometric measurements by means of Genetic Algorithm regression models. Food Chem., *100*(1), pp.211-218.

Cambrai, A., Marcic, C., Morville, S., Sae Houer, P., Bindler, F. and Marchioni, E., 2010. Differentiation of chocolates according to the cocoa's geographical origin using chemometrics. J. Agric. Food Chem., *58*(3), pp.1478-1483.

Carvallo, F. D. L., Hine, W. S. and Helmreich, A. V., Kraft Foods, Inc., 2001. Chocolate refining process. U.S. Patent 6,238,724.

Counet, C., Callemien, D., Ouwerx, C. and Collin, S., 2002. Use of gas chromatography-olfactometry to identify key odorant compounds in dark chocolate. Comparison of samples before and after conching. J. Agric. Food Chem., *50*(8), pp.2385-2391.

De Brito, E. S., García, N. H. P., Gallão, M. I., Cortelazzo, A. L., Fevereiro, P. S. and Braga, M. R., 2001. Structural and chemical changes in cocoa (Theobroma cacao L) during fermentation, drying and roasting. J. Sci. Food Agric., *81*(2), pp.281-288.

Diab, J., Hertz-Schünemann, R., Streibel, T. and Zimmermann, R., 2014. Online measurement of volatile organic compounds released during roasting of cocoa beans. Food Res. Int., *63*, pp.344-352.

Ducki, S., Miralles-Garcia, J., Zumbé, A., Tornero, A. and Storey, D. M., 2008. Evaluation of solid-phase micro-extraction coupled to gas chromatography–mass spectrometry for the headspace analysis of volatile compounds in cocoa products. Talanta, *74*(5), pp.1166-1174.

Eklöv, T., Johansson, G., Winquist, F. and Lundström, I., 1998. Monitoring sausage fermentation using an electronic nose. J. Sci. Food Agric., *76*(4), pp.525-532.

Fine, G. F., Cavanagh, L. M., Afonja, A. and Binions, R., 2010. Metal oxide semi-conductor gas sensors in environmental monitoring. Sensors, *10*(6), pp.5469-5502.

Frauendorfer, F. and Schieberle, P., 2008. Changes in key aroma compounds of Criollo cocoa beans during roasting. J. Agric. Food Chem., *56*(21), pp.10244-10251.

Fryer, P. and Pinschower, K., 2000. The materials science of chocolate. Mrs Bulletin, 25(12), pp.25-29.

García, M., Aleixandre, M., Gutiérrez, J. and Horrillo, M. C., 2006. Electronic nose for wine discrimination. Sens. Actuators, B, *113*(2), pp.911-916.

Glicerina, V., Balestra, F., Rosa, M. D., Bergenhstål, B., Tornberg, E. and Romani, S., 2014. The Influence of Different Processing Stages on Particle Size, Microstructure, and Appearance of Dark Chocolate. J. Food Sci. *79*(7), pp.E1359-E1365.

Goldberg, D. E. (1990). A note on Boltzmann tournament selection for genetic algorithms and population-oriented simulated annealing. Complex Syst., *4*(4), 445-460.

Grivetti, L.E. and Shapiro, H.Y., 2011. *Chocolate: history, culture, and heritage*. John Wiley & Sons.

Harsányi, G., 2000. Polymer films in sensor applications: a review of present uses and future possibilities. Sens. Rev., *20*(2), pp.98-105.

Hernandez Bennetts, V., Schaffernicht, E., Pomareda, V., Lilienthal, A. J., Marco, S. and Trincavelli, M., 2014. Combining non-selective gas sensors on a mobile robot for identification and mapping of multiple chemical compounds. Sensors, *14*(9), pp.17331-17352.

Hinze, J. O., 1975. Turbulence McGraw-Hill. New York, 218.

Jinap, S., Rosli, W. W., Russly, A. R. and Nordin, L. M., 1998. Effect of roasting time and temperature on volatile component profiles during nib roasting of cocoa beans (Theobroma cacao). J. Sci. Food Agric., *77*(4), pp.441-448.

Jolly, M. S., Blackburn, S. and Beckett, S. T., 2003. Energy reduction during chocolate conching using a reciprocating multihole extruder. J. Food Eng., *59*(2), pp.137-142.

Labreche, S., Bazzo, S., Cade, S. and Chanie, E., 2005. Shelf life determination by electronic nose: application to milk. Sens. Actuators, B, *106*(1), pp.199-206.

Lilienthal, A. J., Reggente, M., Trincavelli, M., Blanco, J. L. and Gonzalez, J., 2009, October. A statistical approach to gas distribution modelling with mobile robots-the kernel dm+v algorithm. In Intelligent Robots and Systems, 2009. IROS 2009. IEEE/RSJ International Conference on (pp. 570-576). IEEE.

Lozano, J., Santos, J. P. and Horrillo, M. C., 2005. Classification of white wine aromas with an electronic nose. Talanta, *67*(3), pp.610-616.

Markom, M. A., Shakaff, A. M., Adom, A. H., Ahmad, M. N., Hidayat, W., Abdullah, A. H. and Fikri, N. A., 2009. Intelligent electronic nose system for basal stem rot disease detection. Comput Electron Agric, *66*(2), pp.140-146.

Olunloyo, V. O., Ibidapo, T. A. and Dinrifo, R. R., 2012. Neural network-based electronic nose for cocoa beans quality assessment. Agricultural Engineering International: CIGR Journal, *13*(4).

Owusu, M., Petersen, M. A. and Heimdal, H., 2012. Effect of fermentation method, roasting and conching conditions on the aroma volatiles of dark chocolate. J. Food Process. Preserv., *36*(5), pp.446-456.

Pearce, T. C., Schiffman, S. S., Nagle, H. T. and Gardner, J. W. eds., 2006. Handbook of machine olfaction: electronic nose technology. John Wiley & Sons.

Prawira, M. and Barringer, S. A., 2009. Effects of conching time and ingredients on preference of milk chocolate. J. Food Process. Preserv., *33*(5), pp.571-589.

Rodriguez-Campos, J., Escalona-Buendía, H. B., Orozco-Avila, I., Lugo-Cervantes, E. and Jaramillo-Flores, M.E., 2011. Dynamics of volatile and non-volatile compounds in cocoa (Theobroma cacao L.) during fermentation and drying processes using principal components analysis. Food Res. Int., *44*(1), pp.250-258.

Saltini, R., Akkerman, R. and Frosch, S., 2013. Optimizing chocolate production through traceability: A review of the influence of farming practices on cocoa bean quality. Food Control, *29*(1), pp.167-187.

Shoemaker, D. P., Garland, C. W. and Steinfeld, J. I., 1962. Experiments in physical chemistry. New York: McGraw-Hill.

Sivaraj, R., & Ravichandran, T. (2011). A review of selection methods in genetic algorithm. Int. J. Eng. Sci. Res. Technol., *3*(5).

Schnermann, P. and Schieberle, P., 1997. Evaluation of key odorants in milk chocolate and cocoa mass by aroma extract dilution analyses. J. Agric. Food Chem., *45*(3), pp.867-872.

Shraiman, B. I. and Siggia, E. D., 2000. Scalar turbulence. Nature, *405*(6787), pp.639-646.

Squicciarini, M. P. and Swinnen, J., 2016. The Economics of Chocolate. Oxford University Press.

Figures

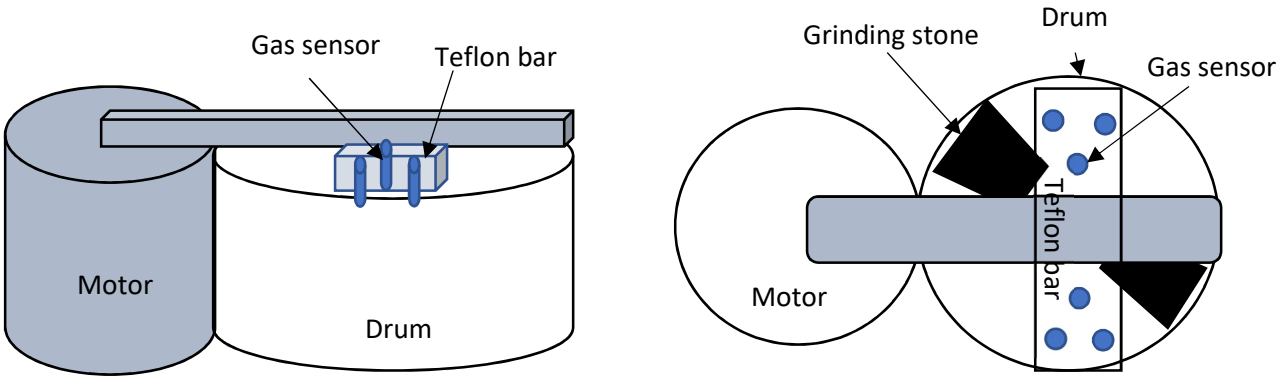

Figure 7.1. Diagram of electronic nose system for monitoring refining/conching.

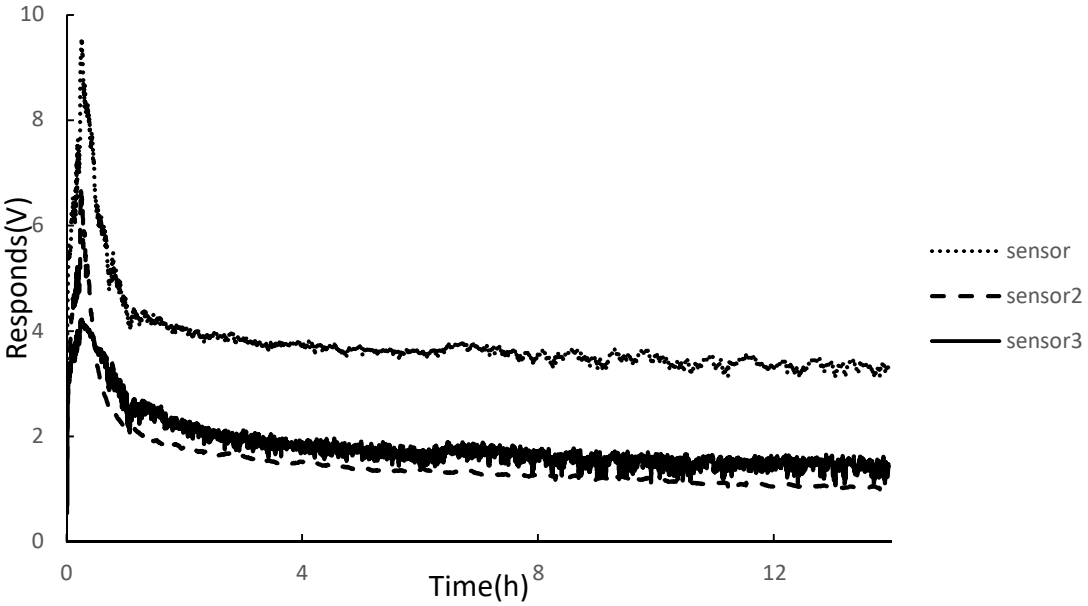

Figure 7.2. The responses of gas sensors during refining/conching.

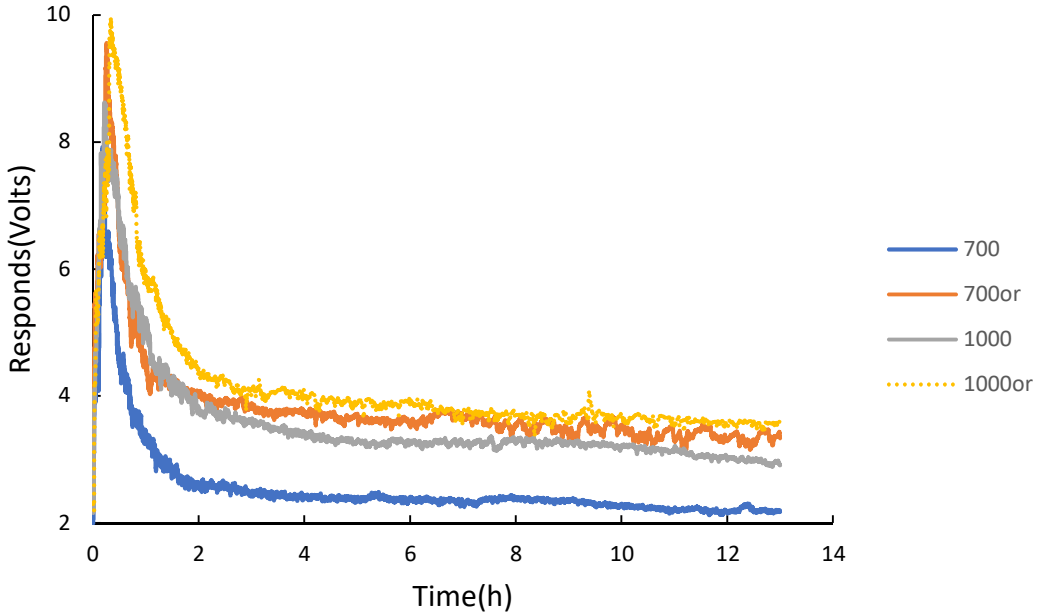

Figure 7.3. The responses of the most sensitive gas sensor from the refining/conching processes of different samples.

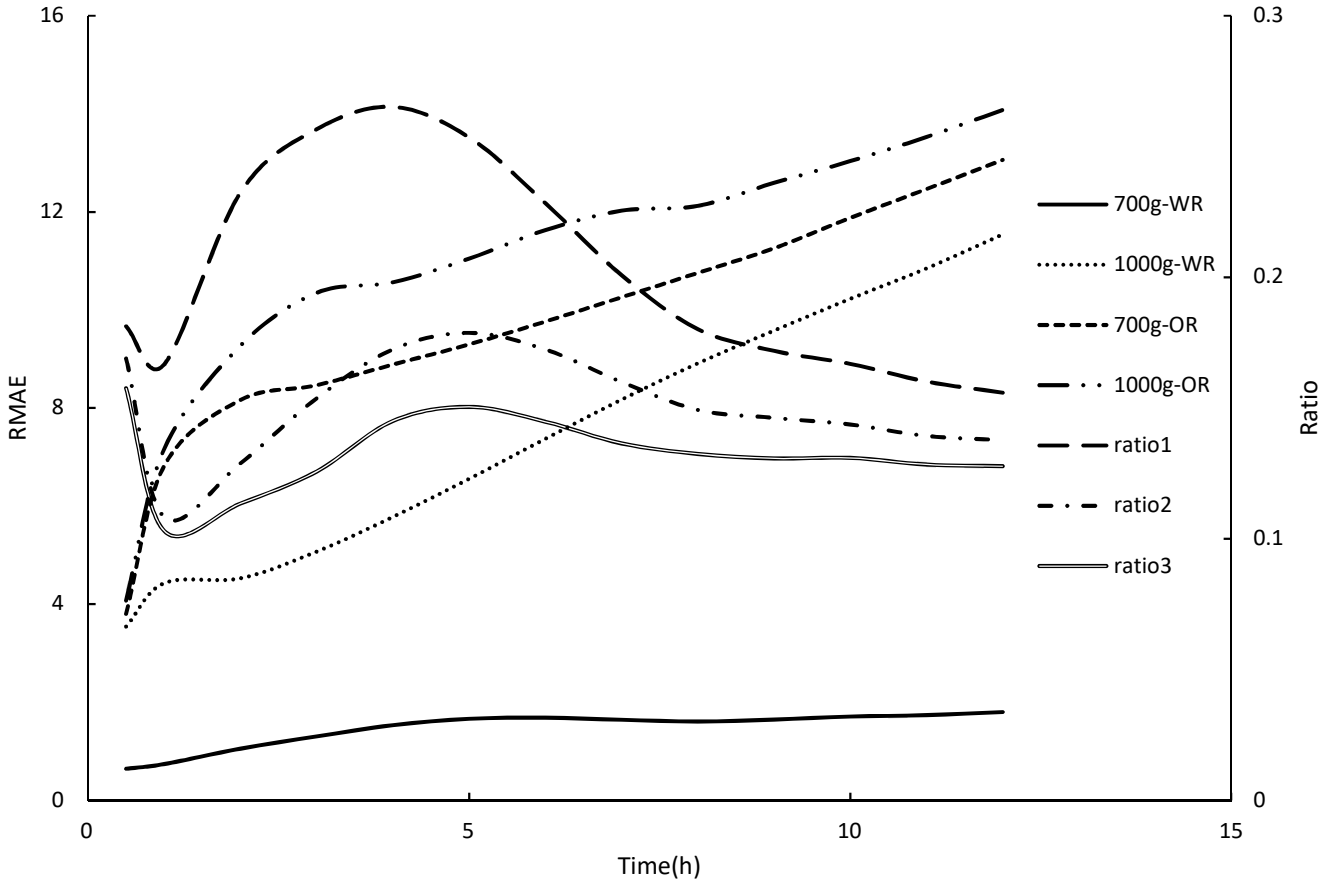

Figure 7.4. The performance of trained Kernel DMs in terms of RMAE and ratio.

Tables

Table 7.1. The P_{area} values for refining/conching processes of different samples.

	2h	4h	8h
700wr	372.41[a]	509.9[a]	737.15[a]
700dr	623.32[b]	1005.46[b]	1674.89[b]
1000wr	663.65[b]	1010.15[b]	1636.72[b]
1000dr	788.8[c]	1167.221[c]	1806.753[c]

wr is "well roasted" sample, "dr" is "dark roasted" sample, and the number represent the sample weight.

Table 7.2. The P_{peak} values for refining/conching processes of different samples.

	Peak valuse
700wr	0.16989[a]
700dr	0.196379[c]
1000wr	0.187003[b]
1000dr	0.215487[d]

wr is "well roasted" sample, "dr" is "dark roasted" sample, and the number represent the sample weight.

Table 7.3. The P_{width} values for refining/conching processes of different samples at different thresholding setting.

	0.2	S0.4	0.6
700wr	1606[a]	914[a]	274[a]
700dr	2439[b]	1113[ab]	615[b]
1000wr	3792[c]	1872[b]	801[bc]
1000dr	4320[d]	2172[c]	1044[c]

wr is "well roasted" sample, "dr" is "dark roasted" sample, and the number represent the sample weight.

Table 7.4. The performance of different trained Kernel DMs in terms of RMAE when applied to different validation groups.

Training group	700g-WR	1000g-WR	700g-OR
Validation group			
700g-WR	1.052[a]	2.927[c]	5.186[d]
1000g-WR	4.527[b]	1.382[a]	3.984[c]
700g-OR	8.163[c]	1.987[b]	1.792[a]
1000g-OR	9.271[d]	5.765[d]	2.781[b]

wr is “well roasted” sample, “dr” is “dark roasted” sample, and the number represent the sample weight.

CHAPTER 8

SUMMARY

Determination of glass transitions in boiled candies by capacitance based thermal analysis (CTA) and genetic algorithm (GA)

When the Tg of the candy was below ~15 ℃, the measurement from the GA-CTA was higher (2-3 ℃) than that from DSC. However, if Tg of the candy was higher than 15 ℃, the two methods gave similar values. GA based CTA provides a feasible new way to measure phase transitions in candies with relatively inexpensive equipment, and with less need for user interpretation of data.

Determination of chocolate melting properties capacitance based thermal analysis (CTA)

PSD of the samples did not significantly influence their melting onset temperature (~25℃) and peak temperature (33℃) measured by DSC. However, samples with finer particles had lower ending temperatures than those with coarser particles (range 36.59 to 37.28°C). Varying fat content in chocolate samples did not result in differences in the DSC melting curves. Samples with smaller particle sizes had lower temperatures at peak capacitance than those with larger particles, with peak temperatures ranging from 30.84 to 39.29℃, while higher peak capacitance values (range 2.61 to 2.84 10^{-11} F) were measured by contact area based CTA. Samples with higher fat content had lower peak temperatures (range 34.7 to 39.71 ℃) but higher peak capacitance values (range 3.29 to 4.3 10^{-11F}). While not yielding identical melting

temperatures, the values from the CTA system could be correlated with DSC results. In addition, the capacitance-based system was much simpler to use and relatively inexpensive to build.

Particle size measurements and scanning electron microscopy (SEM) of cocoa particles refined/conched by conical and cylindrical roller stone melangers

The performances of the two melangers (conical roller and cylindrical roller) were similar, however, cylindrical roller stones tend to generate thin and flat particles during the first 4 h of refining. Varying sample weights only influenced particle size reduction at early stages of refining. From the SEM images, a decreasing trend in the number of large spherical particles and an increasing trend in the number of small flat irregularly shaped particles were observed. The particle size measurements by the micrometer of cocoa particles refined for 0.5 h was greater than all other methods. However, the particle size measurements by the micrometer of particles refined for 2 h, 4 h, and 24 h were smaller than the measurements made by any other methods. On the other hand, except for cocoa being refined for 0.5 h, the particle size measurements tested by light microscopy image analysis for all cocoa samples were much greater than other measurement methods. Both the micrometer and light microscopy image analysis can be used to monitor the PSD of cocoa particles during refining/conching. However, the Hegman gauge failed to provide meaningful measurements.

Determining degree of roasting in cocoa beans by artificial neural network (ANN) based electronic nose system and gas chromatography/mass spectrometry (GC/MS)

In this study, an electronic nose system was constructed consisting of an array of gas sensors and used to detect volatiles emanating from cocoa beans roasted at 0, 20, 30, and 40min. The several signals were used to train a three-layer artificial neural network (ANN). Headspace samples were also analyzed by GC-MS with 23 select volatiles used to train a separate ANN. Both

ANNs were used to predict the degree of roasting of cocoa beans. The electronic nose had a prediction accuracy of 94.4% using signals from TGS 813, 826, 820, 880, 830, 2620, 2602 and 2610 sensors. In comparison, the GC-MS predicted the degree of roasting with an accuracy of 95.8%.

Characterizing cocoa conching and refining processes by kernel distribution model (Kernel MD) based electronic nose

The three parameters were able to detect the overall influence of roasting and sample weight on the volatile compound profile, however, they failed to characterize the influences introduced by single factor. On the other hand, the trained Kernel DM models were able to characterize the total volatile compounds profiles of samples with different treatment. Classification and discrimination based on volatile compounds profiles were correctly conducted by trained Kernel DM models.